INTERNAL GRAVITY WAVES FROM ATMOSPHERIC JETS AND FRONTS

Riwal Plougonven[1] and Fuqing Zhang[2]

R. Plougonven, Laboratoire de Météorologie Dynamique, Ecole Normale Supérieure, 24 rue Lhomond, 75005 Paris, France.

F. Zhang, Department of Meteorology, Pennsylvania State University, 601A Walker Building, University Park, PA 16802, U.S.A.

[1]Laboratoire de Météorologie Dynamique, Ecole Normale Supérieure, IPSL, Paris, France, riwal.plougonven@polytechnique.org

[2]Department of Meteorology, Pennsylvania State University, University Park, Pennsylvania, fzhang@psu.edu

For several decades, jets and fronts have been known from observations to be significant sources of internal gravity waves in the atmosphere. Motivations to investigate these waves have included their impact on tropospheric convection, their contribution to local mixing and turbulence in the upper-troposphere, their vertical propagation into the middle atmosphere and the forcing of its global circulation. While many different studies have consistently highlighted jet exit regions as a favored locus for intense gravity waves, the mechanisms responsible for their emission had long remained elusive: one reason is the complexity of the environment in which the waves appear, another is that the waves constitute small deviations from the balanced dynamics of the flow generating them, i.e. they arise beyond our fundamental, balanced understanding of jets and fronts. Over the past two decades, the pressing need for improving parameterizations of non-orographic gravity waves in climate models that include a stratosphere has stimulated renewed investigations. This review aims at presenting current knowledge and understanding on gravity waves near jets and fronts from observations, theory and modelling, and to discuss and outline challenges for progress in coming years.

1. INTRODUCTION

Internal gravity waves are waves occuring in the interior of a stratified fluid, with buoyancy providing the restoring force which opposes vertical displacements. Such waves are ubiquitous in the atmosphere and ocean and are the internal counterpart to the familiar surface gravtiy waves. In the atmosphere, they have horizontal scales ranging typically from 10 to 1000 km, and frequencies bound between the Coriolis parameter and the Brunt-Väisälä frequency (e.g. *Holton* [1992]). The highest frequencies occur for displacements that are nearly vertical, and high-frequency waves generally have shorter scales (simply reflecting that the forcing at high frequencies occurs at shorter scales). Amplitudes of internal gravity waves (or simply gravity waves, GW) generally are relatively small in the troposphere and stratosphere, in the sense that the dynamics at large scales (synoptic adn larger) is well described by approximations based on a balance such as geostrophic balance, which allows to obtain the wind diagnostically from the rest of the flow. These *balanced* approximations (e.g. quasi-geostrophy) filter out GW by construction, and have provided much of our fundamental understanding of mid-latitude dynamics (e.g. *Vallis* [2006]). For example, baroclinic instability was identified with the development of the quasi-geostrophic approximation [*Charney*, 1948; *Eady*, 1949], and frontogenesis with that of a higher-order approximation, semi-geostrophy [*Hoskins and Bretherton*, 1972]. Nonetheless, gravity waves can be of importance and reach large amplitudes *locally*, and their importance grows as we move up into the stratosphere and mesosphere [*Andrews et al.*, 1987]. Indeed, as they propagate vertically and transfer momentum and energy from their origin (generally in the troposphere) to the level where they dissipate, they contribute to the circulation and variability in the stratosphere, and force the reversal of the meridional thermal gradient in the mesosphere [*Fritts and Alexander*, 2003]. General circulation models (GCMs) that include a middle atmosphere generally do not have sufficient resolution to describe gravity waves explicitly, and hence need *parameterizations* to represent their main effects, namely the forcing due to the deposition of momentum where the waves are dissipated [*Kim et al.*, 2003]. One major difficulty with present parameterizations of gravity waves is the specification of their *sources*, which can be an arbitrary, tunable parameter due to lack of physical understanding and observational constraints.

The main sources of gravity waves include orography, convection and jet/front systems. Flow over orography has long been known and studied as a source (e.g. *Queney* [1948], see also references in *Gill* [1982]). Over the past two decades, several mechanisms have been proposed to explain waves generated by moist convection [*Clark et al.*, 1986; *Fovell et al.*, 1992; *Alexander et al.*, 1995], paving the way for their parameterizations in General Circulation Models. Atmospheric jets and fronts are known from observations to also be a major source of gravity waves. Studies of gravity wave activity have showed a conspicuous enhancement of gravity wave activity in the vicinity of jets and fronts (e.g. *Fritts and Nastrom* [1992]; *Eckermann and Vincent* [1993]). In addition, numerous case studies have analyzed the occurence of strong gravity wave events in the vicinity of a jet/front system. These case studies have isolated specific flow configurations: intense, gravity waves of low frequency have repeatedly been identified in the exit region of jets in the upper troposphere, often upstream of a ridge of geopotential [*Uccelini and Koch*, 1987; *Guest et al.*, 2000]. Such waves of low frequency are often called *inertia-gravity waves.*

However, the exact mechanisms through which the waves are generated near jets and fronts remain an active area of current research and debate. Candidate mechanisms associated with jet-front wave generation have included geostrophic adjustment, Lighthill radiation, unbalanced instabilities, transient generation, shear instability, convection...

Several of these can be considered examples of *spontaneous emission* [*Ford et al.*, 2000], i.e. emission of gravity waves by a flow that initially was well *balanced* (e.g. in geostrophic balance). This highlights one reason for the slow progress in understanding waves generated by jets and fronts: the latter are best known precisely in balanced approximations which by construction filter out gravity waves. Predicting gravity waves that will appear in flows that otherwise remain close to balance amounts to determining the limitations of these balanced approximations [*Vanneste*, 2013].

Recent years have brought significant progress in the understanding of mechanisms of spontaneous emission. Analytical studies have described Lighthill radiation, unbalanced instabilities and transient generation in simple flows and have provided simple asymptotic formulae quantifying the emitted waves [*Vanneste*, 2008]. In more complex flows, emission in a dipole has been simulated and quantitatively explained, providing a clear paradigm for emission in jet exit regions [*McIntyre*, 2009]. These studies have underlined the role of the background flow on the waves that are generated, and hence the importance of considering propagation effects.

With advances in computational power, it has been possible to complement these studies with idealized simulations that describe flows of realistic complexity, starting with *O'Sullivan and Dunkerton* [1995]. The simulated flows consist in the development and saturation of the instability of a baroclinic jet in a stratified, rotating fluid. Such baroclinic life cycles constitute a fundamental paradigm for our understanding of extratropical weather systems [*Thorncroft et al.*, 1993]. Gravity waves emitted in such simulations share features common with observational case studies. The background flow in which these waves appear is still quite complex (fully three-dimensional, time-evolving), so that even the origin of the waves is not always clear. A simpler flow has emerged as a paradigm that retains enough complexity (localized wind maximum, i.e. a jet streak) to produce analogous waves yet allow a quantitative explanation of their generation: it consists in a dipole (one cyclone and one anticyclone of similar size and amplitude) that propagates (quasi-)steadily [*Snyder et al.*, 2007; *Wang et al.*, 2009]. The emission of waves is understood as the response, within a complex background flow, to residual tendencies, i.e. to the small discrepancy between the full flow and its balanced approximation [*Snyder et al.*, 2009; *Wang and Zhang*, 2010].

This review will cover recent advances in many aspects of gravity waves from jets and fronts and discuss their impacts and importance. The review will complement the earlier review of *Uccelini and Koch* [1987] on observed gravity wave events associated with jet streaks, and recent reviews of *Fritts and Alexander* [2003] on gravity waves and the middle atmosphere, of *Kim et al.* [2003] on gravity wave parameterizations and of *Richter et al.* [2007] that summarized findings and discussions from a gravity wave retreat held at NCAR in the summer of 2006.

The paper is organized as follows: observational evidence for the emission of gravity waves from jets and fronts is reviewed in sections 2 and 3, respectively covering climatological studies that establish the general importance of jets and fronts as sources, and case studies which provide insights on favorable flow configurations and characteristics of the emitted waves. Many different generation mechanisms have been proposed in relation to this problem and they are described in sections 4 and 6. Mechanisms that have initially been pinned down through analytical developments, yielding asymptotic results, are described first, in section 4. These theoretical results however do not connect straightforwardly to gravity waves observed in real flows. Understanding the generation and maintenance of gravity waves in more realistic flows requires a preliminary consideration of propagation effects (section 5). This allows to consider the emission in laboratory and numerical experiments (section 6), which occur in more realistic flows and which have led to a consistent explanation of gravity waves in jet exit regions. Impacts and parameterizations of waves generated from jets and fronts are presented in section 7. Our state of understanding and outstanding issues are discussed in section 8.

2. OBSERVATIONS: CLIMATOLOGICAL STUDIES

Broadly, observational studies of relevance can be separated into two categories: climatological studies, which can describe, for example, the importance of strom tracks as source regions of gravity waves, and case studies, which provide specific examples of waves emitted from jets or fronts. The present section describes climatological studies, emphasizing those that quantify waves not only geographically, but relative to the flow and in particular to jets and fronts.

The following is organized by observational platform. This is an opportunity to give an overview of observations available for gravity waves, and to present advantages and limitation of each type of observations.

2.1. Surface and radiosonde networks

Surface observational networks have been available for several decades, and have provided the first opportunity for systematic climatological documentation and characterization of gravity waves. For example, *Einaudi et al.* [1989] performed a monthly-long climatological study of gravity waves at the Boulder Atmospheric Observatory with data, from a network of microbarographs and from sensors on the 300 m tower. They found both coherent and incoherent motions within five frequency ranges with periods range 1-20 min. A similar but much more extensive climatology of gravity waves was performed in *Grivet-Talocia et al.* [1999] using a mesonetwork of barometers over east-central Illinois during 1991-1995. They identified coherent events, for which clear propagation allowed a good estimation of phase velocity, dominant period and horizontal wavelength. Part of these coherent events are attributed to gravity waves, others corresponding to gravity currents, solitary waves or bores. Coherent events were found to occur ~ 20 of the total time in fall and winter and 12% in summer with dominant wave speed at at 25-30 m/s. They attributed the seasonal dependence of gravity wave occurrences to the stronger baroclinicity of the atmosphere (and the mid-latitude jet streams).

The most comprehensive study of gravity waves using surface pressure observations was presented in *Koppel et al.* [2000] who examined the distribution of large hourly pressure changes ($>$ 4.25 hPa) during a 25-yr period over the United States. They found the most frequent occurrences of large-amplitude surface pressure changes are over the Great Plains (which may be related to being in the lee of the Rockies) and over New England (that are in the storm track and jet stream exit region), as illustrated in Figure 1. They also found that the large-amplitude gravity wave activity is more prevalent over winter and spring during the period of strong atmospheric baroclinicity. Their composite analysis shows that the flow patterns are in broad agreement with the gravity wave paradigm of *Uccelini and Koch* [1987] (see section 3).

Gravity waves have also been analyzed systematically using the radiosounding network: these studies contrast with the above by a stronger emphasis on the waves in the upper troposphere and lower stratosphere[1]. Moreover, whereas surface barographs focused on fast waves in time-series (periods less than an hour), vertical profiles from radiosondes favor the analyis of low-frequency waves (also called *inertia-gravity waves*) that have an unambiguous signature in the hodograph [*Hirota and Niki*, 1985].

Wang and Geller [2003] used the high vertical resolution radiosonde wind and temperature data to examine the gravity wave climatology over the United States during 1998-2001 (see their Figure 6). They found that the tropospheric and lower stratospheric gravity-wave energies are both stronger in winter than summer, likely owing to the presence of stronger baroclinic jet-front systems. They found that tropospheric gravity-wave energy maximizes over the Rocky Mountains while the lower stratospheric energy maximized over the southeastern United States. An intriguing result from *Wang and Geller* [2003] is that they found little correlation between the tropospheric and lower stratospheric gravity-wave energies. *Gong et al.* [2008] further examined an 8-year climatology of gravity waves using the high-resolution radiosonde observations with the addition of a ray-tracing model. They found that the gravity wave sources are anisotropic, with wave momentum flux directed mostly upstream of the prevailing wind direction. Whereas a source tied to convection provided the best fit to the observations at low latitudes, a more general source worked better at middle and high latitudes. Investigations were pursued with a more sophisticated use of the energies that can be estimated from radiosondes [*Geller and Gong*, 2010], leading to a better estimation of convective sources [*Gong and Geller*, 2010].

Radiosondes have also been analyzed in other regions, in particular when specific campaigns have made high-resolution profiles available. *Guest et al.* [2000] have analyzed gravity waves in ozonesonde profiles reaching 30 km altitude over Macquarie Island, South of New Zealand. The location guarantees that observed waves are non-orographic. Cases with strong inertia-gravity waves were analyzed and led to the identification of a common meteorological pattern: intense waves were found downstream of a jet streak, between the inflection point and the ridge of geopotential. Using ray-tracing analysis, they confirmed that the origin of the waves observed in the lower-stratosphere originated from a tropospheric jet-front system. *Sato and Yoshiki* [2008] examined stratospheric gravity waves from 3-hourly radiosondes launched from Syowa station in Antarctica. Large and sporadic gravity wave activity was observed during the winter months, with some events of gravity waves generated from the Polar Night Jet, and propagating upward and downward. *Zhang and Yi* [2007] have analyzed gravity waves in several years of twice-daily radiosondes, from several stations in China, and also found that the upper-tropospheric jet was the main source of waves. More precisely, they suggest the strong wind shear induced by the jet as the source of waves [*Zhang and Yi*, 2005, 2008]. As *Guest et al.* [2000], and in contrast to *Wang and Geller* [2003], *Geller and Gong* [2010] or *Sato and Yoshiki* [2008], they found minimum stratospheric gravity wave activity in winter. These differences regarding the seasonal cycle are yet unexplained.

Plougonven et al. [2003] took advantage of the large number of soundings launched from research vessels over the Atlantic Ocean, far from orographic sources, during the FASTEX campaign (January-February 1997, *Joly et al.* [1997]). Gravity wave activity was found to be maximal in the vicinity of the jet stream. More specific analysis led to identify two flow configurations for which intense gravity waves were present: the vicinity of a strong, straight jet, and the jet exit region of a strongly curved jet, either in a trough [*Plougonven et al.*, 2003] or in a ridge [*Plougonven and Teitelbaum*, 2003]. Only in the case of jet exit regions was it possible to carry out case studies of clear, intense inertia-gravity waves consistently identified in several soundings. The waves had frequencies between f and $2f$, wavelengths of a few hundred kilometers, wind perturbation of 5-8$m\,s^{-1}$, similar to *Guest et al.* [2000].

2.2. In-situ aircraft measurements

Analyzing in-situ measurements aboard commercial aircraft during 1978 and 1979, *Fritts and Nastrom* [1992] and *Nastrom and Fritts* [1992] attributed the mesoscale variance enhancements of horizontal velocity and temperature (presumably mostly induced by gravity waves) to four different mechanisms: topography, frontal activity, nonf-rontal convection, and wind shear. Overall, they found variances of temperature and wind at horizontal scales less than approximately 100 km to be 6 times larger in the vicinity of these sources than in a quiescent background, emphasizing the intermittency of gravity waves sources. The relative importance of the different sources were evaluated as shown in Figure 2, indicating strong values of variances above jets and fronts, smaller than those above topography by a factor of $\sim$2 for wind speed, and comparable for temperature.

The interpretation of the small-scale component of winds and temperature as gravity waves received support from *Bacmeister et al.* [1996], who examined the horizontal wavenumber power spectra of 3-D wind velocities and potential temperatures measured at an altitude of about 20 km during 73 NASA ER-2 flights. They argued that the observed velocity and potential temperature spectra are consistent with gravity waves instead of the inverse energy cascade of either 2-D or 3-D turbulence. However, this study did not attempt to identify the sources of these gravity waves.

More recent aircraft based investigations of gravity waves emitted by jets and fronts focus on individual case studies, and are discussed in section 3 and 7.2.

2.3. Balloons and rockets

Beyond the reaches of radiosondes and aircrafts, other in-situ measurements of gravity waves in the middle atmosphere include balloons and sounding rockets, which are usually part of coordinated field campaigns.

Ultra-long-duration, superpressure balloons drift on isopycnic surfaces and behave as quasi-Lagrangian tracers, yielding a direct measurement of intrinsic frequencies which is very valuable for gravity wave studies [*Hertzog et al.*, 2002b]. Whereas flights in the equatorial stratosphere during September 1998 showed largest momentum fluxes associated with convection [*Hertzog and Vial*, 2001], campaigns in the winter polar vortices of both hemispheres (2002, 2005) have allowed the investigation of other sources [*Vincent et al.*, 2007]. Topography (Greenland, Antarctic Peninsula) comes out strikingly as the source associated with the maximum local values of momentum fluxes, but significant values are also found over oceans and smooth terrain, indicating the importance of non-orographic waves. Measurements from the Vorcore campaign (austral spring of 2005, *Hertzog et al.* [2007]) were analyzed in detail using wavelet analysis [*Boccara et al.*, 2008]. *Hertzog et al.* [2008] confirmed that non-orographic sources, although yielding locally weaker values, had an overall contribution that was comparable to or greater than flow over orography (see Figure 3). Complementary to this data analysis, *Plougonven et al.* [2012] have carried out mesoscale simulations ($\Delta x = 20$km) of flows above the polar cap over a wide domain and for a long period (2 months). Overall, a satisfactory, quantitative agreement was found between the simulated and observed gravity wave momentum fluxes, which is very encouraging [*Plougonven et al.*, 2010, 2012]. Nonetheless, specific biases for orographic and non-orographic waves were identified, emphasizing that it is preferable to analyze separately these different types of waves. These simulations confirmed that the contribution fom non-orographic waves to the momentum fluxes integrated over the polar cap were comparable or larger than those of orographic waves for this domain and time, consistent with *Hertzog et al.* [2008] (Figure 3).

In-situ measurements above the upper stratosphere are obtained from sounding rockets. They allow investigation of gravity waves in the mesosphere and lower thermosphere, where their signatures can be very large. The winter MaCWAVE (Mountain and Convective Caves Ascending Vertically) rocket campaign in January 2003 explicitly focused on gravity waves, using both ground-based and rocket-borne instruments [*Fritts et al.*, 2004; *Williams et al.*, 2006]. However, the rocket measurements have not been directly linked to jet-front gravity wave activity.

2.4. Ground-based remote sensing

Besides the aformentioned in-situ measurements, remotely sensed observations from ground-based radars, lidars and airglow are also widely used to detect atmospheric gravity wave activity. Among the ground-based remote sensing instruments, specially designed radars and lidars have the highest temporal and vertical resolution but they are only available at very limited number of locations around the world.

Using observations from an ST (stratosphere-troposphere) radar during four extended observational campaigns in southern Australia, *Eckermann and Vincent* [1993] examine the generation of gravity waves from cold fronts. They found order of magnitude increases in mesoscale variance of winds attributable to gravity waves during frontal passages. They also found it possible to detect certain waves (in the upper-troposphere, with long horizontal wavelengths and large ground-based phase speed) a day before and a day after the fronts' arrival, whereas large amplitude, higher-frequency, shorter horizontal wavelength waves are directly associated with the onset of the frontal circulation at the surface. They speculated that the smaller wave amplitudes observed in the stratosphere may be due to either more oblique propagation of wave energy in a more stable environment or due to the ducting of wave energy below the tropopause.

The MU (middle and upper atmospheric) radar located at Shigaraki, Japan has been providing measurements of gravity waves since 1984. *Sato* [1994] examined gravity wave activity using wind data derived from this radar over 1986-1988, and found the dominant waves in the lower stratosphere tend to have short vertical wavelengths ($\sim$4 km) and long ground-relative periods ($\sim$10 h). The gravity waves are the strongest in winter which is apparently related to the strong substropical jet stream over this region [*Sato*, 1994]. However, she speculated that topography rather than jet/front systems may be the primary sources of these gravity waves.

A mesosphere-stratosphere-troposphere (MST) radar located in Aberystwyth, Wales, has been operated on a quasi-continuous basis since 1997. This VHF wind profiler radar is capable of making continuous measurements of the three-dimensional wind vector at high resolution, and was used for several case studies of inertia-gravity waves excited by jets and fronts [*Pavelin et al.*, 2001; *Pavelin and Whiteway*, 2002], see section 3. *Vaughan and Worthington* [2007] analyze inertia-gravity waves with eight years' observations from this MST radar. They found inertia-gravity waves generally propagating upward in the lower stratosphere and downward in the tropopshere, evidence that the source is at the jet-stream level. Long period waves (> 12h) were not preferentillay associated with a jet stream and showed little seasonal dependence, in marked contrast with shorter period waves (6-8h) which were clearly associated with the jet and had a winter maximum.

The winter maximum in the stratosphere was also found in the 4-year gravity wave climatology derived from Rayleigh lidars located in two different sites in Sourthern France [*Wilson et al.*, 1991] and from a Rayleigh lidar in Japan *Murayama et al.* [1994]. They found strong correlation between the gravity wave activity and the wind speed in the stratosphere, and the waves increase in amplitude while propagating from stratosphere to the mesosphere.

Ground-based airglow imagers are often used as an economical means of measuring gravity waves in the mesosphere and lower thermosphere (e.g., *Taylor and Bishop* [1995]; *Walterscheid et al.* [1999]; *Li et al.* [2011]). Airglows are mostly effective in detecting gravity waves with short periods (< 1 h), short horizontal wavelengths (< 100km) and long vertical wavelength (> 10km) (*Liu and Swenson* [2003]). For example, most recently, *Li et al.* [2011] documented a year-long climatology of gravity waves observed by an airglow imager over northern China. They found the gravity waves occurs more frequently over the summer and winter than the other two seasons. These waves have typical horizontal wavelengths of 10-35 km and phase speeds of 30-60 m/s.

2.5. Satellite observations

There have been a large number of observational studies of gravity waves from satellites since *Fetzer and Gille* [1994] using LIMS (Limb Infrared Monitor of the Stratosphere). On one hand, the satellite-based remote sensing measurements a priori have relatively poor spatial and temporal resolutions, but on the other they provide the most complete coverage of global gravity waves and as such constitute an invaluable source of information. *Wu and Waters* [1996] are one of the first to estimate global activity of gravity waves, using MLS (Microwave Limb Sounder) observations. Further developments led to deriving global gravity wave *momentum fluxes* from satellite observations (*Ern et al.* [2004], using temperature measurements from CRISTA (Cryogenic Infrared Spectrometers and Telescopes for the Atmosphere)).

Overall synthesis of such observations can be found in the recent review paper of *Alexander and et. al.* [2010]. Figure 8 of *Alexander and et. al.* [2010], adapted from *Preusse et al.* [2008], summarizes the spatial and temporal resolution of different satellite-based instruments which include infrared limb sounders, microwave sub-limb instruments, and infrared nadir sounders[2]. *Wu et al.* [2006] compared gravity waves measured by different satellite instruments and found similar gravity wave characteristics from the nadir techniques[3]. The limb-sounding instruments are complementary, having better vertical but poorer horizontal resolution. Higher resolution and accurate measurements of gravity waves can be achieved with the more recently launched HIRDLS instruments (e.g. *Alexander and co authors* [2008]; *Yan et al.* [2010]).

These satellite studies provide global distribiutions, and hence some information on gravity waves generated from jets and fronts. One study which specifically tied gravity wave activity to the tropospheric baroclinic jet front systems is presented in *Wu and Zhang* [2004] using the AMSU-A microwave data (see Figure 6). They particularly focused on the gravity wave properties and variabilities over the northeastern United States and the

North Atlantic in the December-January periods. It is found that gravity waves in this storm-track exit region, found in many winters, can reach the stratopause with growing amplitude. More importantly, this is one of the first studies that directly linked the satellite-derived gravity wave activity with the intensity and location of the tropospheric baroclinic jet front systems. *Wu and Eckermann* [2008] further show strong seasonal fluctuations of the global gravity wave variance derived from Aura MLS for each month of 2006 (their Figure 8).

Estimates of GW momentum fluxes or temperature variances have shown consistently, in different studies, enhanced values in the stratospheric winter polar night jet (e.g. *Wu and Eckermann* [2008]; *Alexander and co authors* [2008]; *Yan et al.* [2010]; *Ern and Preusse* [2011], see Figure 4). This can be interpreted as a signature of significant sources (orographic and non-orographic) in the winter mid-latitudes, but also as the signature of favored propagation within the positive shear of the strong westerlies [*Dunkerton*, 1984; *Ern and Preusse*, 2011]. The zonal asymmetries are indications of enhanced sources, and emphasize orography as a source at mid and high latitudes [*Wu and Eckermann*, 2008]. Interestingly, *Wu and Eckermann* [2008] use the different sensitivity of their instrument between ascending and descending orbits to show that waves in the mid-latitudes have a preferred horizontal orientation, with phaselines extending from south-west to north-east in the Northern Hemisphere, and from north-west to south-east in the Southern Hemisphere. This is consistent with the momentum fluxes estimated over the Southern ocean from balloon observations [*Hertzog et al.*, 2008] and numerical simulations [*Plougonven et al.*, 2012].

2.6. Analyses and forecasts from meteorological models

With increased model resolution and advanced model physics, along with enhanced observations and improved data assimilation methods, numerical weather prediction (NWP) models are increasingly capable of resolving at least part of the gravity wave specta in the trophere and stratosphere in both their analyses and forecasts. Even at moderate resolutions, relevant information about the location and intrinsic frequency of gravity waves can be obtained [*Plougonven and Teitelbaum*, 2003]. *Wu and Eckermann* [2008] showed the monthly-mean GW-induced temperature variances at 44 km pressure altitude derived from operational global analysis fields of the European Center for Medium-Range Weather Forecast (ECMWF) Integrated Forecast System in August 2006 (Figure 4). They found qualitative agreement between the gravity wave variances in terms of latitude bands and propagation directions derived from the global analysis and those derived from satellite observations (Aura MLS). At least part of the enhanced gravity wave activity over the Southern Oceans is likely related to strong baroclinic jet-front systems during this winter month.

Consistency of the satellite-derived jet-stream-related gravity waves with those from a NWP model was also shown in *Wu and Zhang* [2004], but with the AMSU-A and a higher-resolution mesoscale model (see section 3 and Figure 6). *Schroeder et al.* [2009] also found good agreement between gravity wave-induced temperature fluctuations derived from satellite observations (SABER, Sounding of the Atmosphere using Broadband Emission Radiometry) and the ECMWF analysis, including those at the edge of the winter polar vortex or the midlatitude jet streams.

More recently, *Shutts and Vosper* [2011] presented an indepth comparison of the gravity wave fluxes derived from both the Met Office and ECMWF forecast models for August

2006 with those from HIRDLS. They concluded that the state-of-the-art NWP models are capable of capturing the correct overall strength and distribution of gravity wave activity. In the Southern mid and high latitudes, they note that waves tend to have phaselines oriented from North-West to South-East, consistent with *Wu and Eckermann* [2008]. *Plougonven et al.* [2012] used observations from the Vorcore balloons *Hertzog et al.* [2007] to systematically assess the realism of the gravity wave field in a mesoscale meteorological model. Relative to the observations[4], the simulations overestimated orographic waves by a factor $\sim 2-3$, whereas non-orographic waves were slightly underestimated (factor ~ 0.8 for the time-averaged value).

These recent investigations advocate NWP models as a relevant means to document the global variations and impacts of gravity wave activity and fluxes [*Alexander and et. al.*, 2010]. Combining NWP output with observations and a careful assessment of biases and limitations of each promises to lead, in coming years, to a converging estimation of gravity wave momentum fluxes.

3. OBSERVATIONS AND MESOSCALE MODELLING: CASE STUDIES

In contrast to the climatological studies above, individual case studies isolate specific configurations in which intense gravity waves are unambiguously identified. They are described below in section 3.1. Finally, an overview of the observational studies is given in section 3.2, discussing the limitations and biases of the different observational platforms, and the needs for future observations.

3.1. Case studies

Tropospheric jets and fronts were long hypothesized to be responsible for numerous observed gravity wave events, both in the troposphere [*Tepper*, 1951] and in the upper atmosphere above the tropopause [*Hines*, 1968]. However, given the limitation in the observing techniques, there were inherent uncertainties in the source attribution of these earlier observations [*Hines*, 1968; *Gossard and Hooke*, 1975]. Below we review case studies starting from the review of *Uccelini and Koch* [1987]. Whereas early studies emphasized tropospheric (ducted) waves, the focus over the last decade has shifted to upper-tropospheric waves propagating into the stratosphere.

Uccelini and Koch [1987] (hereafter UK87) reviewed 13 long-lived observed lower-tropospheric gravity wave events in literature (see refs therein). These mesoscale disturbances have wave periods of 1-4h, horizontal wavelengths of 50-500km and surface pressue perturbations of 0.2-7 mb, all of which have been shown to influence the mesoscale structure of precipitation systems. They found a common synoptic environment for the generation and maintenance of these waves as being in the exit region of upper-level jet streaks and cold-air side of a surface frontal boundary (Figure 5). They further hypothesized that these gravity waves are likely to be generated by the unbalanced upper-tropospgeric jet-front systems through geostrophic adjustment [*Rossby*, 1938; *Cahn*, 1945; *Blumen*, 1972], and to be maintained through wave ducting (*Lindzen and Tung* [1976], and section 5.1).

Case studies in the years following UK87 increasingly involved mesoscale numerical modelling. The earliest simulations of mesoscale gravity waves using numerical weather prediction models were first conducted by *Zhang and Fritsch* [1988]; *Schmidt and Cotton* [1990] and *Cram et al.* [1992]. Gravity waves in these studies were generated by the simulated mesoscale convective systems. However, detailed verification of these waves against mesoscale observations was not performed due to the unavailability of the mesoscale data sets. Mesoscale numerical models have subsequently been developed into powerful tools for the detailed study of gravity wave structure, energy sources, and maintenance mechanisms, all of which are difficult to detect with standard observations.

The first published attempt to use a mesoscale model for the sole purpose of simulating and studying an observed gravity wave event, and for which verification was performed against detailed mesoanalysis, was provided by *Powers and Reed* [1993]. The case simulated was the long-lived, large-amplitude gravity wave event on 15 December 1987 over the Midwest of the US which is believed to have created life-threatening blizzard conditions with peak pressure falls up to 11mb in 11 min as documented in *Schneider* [1990]. *Powers and Reed* [1993] concluded that the mesoscale NWP model used can successfully simulate mesoscale gravity waves and can capture many aspects of the observed waves in terms of both timing and magnitudes. Although this event had characteristics of mesoscale gravity waves under typical synoptic settings conceptualized by Uccellini and Koch (1987), the authors suggested the model waves were maintained and amplified by wave-CISK processes. *Powers* [1997] further concluded that elevated convection above a stable wave duct was the forcing mechanism in the model. *Pokrandt et al.* [1996], who studied the same case also with numerical simulations, on the other hand hypothesized that a transverse circulation about the approaching jet streak produced a mesoscale potential vorticity anomaly at midlevels that subsequently forced the mesoscale waves.

One of the cases reviewed in UK87 is the 11-12 July 1981 gravity wave event that is believed to be responsible for triggering and organizing mesoscale convection over southeast Wyoming into the Dakotas during CCOPE [*Koch and Golus*, 1988; *Koch and Dorian*, 1988; *Koch et al.*, 1988, 1993]. There are at least two distinct wave episodes detected by the CCOPE high-resolution surface mesonet [*Koch and Golus*, 1988]. The synoptic-scale analysis in *Koch and Dorian* [1988] showed that the waves are confined to the region between the axis of inflection and the ridge in the 300 hPa height field, downstream of a jet streak and to the cold air side of a surface quasi-stationary front. There is also evidence of strong flow imbalance associated with the upper-level jet from observational analysis [*Koch and Dorian*, 1988] and from mesoscale modeling [*Kaplan et al.*, 1997]. Subsequent numerical simulations by *Zhang and Koch* [2000] and *Koch et al.* [2001] did simulate reasonably well the observed gravity waves. However, these latter studies concluded that, despite the proximity of the wave generation with the jet streaks, the thermally-driven mountain-plains circulation (MPS) is responsible for the generation of both wave episodes: the first through an orographic density current relegated from a remnant daytime MPS circulation [*Zhang and Koch*, 2000] and the second by convection triggered by the developing MPS [*Koch et al.*, 2001].

The relevance of the UK87 paradigm has been highlighted in a number of case studies and shown to be robust for the presence of waves (e.g. *Ramamurthy et al.* [1993]). Often it is found that the waves have an impact on convection and precipitation [*Trexler and Koch*, 2000; *Richiardone and Manfrin*, 2003], although the relation varies. This impact has been one motivation for the development of an automated system for predicting and detecting mesoscale gravity waves using surface observations [*Koch and O'Handley*, 1997; *Koch and Saleeby*, 2001]. Both studies suggest the hypothesis that the unbalanced flow in the jet streak exit region or near frontal boundaries is associated to mesoscale gravity wave generation.

Another well-studied case is the 1992 St. Valentine's Day mesoscale gravity wave event observed during STORM-FEST [*Trexler and Koch*, 2000; *Rauber et al.*, 2001]. High-resolution mesoscale NWP models had been used to simulate the event with varying degrees of success, while the mechanisms derived from different simulations differ greatly. Through unbalanced flow diagnosis of the model simulations, *Jin* [1997] and *Koch and O'Handley* [1997] believe this event followed closely the jet-gravity wave paradigm of UK87, though as in previous studies, *Jin* [1997] also finds convection is important for maintaining and amplifying the mesoscale waves. Through numerical experiments with and without evaporative processes, *Jewett et al.* [2003], on the other hand, singled out the importance of the evaporatively driven downdrafts that impinges upon the surface warm-frontal inversion on the wave genesis.

Whereas observations alone have recurrently been insufficient to support conclusions on the relation of gravity waves and convection (e.g. *Ralph et al.* [1993]), high-resolution mesoscale simulations in complement to observations can provide key insights. A large-amplitude gravity wave event over the northeastern United States on 4 January 1994 was documented in *Bosart et al.* [1998] that showed wavelengths of 100-200km and peak crest-to-trough pressure falls exceeding 13 hPa within 30 min associated with short-term blizzard conditions. The synoptic-scale pattern of this wave event is again consistent with the UK87 paradigm from the observational analysis. Through successful simulation of this event with a high-resolution mesoscale model, *Zhang et al.* [2001, 2003] demonstrated the radiation of the gravity waves to the lower-troposphere from an unbalanced upper-tropospheric jet streak. The wave packet emitted from the upper-level jet streak subsequently merged with a mid-tropospheric cold-front aloft and triggered moist convection. A ducted wave-CISK mode was responsible for the subsequent wave maintenance and amplification. Hence, although moist processes were not at the origin of the wave, they played a crucial role to amplify it, as shown by dry simulations.

It is worth noting that a number of case studies fall outside the flow configuration of the UK87 paradigm. For example, *Ralph et al.* [1999] described gravity waves found ahead of a cold front, suggesting that the cold front plays the role of an obstacle to the flow impinging on it. These waves are very similar to some of the waves simulated in idealized studies of frontogenesis (see section 6). The flow pattern in this case was significantly constrained by the presence of mountains to the West of the cold front, and further investigations would be necessary to determine whether this 'obstacle effect' of cold fronts was exceptional, or commonly occurs.

The above case studies have focused on tropospheric waves, their interactions with convection and their effects near the surface. The flow configuration identified by UK87 has also been found to be relevant for emission into the lower stratosphere. *Guest et al.* [2000] have highlighted the jet exit region of a jet streak approaching the inflection point between the base of a trough and a ridge as a configuration conducive to intense gravity waves in the lower stratosphere. Ray-tracing was used to identify the origin of clear, intense inertia-gravity waves observed in the lower stratosphere, and has highlighted the upper-level jet as the region of emission [*Guest et al.*, 2000; *Hertzog et al.*, 2001]. Case studies based on FASTEX radiosoundings also highlighted jet exit regions, either upstream of a ridge *Plougonven and Teitelbaum* [2003] or upstream of a deep trough *Plougonven et al.* [2003]. Instances of generation from jets in a region a priori dominated by orographic waves were documented by *Spiga et al.* [2008]. They combined global reanalysis, satellite and radiosoundings data along with mesoscale model simulations in the Andes Cordillera region to identify the cases where, respectively, the jet-stream source, the convective source and the topography source are predominantly in action.

Case studies focusing on upper-tropospheric and lower-stratospheric observations have often emphasized the presence of both upward and downward waves from the jet as a disctinctive signature of emission by the jet *Thomas et al.* [1999]; *Plougonven et al.* [2003]; *Wu and Zhang* [2004]; *Spiga et al.* [2008]. From 17 radiosoundings launched at 3-hour intervals over Northern Germany, *Peters et al.* [2003] clearly identified inertia-gravity waves propagating upward and downward from the jet which amplified downstream of the jet streak. Complementing similar radiosonde observations with mesoscale simulations, *Zülicke and Peters* [2006] investigated the spontaneous generation of waves from the upper-level jet streak in a poleward-breaking Rossby wave. They identified subsynoptic (horizontal wavelength $\lambda_h \sim 500$km) and mesoscale waves ($\lambda_h \sim 500$km), and showed the waves to propagate upward and downward from the level of the jet stream. Their study provides further evidence that the jet exit region is hereby the key feature of the background flow. Numerical simulations have also been carried out in complement to satellite observations by *Wu and Zhang* [2004]. A good level of agreement was found between the waves interpreted from radiance perturbations east of Newfoundland, and the simulated waves (see Figure 6). Such comparison serves both to validate the interpretation of the observations and to assess the realism of the model.

First systematic measurements of upper-tropospheric and lower-stratospheric gravity waves with a dedicated research aircraft conducted during the 2008 field experiment of Stratosphere-Troposphere Analyses of Regional Transport (START08; *Pan et al.* [2010]).

During one of the research flights, accompanied with a strong baroclinic jet-front across the continental United States, apparent activity of gravity waves at different scales near or just above the tropopause region were sampled during nearly the entire flight mission that covered a distance of a few thousand kilometers. While research is still ongoing to examine the sources of these gravity waves observed during START08, it is apparent the tropopopheric jet-front systems, in interaction with the local topography and moist convection, were playing essential roles in the forcing and characteristics of theses gravity waves [*Zhang et al.*, 2009].

Regarding generation mechanisms, case studies have often referred to geostrophic adjustment (e.g. *Pavelin et al.* [2001]). The justification is that observed and simulated GW are often found in the vicinity or just downstream of regions of imbalance, with Lagrangian Rossby numbers serving as an indicator of imbalance [*Koch and Dorian*, 1988; *Ramamurthy et al.*, 1993; *Spiga et al.*, 2008]. A more sophisticated indicator is provided by the residual of the nonlinear balance equation *Zhang et al.* [2000, 2001], and has been used efficiently (e.g. *Hertzog et al.* [2001]). However, the relation is merely a colocation (the waves are found where or near maxima of indicator of imbalance), but it is not systematic (e.g. there are other maxima that are not associated to waves) and a quantitative relationship is still lacking.

3.2. Limitations and challenges

Observational estimates of gravity wave activity or momentum fluxes face several difficulties: first, each observational platform has its own limited resolution (spatial and/or temporal), making it sensitive only to a certain portion of the gravity wave spectrum (see *Preusse et al.* [2008]; *Alexander and et. al.* [2010]). Second, each observational platform has limitations in terms of spatial and/or temporal coverage. For instance, high-resolution radiosondes describe *in situ* gravity waves with low frequencies and with vertical wavelengths of a few kilometers, but each station only samples one location and with a limited frequency. In contrast, satellite observations can provide a nearly global coverage, but with limited spatial resolution and significant assumptions used in the process of converting, say, radiance anomalies to momentum fluxes.

Numerical simulations have also been used to explore the uncertainties in the current gravity-wave observing techniques. For example, *Zhang et al.* [2004] examined the uncertainties in the commonly used hodograph method in retrieving inertio-gravity wave characteristics from individual vertical profiles of the winds. Analysis of mesoscale numerical simulations of a gravity wave event in which a seeminly coherent quasi-monochromatic inertia-gravity wave packet showed that important uncertainties were found to exist for all the wave characteristics derived from single vertical profiles using the hodograph method. Large uncertainties were found in particular in estimating derived quantities such as horizontal wavelengths. Similar approaches can be performed to assess the uncertainties in the gravity wave observations by in-situ or remotely sensing instruments (reviewed in section 2). One such example is presented in *Wu and Zhang* [2004] which compared the mesoscale simulations of gravity waves with those derived from space-borne sense on AMSU (see Figure 6).

Observations have provided substantial evidence for the importance of jets and fronts as sources of gravity waves and case studies have identified flow configurations favorable to the presence of significant waves. Two limitations need to be mentionned: one is that observations identify where gravity waves are found, not necessarily where they are generated. Second, case studies may introduce a bias towards cases that lend themselves well to case studies, i.e. where conspicuous gravity waves (large amplitude, large enough scale and time span that the wave can be identified, say, in several radiosondes. . .) that can be well identified and interpreted. Generally, perturbations that occur on smaller scales, and in particular those that are tied to moist convection, prove more difficult to interpret beyond statistical approaches (e.g. *Fritts and Nastrom* [1992]; *Eckermann and Vincent* [1993]). Now, as described above a number of case studies have emphasized the possible role of moist processes in generating or amplifying waves near fronts. Gravity waves directly generated by convective cells will have clearly higher intrinsic frequencies (and shorter horizontal scales) than waves excited dynamically by jets and fronts. Nonetheless, clarifying the contribution of moist processes to waves in the vicinity of jets and fronts calls for dedicated research efforts.

A first challenge, that is presently being addressed given the maturity of observational gravity wave studies (in particular from satelites), will be to make the different analyses of the gravity wave field converge [*Alexander and et. al.*, 2010]. Comparisons of estimates from different satellites [*Ern and Preusse*, 2011], between satellites and analyses *Shutts and Vosper* [2011], or between mesoscale simulations and balloon observations *Plougonven et al.* [2012] provide indications on the biases of these different sources of information, and suggest that these different estimates may soon converge. A second challenge is to define and obtain a complete description of the useful characteristics of the gravity wave field: whereas mean momentum fluxes have very much been emphasized, they are not the only relevant quantity. For example, the intermittency of the wave field also matters, and this may be described through the probability distribution function of the momentum fluxes

[*Hertzog et al.*, 2012]. A final challenge will consist in extracting information on the wave sources from a combination of observations and simulations. Investigation of the gravity wave field relative to the flow (both the tropospheric flow which may act as a source, and the stratospheric flow which acts as a background) will be a path to help identify sources, going beyond geographical and seasonal variations.

Despite the availability of near continuous 4-dimensional model output, difference between different modeling studies of the same events highlight the difficulties in pinpointing the forcing and generation mechanisms. These difficulties have at least partially driven the need for more idealized simulations with simpler flow patterns, which will be described in section 6.

4. GENERATION MECHANISMS: ANALYTICAL RESULTS

This section and section 6 review theoretical studies of generation mechanisms that have been invoked to explain gravity waves in the vicinity of jets and fronts. The present section restricts mainly to analytical studies[5] and hence simple flow configurations, allowing asymptotic results. This section is complemented, in Section 6, by a review of studies for which laboratory or numerical experiments have been a necessary component, providing an examination of emission in more realistic flows.

The observational evidence for a strong enhancement of gravity waves in the vicinity of jet/front systems has been one motivation for investigations of dynamical mechanisms generating gravity waves from predominantly *balanced* features of the flow. Another fundamental motivation has been to identify the limitations of balanced approximations, i.e.

to determine when the evolution of the flow, while remaining predominantly balanced, includes the *spontaneous* generation of gravity waves.

The fundamental difficulty for the emission is the scale separation between the slow balanced motions and the fast gravity waves, making it difficult for both types of motions to interact. The Rossby number measures this separation of the time scales: balanced motions evolve on the advective time-scale L/U, whereas the longest time scale for gravity wave motions is $1/f$. Their ratio yields the Rossby number

$$Ro = \frac{U}{fL}, \tag{1}$$

which is typically small for mid-latitude flows. To a very good approximation, atmospheric and oceanic motions at small Rossby numbers are balanced, i.e. a diagnostic relation can be established between the wind and other variables. The simplest balance relation is geostrophic balance, but there are more accurate relations (e.g. *Hoskins et al.* [1985]; *Zhang et al.* [2000]). Additionnally, the flows considered in this review nearly all have aspect ratios justifying hydrostatic balance in the vertical (e.g. *Vallis* [2006]). These balances provide diagnostic relations which can reduce the number of time-derivatives in the system: balanced approximations such as quasi-geostrophy provide a simple description of the balanced flow, consisting of an inversion relation and a *single* prognostic equation, the advection of the materially conserved potential vorticity *Hoskins et al.* [1985]. Other motions, such as gravity waves, have been filtered out. Balanced models have provided much of our understanding of mid-latitude dynamics and are helpful for initialization issues in numerical weather forecasting (e.g. *Kalnay* [2003]). The occurence of gravity waves in the vicinity of jets and fronts constitutes a deviation from balance.

First we describe geostrophic adjustment, because it has very regularly been invoked (section 4.1). Studies of geostrophic adjustment address how an initial imbalance projects onto gravity waves, but not the origin of the imbalance. The discussion on the relevance of geostrophic adjustment in the present context is deferred to section 8.1. Next we describe explicit examples of spontaneous emission (or spontaneous adjustment emission, SAE), mechanisms explicitly addressing how balanced motions excite, in the course of their evolution, gravity waves: Lighthill radiation (section 4.2.2), unbalanced instabilities (section 4.3) and transient generation (section 4.4). Further studies of spontaneous emission, in more realistic flows, are discussed in section 6. Finally, generation mechanisms involving shear instability are discussed in section 4.5.

4.1. Geostrophic adjustment

Geostrophic adjustment occurs when a rotating fluid is forced away from a balanced state on timescales that are short relative to the inertial timescale. The process forcing the fluid away from balance need not be specified: for example a wind burst forcing the upper ocean [*Rossby*, 1938], heating due to convection [*Schubert et al.*, 1980], an absorbed gravity wave [*Zhu and Holton*, 1987], or mixing due to shear instabilities [*Bühler et al.*, 1999]. It only matters that this forcing be fast relative to the inertial timescale, so that it can be considered instantaneous, yielding the classical initial value problem. More generally, this is only a special case of the adjustment to a time-dependent local body forcing [*Weglarz and Lin*, 1997; *Chagnon and Bannon*, 2005a]. Below, we reserve the term 'geostrophic adjustment' for the classical initial value problem with geostrophy as the underlying balance.

The classical problem of geostrophic adjustment describes how an arbitrary initial condition, in a rotating fluid subject to gravity, splits into a geostrophically balanced part that remains and inertia-gravity waves which propagate away [*Rossby*, 1938; *Cahn*, 1945; *Obukhov*, 1949]. *Rossby* [1938] considered as an initial condition a rectilinear current in the upper layer of the ocean, with limited horizontal extent and with no surface height anomaly. Hence the initial current is out of balance and the fluid adjusts so as to find a state in which velocity and pressure (here surface height) are in geostrophic balance and which preserve the potential vorticity and mass realtive to the initial state. The excess energy contained in the initial condition is shed off, in the form of inertia-gravity waves that propagate away.

Studies on geostrophic adjustment have focused on configurations for which the problem is well-posed:

1. if all motions are small perturbations to a state of rest, the adjustment can be described asymptotically in Rossby number [*Blumen*, 1972]. To leading order, the balanced part of the flow is described by quasi-geostrophic dynamics for Burger number of order unity [*Reznik et al.*, 2001].

2. if the flow is rectilinear or axisymmetric, the separation is again unambiguous because the balanced part of the flow, even for large Rossby numbers, has a trivial time evolution: it is stationary. Adjustment has been investigated for purely zonal flows (e.g. *Rossby* [1938]; *Yeh* [1949]; *Ou* [1984]; *Kuo and Polvani* [1997]; *Kuo* [1997]; *Zeitlin et al.* [2003]) and axisymmetric flows (e.g. *Paegle* [1978]; *Schubert et al.* [1980]; *Kuo and Polvani* [2000]). In both cases, the unambiguous separation made it possible to describe analyt-

ically nonlinear adjustment (e.g. *Glendening* [1993]; *Blumen and Wu* [1995]; *Wu and Blumen* [1995]; *Plougonven and Zeitlin* [2005]).

Note that in both cases, the initial imbalance is prescribed. The origin of this imbalance lies outside the scope of these studies. They only describe the response of the fluid, in certain limited configurations (small perturbations to a state of rest (1), or symmetric flows (2)).

Numerous aspects of the geostrophic adjustment problem have been studied, e.g. the dependence of the response to the scale of the initial perturbation (e.g. *Matsumoto* [1961]; *Blumen and Wu* [1995]; *Kuo* [1997]), or the interpretation of geostrophic adjustment as a minimization of energy for a given potential vorticity distribution [*Vallis*, 1992]. With the emission from jets in mind, *Fritts and Luo* [1992] have considered, in a stratified fluid at rest, initial imbalances having dimensions comparable with those of a jet stream. They found emitted waves that have low frequencies, consistent with the dispersion relation and the spatial scales of the prescribed imbalance. Their first, two-dimensional study was complemented by consideration of three-dimensional imbalances having long scales in the along-jet direction *Luo and Fritts* [1993].

In all of the examples above, the gravity waves originate from the initial, prescribed imbalance, and hence these examples provide little insight into generation from balanced motions. The geostrophic adjustment problem was in fact used to investigate the interactions of gravity waves and balanced motions: in the first several orders of the asymptotic theory, *Reznik et al.* [2001] showed a complete decoupling of the balanced motions and gravity waves (see also *Dewar and Killworth* [1995]), yielding an unambiguous separation, and hence no spontaneous emission [*Zeitlin*, 2008].

Now, various diagnostics of flow imbalance, as surveyed in *Zhang et al.* [2000], have been widely and successfully used to identify the sources of gravity waves with respect to the balanced flow (e.g., *O'Sullivan and Dunkerton* [1995]; *Jin* [1997]; *Zhang et al.* [2001]). In consequence, 'geostrophic adjustement' has very often been referred to explain emitted waves near jets and fronts (e.g. *O'Sullivan and Dunkerton* [1995]). In a related study of an idealized baroclinic life cycle, and in order to emphasize the differences with classical geostrophic adjustment, *Zhang* [2004] proposed the term *balanced adjustment*[6] to describe the spontaneous generation of gravity waves from a predominantly balanced flow that continuously produces imbalance (as can be diagnosed from the residual of the nonlinear balance equation for example), with an associated, continuous emission of gravity waves. The investigation of this mechanism relies heavily on numerical simulations and will be described in section 6.

4.2. Lighthill radiation

It is preferable to briefly recall the context in order to understand the change in paradigm between the previous section and the present one.

4.2.1. A foreword on slow manifolds

The atmosphere and oceans are and remain so close to a balanced state on synoptic scales that the existence of a *slow manifold* [*Lorenz*, 1980; *Leith*, 1980] was suggested and investigated: within the phase space of the full equations, this would be an invariant subspace of reduced dimensionality containing only balanced dynamics (for more general definitions, see discussions in *Warn et al.* [1995] and *Ford et al.* [2000]). Investigating whether such a manifold exists is equivalent to investigating whether motions that are at one initial time purely balanced (or more precisely on the slow manifold) can produce, in the course of their evolution, unbalanced motions, i.e. gravity waves.

Several lines of evidence have progressively shown that such emission is inevitable, i.e. that an exactly invariant slow manifold in fact does not exist and that one should rather think slow manifolds of various accuracies (*MacKay* [2004]; *Vanneste* [2013] and references therein). One line of evidence came from low-order models such as the Lorenz-Krishnamurty model [*Lorenz*, 1986; *Lorenz and Krishnamurty*, 1987] describing with 5 Ordinary Differential Equations (ODEs) the interactions of 3 slow vortical modes and 2 fast gravity wave modes[7]. The divergence of perturbative procedures [*Vautard and Legras*, 1986; *Warn and Ménard*, 1986], numerical simulations [*Lorenz and Krishnamurty*, 1987; *Camassa*, 1995; *Bokhove and Shepherd*, 1996], and exponential asymptotics *Vanneste* [2004] have demonstrated the spontaneous generation of fast motions is inevitable(Figure 7). *Vanneste* [2004] has explicitly quantified the emission in this model as exponentially small in Rossby number, i.e. of a form involving $e^{-\alpha/Ro}$, with a prefactor that involves algebraic powers of the Rossby number Ro.

A second line of evidence comes from mechanisms of spontaneous emission identified in full flows, i.e. described by a system of Partial Differential Equations. The first is Lighthill radiation, and constitutes an explicit example of spontaneous generation (section 4.2.2). Two other mechanisms of SAE are unbalanced instabilities (section 4.3) and transient generation in shear (section 4.4).

4.2.2. Lighthill radiation

'Lighthill radiation' of gravity wave motions by balanced vortical motions [*Ford*, 1994a, b, c] is analogous to the radiation of acoustic waves by turbulent vortical motions described by *Lighthill* [1952]. The analogy is straightforward for the non-rotating shallow water equations which are equivalent to the two-dimensional equations for gas dynamics, with gravity waves replacing acoustic waves, and the Froude number $F = U/\sqrt{gH}$ replacing the Mach number $M = U/c_s$, where c_s is the sound speed. The inclusion of rotation inhibits the emission of waves, as frequency matching between the vortical motion and the inertia-gravity waves only occurs for $Ro > 1$ [*Ford*, 1994a]. The smallness F allows asymptotic investigation of the problem, and has an essential implication regarding the scale of the waves: the excited gravity waves having frequencies matching those of the balanced motions, of order U/L, the dispersion relation for shallow water waves imposes that they have spatial scales $\lambda \sim L/F >> L$. Hence there is a scale separation between the small balanced motions and the large-scale gravity waves that are emitted.

Many aspects of the emission can be summarized by rearranging the equations of motions in such a way as to obtain a wave equation on the left-hand side (lhs), forced by nonlinear terms on the right-hand side (rhs) *Ford* [1994c]; *Ford et al.* [2000]:

$$\left(\frac{\partial^2}{\partial t^2} + f^2 - g\,h_0\nabla^2\right)\frac{\partial h}{\partial t} = \frac{\partial^2}{\partial x_i \partial x_j}T_{ij}\,, \qquad (2)$$

where h is the height of the surface, h_0 is the height at rest, f is the Coriolis parameter and T_{ij} result from the combination of the nonlinear terms of the equations. In itself, this rearrangement does not prove anything [*Snyder et al.*, 1993; *Plougonven et al.*, 2009]. When one adds assumptions on the regime parameter, as above ($Ro > 1, F << 1$), one deals with Lighthill radiation: as the waves are large-scale and as the small-scale balanced motions are supposed to occur only in a compact region, it is appropriate to consider that the waves are propagating on the background of a fluid at rest and that the forcing is a point, quadrupolar source. The quadrupolar nature of the forcing implies, in this setting, significant destructive interferences and hence weak emission (order F^2, [*Ford et al.*, 2000]).

As *Ford et al.* [2000, 2002] emphasized, one key feature of Lighthill radiation were that the emission is weak enough that the source can be described without taking the emission into account, e.g. from a balanced model. The lhs of (2) being the standard equation for gravity waves for a fluid at rest, standard intuitions apply: for example, Fourier transforms [*Ford*, 1994c] can be used to isolate the part of the rhs forcing that produce gravity waves (frequencies larges than f). Matched asymptotic expansions or Green's functions can be used to solve the forced problem [*Ford*, 1994a, b; *Ford et al.*, 2000]. Gravity wave emission by balanced motions was investigated in rotating shallow water for unstable modes of axisymmetric vortices [*Ford*, 1994a], for the emission by an elliptic vortex [*Ford*, 1994b], for arbitrary localized balanced motions [*Ford et al.*, 2000] and for the roll-up of an unstable shear layer [*Ford*, 1994c]. In the latter case, numerical simulations were used to describe the small-scale vortical motions, and knowledge of the resulting forcing, averaged in the streamwise direction, was successfully used to predict the large-scale inertia-gravity waves in the far field (see Figure 8).

The analysis of Lighthill radiation was extended to a continuously stratified fluid for the emission by an ellipsoidal vortex [*Plougonven and Zeitlin*, 2002]. The radiative instability of an axisymmetric vortex [*Ford*, 1994a] and the evolution of the elliptic vortex [*Ford*, 1994b; *Plougonven and Zeitlin*, 2002] can be interpreted as a coupling of Rossby waves on the PV gradient on the edge of the vortex [*Brunet and Montgomery*, 2002] with inertia-gravity waves in the far-field. The emitted waves are found to scale as F^2, and hence the backreaction on the vortical motions only occur on very slow timescales (F^{-4}).

Rankine vortices were used for the above studies, for analytical tractability. In more realistic cases, when the vortices have a continuous distribution of PV, mixing at a critical level in the skirt of the vortex may inhibit the growth of these radiative instabilities [*Schecter and Montgomery*, 2006]. The regime of parameters for Lighthill radiation make it relevant for strong supercell mesoscylcones and hurricanes (*Schecter* [2008] and ref. therein).

The study of Lighthill radiation was recently extended with numerical experiments to carry out a systematic parameter sweep [*Sugimoto et al.*, 2008], and also to spherical geometry *Sugimoto and Ishii* [2012].

4.3. Unbalanced instabilities

Unbalanced instabilities (also called non-geostrophic or ageostrophic instabilities) are instabilities of a balanced flow that involve unbalanced motions, typically gravity waves. These constitute a mechanism for spontaneous emission, provided that there is an initial deviation, however small, from the balanced flow under consideration [*Vanneste*, 2008].

A flow for which unbalanced instabilities have received considerable attention is an unbounded vertical shear above a flat surface. The quasi-geostrophic solution of *Eady* [1949] was extended beyond the Eady cutoff by *Stone* [1970] and *Tokioka* [1970], independently. The spatial structure of the modes they obtained was elucidated by *Nakamura* [1988], who showed that the modes changed character through the inertial-critical level (ICL) present in the flow. At the ICL, the Doppler shifted wave period is equal to the inertial period. The stability analysis was extended to nonzero meridional wavenumber l by *Yamazaki and Peltier* [2001a, b]. The growth rates of these modes [*Molemaker et al.*, 2005] and the spatial structure [*Plougonven et al.*, 2005] were both revisited recently. The unstable modes consist of an Eady edge wave between the ground and the ICL, and of sheared gravity waves above (see Figure 9). A WKBJ approximation can give an accurate description of the normal mode, including its exponentially small growth rate (Vanneste, personal communication).

Unbalanced instabilities can involve different types of waves, from IGW (e.g. *Plougonven et al.* [2005]) to Kelvin waves (e.g. *Kushner et al.* [1998]), and have been identified in different flows: two layer sheared flow [*Sakai*, 1989], sheared flow over a slope [*Sutyrin*, 2007, 2008], horizontal shear [*Vanneste and Yavneh*, 2007], stratified Taylor-Couette flow [*Yavneh et al.*, 2001; *Molemaker et al.*, 2001], vortices [*LeDizès and Billant*, 2009], a front of potential vorticity [*Dritschel and Vanneste*, 2006], elliptical instability *McWilliams and Yavneh* [1998]; *Aspden and Vanneste* [2009].

A strong motivation for the study of these various unbalanced instabilities has come from the suspicion that they play a significant role in the ocean interior (see section 7.4), in the forward cascade necessary to transfer energy from the anisotropic, balanced large-scale flow down to more nearly isotropic flows leading to dissipation [*McWilliams et al.*, 2001].

Another motivation has been to better understand the dynamics of two-layer systems encountered in laboratory experiments (see section 6.1). Instabilities coupling a Rossby wave and a Kelvin wave in a two-layer rotating fluid were recently revisited with an emphasis on their nonlinear development [*Gula et al.*, 2009a]. Simulations suggested that the instability saturated early on, leaving behind only a limited signature of gravity waves. Recently, careful laboratory experiments (see Section 6.1) have provided the first evidence of these instabilities in real flows, and confirmed the weakness of their growth.

The stability study of realistic (continuous) frontal states [*Snyder*, 1995] also provides evidence for the weakness of unbalanced instabilities.

4.4. Transient generation by sheared disturbances

The evolution of potential vorticity anomalies in a horizontal shear [*Vanneste and Yavneh*, 2004] leads to a transient generation of gravity waves. This differs from the unbalanced instabilities described above in several respects: **1)** the generation of gravity waves occurs at a specific time; **2)** the final amplitude of the waves can be predicted within the linear theory[8], and **3)** it is not necessary to include, in the initial condition, a small perturbation *Vanneste* [2008]. *Vanneste and Yavneh* [2004] quantified the emission of gravity waves for a sheared disturbance at one along-shear wavenumber, and demonstrated that the final amplitude of the waves is proportional to

$$\varepsilon^{-1/2} \exp(-\alpha/\varepsilon)$$

. As for the spontaneous generation in the Lorenz-Krishnamurty model *Vanneste* [2004], exponential asymptotics were necessary to describe this exponentially weak emission. The solutions obtained for one wavenumber can be combined (as a Fourier decomposition) to describe the emission by localized features of the flow such as a sheared vortex [*Olafsdottir et al.*, 2008].

The transient generation of sheared potential vorticity anomalies in a vertical shear was calculated by *Lott et al.* [2010] for 2D and *Lott et al.* [2012b] for 3D anomalies. These two studies illustrate transient emission in a vertical shear, and hence can be read as a vertical counterpart of *Olafsdottir et al.* [2008]. However, they are based on a modal (Fourier) decomposition, and hence can be read as a counterpart of *Plougonven et al.* [2005] without a surface. The same equation for the vertical structure of modes is solved in both cases, what differs are the boundary conditions, leading to unstable modes when a lower boundary is present, and neutral modes when no boundary is present but a Dirac-δ PV anomaly is included. Physically, the key process in both cases is the coupling, by differential advection, of balanced motions and gravity waves, on one and the other side of an inertial critical level (ICL). Despite this commonality, the results on shear disturbances [*Vanneste and Yavneh*, 2004] appear very different from those on unbalanced instabilities in the same flow [*Vanneste and Yavneh*, 2007]. This is in part due to the different approaches used, i.e. nonmodal versus modal. The relationships between the different approaches, in a vertical shear, are discussed by *Mamatsashvili et al.* [2010].

This highlitghts the connections between the different mechanisms of spontaneous emission. Both unbalanced instabilities and transient emission fundamentally rely on shear to connect motions that have different intrinsic timescales.

The transient emission of gravity waves by sheared regions have been investigated also in different contexts, to determine what gravity wave response could be expected from a stochastically perturbed shear layer or jet [*Lott*, 1997; *Bakas and Farrell*, 2008, 2009a, b]. Investigation of momentum transport by gravity waves in a stochastically forced jet has shown for instance that the jet not only passively filters waves, but also amplifies portions of the spectrum, leading to possibly significant decelerations.

4.5. Shear Instability

Another possible route for the excitation of GWs from jets and fronts involves shear instablities on small scales[9]. In the course of frontogenesis, both near the surface and at upper-levels, very intense shear layers are produced, potentially leading to shear instability (e.g. *Snyder* [1995]; *Esler and Polvani* [2004]). As such, this constitues a mechanism for spontaneous emission; however, the scales of shear instability are short enough that it has generally been considered in non-rotating flow, and is not discussed in the literature on spontaneous emission.

Over the past four decades, several candidate mechanisms have been investigated by which shear instabilities excite gravity waves , in a direct or indirect way, in a linear or nonlinear framework. One essential difficulty here lies in the range of scales involved, from tens of meters for the turbulence initiated from the instabbility of a shear layer to thousands of kilometers for the baroclinic instability setting the environmental shear and modulating the background stratification.

The first investigations of possible mechanisms focused on the linear stability analysis of an atmospheric shear layer. The aim was to determine whether unstable modes exist that comprise a radiating GW above the shear layer or a jet [*Lalas and Einaudi*, 1976; *Lalas et al.*, 1976; *Mastrantonio et al.*, 1976]. Although such unstable modes do exist, their growth rates are always considerably smaller than those of KH instability [*Fritts*, 1980]. The latter always occurs on small scales such that their signature above and below the shear layer is evanescent. *McIntyre and Weissman* [1978] point out a fundamental difficulty for shear instabilties to generate gravity waves: to couple propagating gravity waves above the shear layer, it is necessary that the (real part of the) phase speed, c, and the horizontal wavenumber, k, to verify the Phase Speed Condition: $U - N/k < c < U + N/k$, where U is the wind velocity, N is the Brunt-Väisälä frequency. For large values of k, the interval becomes very narrow and only evanescent responses are found in the layer above the shear.

Hence, both the findings of the linear studies and the Phase Speed Condition strongly suggested that generation from shear instabilities likely involved nonlinear mechanisms.

The first nonlinear mechanism to be investigated as a route to larger scales was vortex pairing [*Davis and Peltier*, 1979]. To obtain significantly larger scales, *Fritts* [1982, 1984] and *Chimonas and Grant* [1984] described the interaction of two KH modes having nearby wavenumbers, k and $k + \delta k$. These weak nonlinear interactions produce scales $2\pi/\delta k$, large enough to radiate gravity waves. This mecanism, called 'envelope radiation', has been further investigated by *Scinocca and Ford* [2000]. using direct numerical simulations of the 2D evolution of a region of unstable shear. They focused on the early stages of the instability (when the two-dimensionality is relevant) and on quantifying the momentum fluxes associated to envelope radiation. Going beyond the two-dimensional approximation *Tse et al.* [2003] simulated the three-dimensional turbulence in a forced, unstable jet. In a subsequent study, *Mahalov et al.* [2007] focused on the emission of gravity waves and confirmed their capacity to exert a significant drag on the flow emitting them.

The end effect of the shear instability will be to mix the fluid over the region where it developped. This mixing occurs over a short timescale relative to the inertial period, so the fluid is forced out of balance and will then undergo geostrophic adjustment to recover a balanced state, and emit inertia-gravity waves in the process *Bühler et al.* [1999]. *Bühler and McIntyre* [1999], who calculated the subsequent propagation of the emitted waves in a mean wind profile representative of the summer stratosphere. They concluded that the contribution of this source could not safely be neglected in the global angular momentum budget.

The above studies focused on shear layers in a fluid having constant Brunt-Väisälä frequency. Another possibility consists in having variations of the stratification leading to either propagating wave instabilities [*Lott et al.*, 1992; *Sutherland*, 2006] or to a coupling of the shear instability to upward propagating waves [*Sutherland et al.*, 1994; *Sutherland and Peltier*, 1995]. This may be relevant as the upper-tropospheric jet-stream is indeed just below the tropopause and its sharp jump in stratification [*Gettelman et al.*, 2011].

In summary, theoretical and numerical studies support the notion that gravity waves generated from shear instabilities need to be considered for middle atmospheric dynamics, but the complexity of the flows considered has hindered theoretical progress in quantifying them, while their small scales have made obsevrations difficult.

5. PROPAGATION AND MAINTENANCE

The framework of parameterizations and the resulting demand encourages one to think separately of the gravity wave sources and of their subsequent propagation (in a vertical column for parameterizations). Now, several mechanisms described above (unbalanced instabilities and transient generation, sections 4.3 and 4.4) precisely emphasize the key role played by a varying background wind for the appearance of the waves. In more complex flows (sections 3 and 6), studies of wave emission emphasize the importance of propagation effects. This motivates a pause in the review of generation mechanisms to briefly describe wave ducting, ray-tracing and wave-capture.

5.1. Ducted gravity waves

Ducting of gravity waves between the ground and a layer acting as a partial reflector has been modelled by *Lindzen and Tung* [1976]. It occurs when a stable layer is present near the ground, capped by a layer which efficiently reflects waves (e.g. of low stability, or conditionnally unstable, possibly beneath a critical level). The stable layer needs to be thick enough, and not to contain a critical level. Ducted waves, reflecting off the ground and (partially) at the top of the layer, may travel significant distances in the horizontal, with energy leaking only slowly through the top of the duct. In consequence, such *'almost free'* waves [*Lindzen and Tung*, 1976] need only a weak forcing to be present, and the geometry and stability of the duct selects some of their characteristics. One characteristic selected by the duct is the phase speed

$$C_D \sim \frac{N_D \mathcal{H}}{\pi \left(\frac{1}{2} + n \right)} , \quad n = 0, 1, 2, \ldots \tag{3}$$

where N_D is the Brunt-Väisälä frequency in the duct, and $\mathcal{H}$ its height. The tallest wave ($n = 0$) will be least damped, and is hence of greatest interest. This is a clear example of how the environment in which gravity waves are forced selects certain characteristics of the waves, making it in practice more important to know the duct rather than the details of the forcing.

The relevance of ducting has been shown by numerous case studies focusing on lower-tropospheric waves in the vicinity of surface fronts (e.g. *Eom* [1975]; *Bluestein and Jain* [1985]; *Parsons and Hobbs* [1983]; *Uccelini and Koch* [1987]; *Nicholls et al.* [1991]; *Powers and Reed* [1993]; *Zhang and Koch* [2000]; *Zhang et al.* [2003]). Ducted gravity waves are found propagating ahead of cold fronts, and on smaller-scales ahead of gust fronts *Knupp* [2006], and can play a significant role in triggering convection. The complex interaction between ducted gravity waves and moist convection that maintains and amplifies the mesoscale waves is also referred to "ducted wave-CISK" model [*Powers*, 1997; *Zhang et al.*, 2001]. Other mechanisms leading to maintenance of gravity waves, e.g. solitary wave dynamics [*Lin and Goff*, 1988], lie beyond the scope of the present paper and will not be discussed.

5.2. Ray-tracing

A common approach to investigate the propagation of gravity waves in complex flows has been the use of ray-tracing, which we briefly recall below (see *Lighthill* [1978] or *Bühler* [2009] for a complete discussion, and *Aspden and Vanneste* [2010] for an alternative derivation). It has typically been used in case studies to identify the origin of observed waves [*Guest et al.*, 2000; *Hertzog et al.*, 2001], and in idealized simulations to identify sources and follow emitted waves [*Lin and Zhang*, 2008; *Wang and Zhang*, 2010]. Many of these studies use the ray-tracing software package developed in *Eckermann and Marks* [1996, 1997] with various complex background flows.

Consider a wave-packet described by

$$u(\mathbf{x},t) = A(\mathbf{x},t)\, e^{i\,\theta(\mathbf{x},t} \tag{4}$$

for the x-component of the velocity, with A a slowly changing amplitude and θ a fast-varying phase. The local wavevector and frequency are defined by $\mathbf{k}(\mathbf{x},t) = \nabla\theta$ and $\omega(\mathbf{x},t) = -\theta_t$, where the subscript is used to denote partial derivation. They vary slowly (as A and the background flow), and are assumed to locally satisfy the dispersion relation:

$$\omega = \Omega(\mathbf{k}(\mathbf{x},t),\mathbf{x},t) = \hat{\Omega} + \mathbf{U}\,\mathbf{k}\ , \tag{5}$$

with ω the absolute frequency and $\hat{\Omega}(\mathbf{k},\mathbf{x},t)$ the appropriate dispersion relation.

Now, cross-differentiating the definitions of $\mathbf{k}$ and ω we can obtain $\mathbf{k}_t + \nabla\omega = 0$. Substitution into (5), using the chain rule and the fact that $\nabla \times \mathbf{k} = 0$ yields:

$$\frac{d\mathbf{x}}{dt} = \frac{\partial\Omega}{\partial\mathbf{k}} \quad \text{and} \quad \frac{d\mathbf{k}}{dt} = -\frac{\partial\Omega}{\partial\mathbf{x}} \tag{6}$$

where

$$\frac{d}{dt} = \frac{\partial}{\partial t} + (\mathbf{U} + \hat{\mathbf{c}}_g)\cdot\nabla \quad \text{and} \quad \hat{\mathbf{c}}_g = \frac{\partial\hat{\Omega}}{\partial\mathbf{k}}.$$

An additional equation, generally for the conservation of wave action $A = E/\hat{\omega}$, with E the energy of the wave, is necessary to follow the evolution of the amplitude of the wave-packet *Bühler* [2009].

5.3. Wave capture

Ray-tracing allows to investigate, with simple considerations, how jet exit region may have a specific effect on inertia-gravity waves. In studies that have emphasized jet exit regions as particularly favorable to the occurrence of large-amplitude gravity waves, it has often been assumed, implicitly, that waves were large because they were generated there. This overlooks another possibility of interest: that jet exit regions have a particular significance for gravity waves not only for generation, but also for propagation.

Case studies have highlighted a specific region within the jet, where the flow decelerates and the streamlines are diffluent. The effect of such a background flow on wave packets propagating through them has been emphasized in theoretical studies as 'wave-capture' [*Badulin and Shrira*, 1993; *Bühler and McIntyre*, 2005]). The combination of strong deformation and vertical shear can lead to the contraction of the wave packet to smaller and smaller scales, until dissipation occurs, without having the intrinsic frequency tending to either bound of the GW frequency spectrum.

Quantifying this effect introduces new possible interactions between waves and mean flows [*Bühler and McIntyre*, 2003, 2005], but requires to take into consideration horizontal variations of the background flow, i.e. to consider propagation in $\mathbf{U}(x, y, z)$. This is in contrast to the columnar approximation made for parameterizations (where only $\mathbf{U}(z)$ is considered), and which is encouraged by parallel computing.

For a low-frequency wave packet of sub-synoptic scale, the group velocity is small[10]. This warrants an analogy [*Bühler*, 2009] between the evolution equation for the wavevector and for the evolution of the gradient of a passive, conserved tracer ϕ, respectively:

$$\frac{d\mathbf{k}}{dt} = -(\nabla\mathbf{U})\cdot\mathbf{k} \quad \text{and} \quad \frac{D\nabla\phi}{Dt} = -(\nabla\mathbf{U})\cdot\nabla\phi\ , \tag{7}$$

the two equations differing in their operators on the lhs by

$$\frac{d}{dt} - \frac{D}{Dt} = \hat{\mathbf{c}}_g\cdot\nabla\ .$$

Now, assuming the background flow to be layerwise non-divergent, $\mathbf{U} = (U, V, 0)$, with $U_x + V_y = 0$, which is relevant as a leading-order description of the background balanced flow, the evolution of the advected tracer gradient is governed by the sign of

$$D = -U_x\,V_y + V_x\,U_y \tag{8}$$

$$= \tfrac{1}{4}\left((U_x - V_y)^2 + (V_x + U_y)^2 - (V_x - U_y)^2\right)\ . \tag{9}$$

The first two terms on the rhs of (9) constitute the strain [*Batchelor*, 1967], and the last is the vertical component of the relative vorticity. D is also referred to as the Okubo-Weiss parameter and extensively discussed in studies of tracer advection (e.g. *Lapeyre et al.* [1999] and refs. therein).

If the wavepacket remains where the strain dominates ($D > 0$), the wavenumber experiences exponential growth (see *Bühler* [2009], section 14.3). As a simple example, consider a pure deformation flow with extension along the y-axis, with vertical shear: $U = -\alpha x + \beta z$ and $V = \alpha y + \gamma z$. Equation 7 then yields $k = k_0 e^{\alpha t}$, $l = l_0 e^{-\alpha t}$ and $m \to -\alpha^{-1}\beta\, k(t)$ as $t \to +\infty$. Asymptotically, the wavevector will tend to

$$(k, l, m) \to k_0\, e^{\alpha t} \left(1,\, 0,\, \frac{U_z}{U_x}\right)$$

for $t \to \infty$, and with k_0 the initial value of wavenumber k. More generally, the above considers the action of only one region of strain on a wavepacket. As a packet moves within the flow (by advection and by its own propagation), it may encounter different regions of strain, and *Aspden and Vanneste* [2010] show that this will lead to growth of the wavenumber, as for tracer gradients [*Haynes and Anglade*, 1997].

We emphasize two implications: first, in jet exit regions, deformation and shear are large. For wave packets that have a long enough residence time in such regions, propagation effects will favor certain orientation and intrinsic frequency, with little sensitivity to the initial condition, and contraction of the wavelength. Second, this is only an asymptotic result, neglecting spatial variations of the background shear and strain. Its efficiency will depend on the residence time of the wave packet in the jet exit region. This effect has been named 'wave-capture', because the asymptotic calculation suggests contraction of the wavelength down to dissipation. In practice, it may be that capture is only partially realized, but this effect will nonetheless constrain wave characteristics, and the term wave-capture will be used to designate this influence.

6. GENERATION MECHANISMS: LABORATORY AND MODELLING EXPERIMENTS

There is a certain discrepancy between the simplicity necessary for analytical studies, e.g. plane-parallel unbounded shears (sections 4.3-4.4), and the complex, three-dimensional flow patterns highlighted in observations, e.g. jet exit regions (section 3). Laboratory experiments (section 6.1) and idealized simulations (sections 6.2-6.5) have provided a realm for exploring spontaneous emission in flows of intermediate complexity, bridging the two, and establishing a convincing sketch of the generation mechanism involved near jet exit regions.

6.1. Laboratory experiments

Laboratory experiments provide valuable examples of *real* flows, in which a fundamental dynamical mechanism may be identified, and to some extent isolated. Understanding these experiments can greatly enhance our understanding of the atmosphere and ocean, provided the mechanisms at play are the same.

Several experiments have been reported as exhibiting spontaneous generation of gravity waves in stratified fluids, mainly in a rotating annulus, either thermally or shear-driven, but also in other configurations.

A classical laboratory experiment of baroclinic instability has focused on a shear-driven fluid in a rotating annulus [*Hart*, 1972]. For such a configuration, with two immiscible fluid layers having each an aspect ratio of 2 (height / width), *Lovegrove et al.* [2000] and *Williams et al.* [2005] reported the appearance of inertia-gravity waves in a flow dominated by baroclinic instability. The flow is investigated from measurements of the interface height. In a regime dominated by large scale baroclinic waves (wavenumber 2), small-scale features (wavenumber between 30 and 40, *Williams et al.* [2008]) occur which are interpreted as inertia-gravity waves. The amplitude is estimated, in the range

$0.05 < Ro < 0.14$, to vary linearly with Rossby number [*Williams et al.*, 2008]. The generation mechanism was argued by *Williams et al.* [2005] to be Lighthill radiation, because the 'forcing terms' (as in equation (2) [*Ford et al.*, 2000] and assuming shallow water) are colocated with the gravity waves. However, given that the flow regime ($Ro \ll 1$, and not shallow water) and the scale separation (small-scale waves) differ so completely from those for Lighthill radiation, and that the amplitude varies linearly although the hypothesized forcing is quadratic, one may say that the generation mechanism remains to be explained.

A similar experiment has recently been carried out by *Scolan et al.* [2011], but with a salt stratification including a sharp transition rather than immiscible fluids, and with an aspect ratio (~ 0.2) compatible with a shallow water interpretation. Interpretation is supported by the complete stability analysis for two-layer shallow water sheared flows in an annulus obtained by *Gula et al.* [2009b], which includes an *unbalanced instability* (Rossby-Kelvin, see Section 4.3). *Scolan et al.* [2011] identify this unbalanced instability, for the first time in laboratory experiments. They also find that small-scale perturbations are present in many regimes of parameters. These small-scale features are argued in many cases to result from Hölmböe instability (e.g. *Lawrence et al.* [1991]). This instability occurs when a sharp density interface is colocated with a thicker shear layer, and is hence particularly relevant for the experiments with immiscible fluids of *Williams et al.* [2005].

Thermally-driven annulus experiments have also reported small-scale features [*Read*, 1992] which could be gravity waves. Numerical simulations have proved necessary to confirm this [*Jacoby et al.*, 2011], and have further identified an instability of the lateral boundary layer as the generation mechanism. Its location in azimuth remains unexplained, but is likely tied to be the separation of the large-scale geostrophic jet from the inner boundary. This example, and the reinterpretation of the 'waves' investigated by *Williams et al.* [2005] as Hölmböe instability *Scolan et al.* [2011], emphasizes the importance of boundary or interfacial layers in such laboratory experiments, making it more difficult to relate these results to atmospheric or oceanic flows.

Another unbalanced instability has been identified in laboratory experiments: *Riedinger et al.* [2010a] have analyzed the radiative instabilities of axisymmetric, columnar vortices in non-rotating, stratified fluid. The radiative instability of the flow around a rotating cylinder has been described theoretically and very clearly displayed in experiments *Riedinger et al.* [2011]. The robust agreement between theory and experiments in this somewhat contrived configuration makes the (difficult) experimental identification [*Riedinger et al.*, 2010b] of the radiative instability of a columnar vortex all the more convincing. Remarkably, this is the first laboratory evidence of an unbalanced, radiative instability.

Spontaneous emission was also investigated during the collision and rearrangement of two dipoles in the interior of a two-layer, non-rotating fluid [*Afanasyev*, 2003]. The experiments confirmed the radiation of interfacial gravity waves, occuring when fluid parcels underwent strong accelerations, such that the spatial scale and the Lagrangian timescale matched the dispersion relation.

Perhaps the clearest experimental evidence of spontaneous emission was provided by study of an unstable coastal jet in a two-layer fluid [*Afanasyev et al.*, 2008]. A clever visualisation technique (Altimetric Imaging Velocimetry, *Rhines et al.* [2006]) allowed to detect and quantify precisely the waves emitted, and to describe with a very high resolution the vortical flow emitting the waves. A notable difference relative to other studies on spontaneous generation is that the emitted waves are inertial waves in the unstratified lower layer, hence not constrained by $\hat{\omega} \geq f$. Waves were radiated away from the meanders of the baroclinic instability when the deformation radius was short enough that the characteristics of the meanders matched the dispersion relationship for the inertial waves, see Fig. 10. In experiments with larger deformation radius, single events of emission could be isolated, emphasizing regions of strong curvatures and large accelerations. Emitted waves represented only a small fraction, about 0.5%, of the total energy of the flow.

6.2. Early Simulations

The numerical study of geostrophic adjustment of a jet streak by *Tuyl and Young* [1982] deserves to be highlighted because they identified several essential issues which, although simple, have sometimes been overlooked thereafter. They simulated, in a two-layer model, the adjustment of perturbations added to a jet streak and emphasize how the background flow crucuially changes the adjustment and the wave dynamics. They give three reasons why traditional approaches (more specifically, the normal mode techniques of *Machenhauer* [1977]; *Baer and Tribbia* [1977]) fail to separate gravity waves and balanced motions in the vicinity of jet streaks: *1) the gravity-inertia modes are eigenfunctions for a base state of rest, rather than a sheared, time-dependent jet; 2) the methods may not work for strong accelerations (Rossby number of order unity (...)); and 3) the frequency separation has been based upon Eulerian (fixed frame) frequencies, rather than Lagrangian (Doppler shifted) ones,'* (*Tuyl and Young* [1982], p 2039). Indeed, points 1 and 3 underlie the spontaneous generation of gravity waves in a shear (sections 4.3 and 4.4), and point 2 is an ingredient of Lighthill radiation.

The simulations of *Tuyl and Young* [1982] may be regarded as an early prototypes of the recent dipole experiments (section 6.5). With anticipation, they suggest that gravity wave modes near jet streaks, although usually discarded as meteorologcal noise, *'may eventually show their more persistent members to be a complex part of the jet streak signal* (p 2038).

6.3. Two-dimensional frontogenesis

Early numerical experiments of spontaneous generation described two-dimensional frontogenesis. This is understandable for two reasons: physically, fronts are regions of the flow where short scales are produced (collapse to a near-discontinuity in a finite time [*Hoskins and Bretherton*, 1972] and large velocities are encountered. Practically, major features of frontogenesis can be understood in a two-dimensional framework [*Hoskins*, 1982], which greatly simplifies the problem and made it possible to attain higher resolutions. Although frontogenesis has sometimes been considered as an *adjusmtent* (e.g. *Kalashnik* [1998, 2000]), it is a specific process, central to mid-latitude dynamics, and deserves its own discussion, distinct from that of geostrophic adjustment (section 4.1).

A first study of gravity waves emitted by fronts was carried out with a mostly analytical approach by *Ley and Peltier* [1978]. They calculated the far-field gravity wave response to a frontogenesis event modeled by SG, assuming the background to be at rest when calculating the gravity wave response. Subsequent studies explicitly simulated the frontal collapse with different numerical methods [*Gall et al.*, 1987, 1988], including a Lagrangian description [*Garner*, 1989], with contradictory results regarding gravity waves. *Snyder* *et al.* [1993] showed that some of the excited waves were spurious, due to poor initialization and an inconsistency between the aspect ratio of the grid ($\Delta z/\Delta x$) and of the frontal slope yielding spurious waves [*Lindzen and Fox-Rabinowitz*, 1989].

Snyder et al. [1993] simulated both inviscid frontogenesis prior to frontal collapse, and postcollapse frontogenesis with horizontal diffusion, with frontogenesis forced by either deformation or shear. They used a nonhydrostatic model and their domain was bounded in the vertical by a flat surface and a rigid lid. Significant gravity waves, i.e. dominating other corrections to semi-geostrophy, are emitted when the frontogenesis is sufficiently intense, and are most prominent in the postcollapse solutions, above the surface front. Emission occured when the advective time-scale, which decreases as frontogenesis proceeds and the cross-frontal scale shrinks, became comparable to or shorter than the inertial period. This emission was explained as the linear response, in the frontogenetical background flow, to the cross-front accelerations neglected by semi-geostrophy.

More realistic simulations focused on gravity waves generation were carried out by *Griffiths and Reeder* [1996], who considered a domain including a stratosphere. Three cases of deformation frontogenesis were simulated: without, with negative and with positive vertical shear in the transverse direction (this transverse shear makes the large-scale frontogenetical forcing time-dependent). Emission of large-scale, low-frequency waves from the upper-level front and propagating up into the stratosphere was found in all three cases. Their comparison revealed that a determining factor for the amplitude of the emitted waves was the rapidity of the frontogenesis rather than its intensity (estimated by the maximum cyclonic vorticity). In other words, the emission is limited by the fact that the forcing (the transverse, frontogenetic circulation) poorly 'projects' on gravity wave modes. *Reeder and Griffiths* [1996] used ray-tracing to confirm the origin of the waves from the upper-level front, and its inital near-inertial frequency ($\hat{\omega} \sim 1.3\, f$). The emission was analyzed, with reference to Lighthill radiation *Ford* [1994c], as the linear response, *in a background flow consisting of the imposed deformation and transverse shear*, to the nonlinear terms from the frontal circulation. Linear forced simulations reproduced satisfactorily the emitted waves away from the fronts, whether using the full simulation or a balanced approximation to estimate these forcing terms. Crucially, the linear simulations include the background deformation and time-dependent shear, leading respectively to contracting wavelengths (from 1000 km to 500 km) and increasing vertical wavelength (from 3 km to 10 km). Inclusion of this background flow profoundly modifies the problem relative to Lighthill radiation (see section 6.5).

6.4. Idealized baroclinic life cycles

Idealized life cycles of baroclinic instability provide more realistic flows to investigate spontaneous emission, but requires significant computational resources as an additional spatial dimension is needed. *O'Sullivan and Dunkerton* [1995] simulated a baroclinic life cycle on the sphere (wavenumber 6, following *Simmons and Hoskins* [1978]) with a spectral truncation at wavenumber 126 (T126, approximately equivalent to a horizontal grid spacing of 1°). Inertia-gravity waves with intrinsic frequencies between f and $2f$ arose during the nonlinear stage of the development of the baroclinic wave, principally in the jet-stream exit region in the upper troposphere (see Figure 12). Surface fronts were shown not to be the source of these waves. They subsequently propagated horizontally within the jet, but only few IGWs penetrated the lower stratosphere. *O'Sullivan and Dunkerton* [1995] showed maps of the Lagrangian Rossby number with a large-scale maximum roughly coincident with the waves and put forward geostrophic adjustment as the generation mechanism.

The simulations and interpretations of *O'Sullivan and Dunkerton* [1995] have become a milestone for several reasons: they explicitly showed IGWs generated by jets, with more realism than 2D frontogenesis simulations, allowing essential features emphasized from observations (low frequency, jet exit region) to be reproduced. As a consequence, their interpretation in terms of geostrophic adjustment, and the confirmation of the relevance of the Lagrangian Rossby number as a diagnostic, have guided interpretations in subsequent studies, in particular for observations (e.g. *Pavelin et al.* [2001]; *Plougonven et al.* [2003]).

As shown by sensitivity tests, the simulations of *O'Sullivan and Dunkerton* [1995] did not converge numerically (see their Fig. 9), which was somewhat controversial at the time[11]. In fact, a contemporaneous study by *Bush et al.* [1995] used very similar idealized baroclinic life cycles (with $\Delta x \sim 60km$) to analyze the degree of balance of the flow. Gravity waves were found to be more intense near the cold fronts than in the upper-troposphere, but the analysis of these frontal waves strongly suggested that they were a numerical artifact, again due to the shallow slope of the front near the surface, shallower than $\Delta z/\Delta x$. These numerical issues raise two questions: **1)** at what resolution would the gravity waves converge, and what small-scale gravity waves would then be obtained? **2)** how should one interpret such gravity waves from simulations that have not converged?

Regarding the first question, the resolution used by *O'Sullivan and Dunkerton* [1995] only allowed subsynoptic scale inertiagravity waves with horizontal wavelengths of 600-1000 km to be described. However, as reviewed in section 3, it is mesoscale gravity waves with horizontal wavelengths of 50-500 km that are found to be prevalent in the vicinity of the unbalanced upper-level jet streaks. This has been demonstrated repeatedly from observational studies of gravity waves (e.g., *Uccelini and Koch* [1987]; *Bosart et al.* [1998]; *Thomas et al.* [1999]) and the corresponding numerical investigations (e.g., *Powers and Reed* [1993]; *Zhang and Koch* [2000]; *Zhang et al.* [2001]). These mesoscale waves may have a greater impact on the transport of momentum than the subsynoptic waves [*Fritts and Nastrom*, 1992].

Consequently, *Zhang* [2004] performed multiply nested mesoscale numerical simulations with horizontal resolution up to 3.3 km to study the generation of mesoscale gravity waves during the life cycle of idealized baroclinic jetfront systems. Long-lived vertically propagating mesoscale gravity waves with horizontal wavelengths ∼100-200 km are simulated originating from the exit region of the upper-tropospheric jet streak, in a manner consistent with past observational studies. The residual of the nonlinear balance equation is found to be a useful index in diagnosing flow imbalance and predicting the location of wave generation. *Zhang* [2004] proposed the term *balanced adjustment* to describe the continuous radiation of waves within the developing baroclinic wave. A framework to describe this emission was proposed by *Plougonven and Zhang* [2007] through scale analysis and analytical derivation of a wave equation linearized on the balanced background flow that is forced by synoptic-scale flow imbalance. This was implemented and expanded to explain gravity waves emitted in dipoles [*Wang and Zhang*, 2010], and has recently been used to explain at least some of the jet-exit region gravity waves found in baroclinic life cycles *Wang* [2008].

To further investigate the sources and propagation of gravity waves in the baroclinic jet-front systems, *Lin and Zhang* [2008] carried out ray-tracing from the four groups of waves they identified in the lower stratosphere: a northward-propagating short-scale wave packet (horizonatal wavelength $\lambda_H \sim 150$ km), and a northeastward-propagating medium-scale wave packet ($\lambda_H \sim 350$ km) in the exit region of the upper-tropospheric jet, a third packet in the deep trough region above (and nearly perpendicular to) the jet ($\lambda_H \sim 100$-150 km), and a fourth group far to the south of the jet right above the surface cold front ($\lambda_H \sim 100$-150 km). The ray-tracing analysis suggests that the medium-scale gravity waves originate from the upper-tropospheric jet-front system where there is maximum imbalance, though contributions from the surface fronts cannot be completely ruled out. The shorter scale wave packets, on the other hand, possibly originate from the surface front: this is a possibility for the northward-propagating gravity waves in the jet-exit region, and a certainty for the other two packets. Ray-tracing analysis also reveals a very strong influence of the spatial and temporal variability of the complex background flow on the characteristics of gravity waves as they propagate.

Wang and Zhang [2007] investigated the sensitivity of mesoscale gravity waves to the baroclinicity of the background jet-front systems by simulating different life cycles of baroclinic waves with a high-resolution mesoscale model. In all experiments, vertically propagating mesoscale gravity waves are found in the exit region of upper-tropospheric jet streaks. The intrinsic frequencies of these gravity waves tend to increase with the growth rate of the baroclinic waves. They further found that the growth rate of flow imbalance also correlates well to the growth rate of baroclinic waves and thus correlates to the frequency of gravity waves.

Regarding the second question, *Plougonven and Snyder* [2005] have shown that simulations that did not converge numerically nevertheless could carry relevant information regarding the location, the horizontal orientation and the intrinsic frequency $\tilde{\omega}$ of the waves in jet exit regions. The reason is that those characteristics are largely determined by propagation through the large-scale flow (see section 5.3), which is well described. The large-scale strain causes a wavepacket's wavenumber to increase exponentially along a ray, so that details of the waves will always be sensitive to resolution. Nonetheless, even at low resolution the location, orientation and $\tilde{\omega}$ of waves may be relevant because they are constrained by the large-scale deformation and shear. Evidence for this effect also comes from comparison of simulated waves with observations [*Plougonven and Teitelbaum*, 2003] and from the remarkable insensitivity to resolution of $\tilde{\omega}$ for waves in jet exit regions [*Plougonven and Snyder*, 2007].

Now, the above studies focused each on one idealized life cycle, emphasizing gravity waves emanating from the upper-level jet[12]. One issue then concerns the relation of these three-dimensional simulations to the evidence from 2D frontogenesis simulations and from some observations (*Eckermann and Vincent* [1993]; *Fritts and Nastrom* [1992]) indicating wave generation from the surface fronts.

In order to test the sensitivity of the wave generation to the background flow, *Plougonven and Snyder* [2007] ran two very different baroclinic life cycles, following the paradigm of *Thorncroft et al.* [1993] who highlighted two types of nonlinear Rossby wave breaking, cyclonic and anti-cyclonic. In the cyclonic run, gravity waves were found in the jet exit region, clearly emitted by the jet (both an upward and a downward wavepacket are found), have sub-synoptic scale, similar to those described by *O'Sullivan and Dunkerton* [1995]. In the anticyclonic run, the most conspicuous waves are found ahead of the surface cold front (see Figure 14), reminiscent of those found in 2D frontogenesis studies, and have a different sensitivity to resolution: as resolution increases, their vertical wavelength remains unchanged while the horizontal one decreases, yielding higher frequencies (up to $3f$): these waves are *not* undergoing wave capture. Their generation seems tied to an obstacle effect (strong surface winds impinging on the cold front), as in the case study of *Ralph et al.* [1999].

Baroclinic life cycles in a very different configuration (triply periodic domain, initial jet specified by strong interior PV anomalies) have been carried out by *Viúdez and Dritschel* [2006] to study spontaneous emission with a sophisticated code and inversion for the balanced flow. Waves with intrinsic frequencies close to inertial ($N/f \sim m/k$) were produced in very localized bursts where the flow has strong curvature, on the anticyclonic side of the jet. One packet remains trapped withing the vortices, while another propagates significantly outward.

Waite and Snyder [2009] carried out baroclinic life cycle experiments at high resolution ($\Delta x = 10$km, $\Delta z = 60$m), which revealed three types of waves spontaneously generated (a long packet tied to the cold front [*Snyder et al.*, 1993], a compact one east of the ridge, turning into the cyclone, east of the ridge [*Zhang*, 2004], and a long packet from the jet exit region in the ridge down into the trough [*Plougonven and Snyder*, 2007]). At later times, these localized packets give way to more disordered wave signatures filling the whole region of the baroclinic jet and vortices. *Waite and Snyder* [2009] investigated the contribution to the mesoscale energy spectrum of the spontaneously emitted IGW (both by a direct cascade and by vertical propagation), and showed that they could yield a -5/3 spectrum, but only in the lower stratosphere and with too low amplitude. This suggests that other contributions to the mesoscale spectrum (convection, topography) are crucial.

6.5. Dipoles

Both observations and idealized baroclinic life cycles have stressed jet exit regions as favored sites for the appearance of conspicuous inertia-gravity waves. Now, a simple model of jet exit regions is provided by dipoles (e.g. *Cunningham and Keyser* [2000]). Numerical simulations of dipoles have been carried out by several different groups, using different configurations and very different models: *Snyder et al.* [2007] simulated a surface dipole, from an initial dipole that is an exact solution in the quasi-geostrophic approximation [*Muraki and Snyder*, 2007]. *Viudez* [2007, 2008] simulated a dipole in the interior of the fluid with constant stratification, from an initial condition with PV anomalies of opposite magnitudes but slightly different structures. Their model uses potential vorticity (PV) as one of the prognostic variables [*Dritschel and Viúdez*, 2003] and evolves it using contour advection to ensure a good conservation. They invert the initial PV distribution with a unique method which iteratively finds an optimal balanced state which minimizes the unbalance in the full dynamics [*Viúdez and Dritschel*, 2003]. *Wang et al.* [2009] simulated both surface and interior dipoles. Antisymmetric initial PV anomalies are inverted using the Nonlinear Balance Equations [*Davis and Emanuel*, 1991], producing asymmetric dipoles. *Snyder et al.* [2007] and *Wang et al.* [2009] use different models based on finite differences, and *Viudez* [2008] has checked his results with a pseudospectral code. All these simulations were carried out on the f-plane, with domains that are doubly periodic in the horizontal, or bounded [*Wang et al.*, 2009].

In all cases, the dipoles proved to be robust structures: after an initial adjustment, the dipoles propagated steadily and for long periods (tens of days), along trajectories that curve with a radius of curvature very large relative to the dipole size. Hence they have the great advantage of providing a background flow that retains a jet exit region, but that is nearly stationary in the appropriate frame of reference.

A robust phenomenology emerged from these simulations: a gravity wave packet was systematically found in the front of the dipole, in the jet exit region, with phase lines rather normal to the jet and wavelengths contracting to smaller scales in the front of the wavepacket (see Fig. 15). The phase lines extend into the anticylcone. The intrinsic frequencies are close to the inertial frequency ($f < \hat{\omega} < 2f$). In these diverse simulations, the presence, orientation and relation to the background flow is strikingly robust, making these Jet Exit Region Emitted (JEREmi) waves a paradigm to understand similar wave packets found in baroclinic life cycles. Some minor aspects differ between the simulations, such as the importance of the bias toward the anticyclone and the rather weak amplitude of the simulated waves.

The origin of the waves has been carefully examined and discussed, demonstrating unambiguously that they are not remnants of the adjustement of the initial condition but truly result from spontaneous generation [*Snyder et al.*, 2007; *Wang and Zhang*, 2010]. Vertical cross-sections through the dipole axis clearly suggest that the waves originate in the jet core, where fluid parcels undergo significant acceleration then deceleration, accompanied with vertical displacements *McIntyre* [2009]. The waves appear as a conspicuous component of the flow downstream, in the jet exit region, and are there consistent with wave-capture [*Bühler and McIntyre*, 2005]. This influence, due to the background deformation and shear, can be seen graphically from the tendency of the phase lines to align with the isolines of along-jet velocity (Fig. 15, or Figure 4.b of *Wang et al.* [2009]), and was verified using ray-tracing by *Wang et al.* [2010]. This was highlighted in other simulations and discussed independently, but yielding the same conclusion *Viudez* [2008]. The waves were found not to be detectable when the Rossby number was too small (less than 0.15 *Snyder et al.* [2007] or less than 0.05 *Wang et al.* [2009]), and showed an algebraic dependence above that (exponents between 2 and 6). The dependence on the Rossby number however is very sensitive to resolution *Wang et al.* [2009], and is obtained only for a narrow range of Rossby numbers (e.g. 0.15-0.30 in *Snyder et al.* [2007])). Hence it could not be conclusive to compare this dependence with theoretical predictions, in particular a non-algebraic one such as an exponential dependence in Rossby number.

The waves have been explained as a linear response to a forcing which is akin to the imbalance produced by the balanced flow. The idea of such a linearization goes back, in the context of frontogenesis, at least to *Ley and Peltier* [1978]*Snyder et al.* [1993] and *Reeder and Griffiths* [1996], and more generally to *Lighthill* [1952]. Building on the (spontaneous) balance adjustment hypothesis proposed in *Zhang* [2004], a general framework for such linearization has been discussed by *Plougonven and Zhang* [2007], emphasizing the need to linearize around the large-scale background flow. The basic assumption is that the waves are small enough to be described by linearized dynamics around a balanced approximation of the flow.

As a crude sketch of this linearization, we consider the equation for the velocity in the x direction, u, in the Boussinesq approximation on the f-plane (e.g. *McWilliams and Gent* [1980]):

$$\frac{\partial u}{\partial t} + \mathbf{u}\nabla u - fv + \frac{\partial \Phi}{\partial x} = 0 \,, \tag{10}$$

where f is the Coriolis parameter and Φ is geopotential. Now, the flow can always be decomposed into two components $u = \bar{u} + u'$, where $\bar{u}$ is a balanced approximation of the flow (or its large-scale part) and u' the residual, including gravity waves and higher-order balanced corrections. For Rossby numbers smaller than one but finite, it is expected that the background flow will well be approximated by a balanced relation ($|u'| \ll |\bar{u}|$), but that the emission of gravity waves will dominate u'. Injecting the decomposition into (10), three types of terms appear: terms involving only the balanced flow are moved to the right hand side (*rhs*), terms linear in the perturbations are kept on the *lhs*, and terms that are quadratic in perturbations are neglected. This yields forced equations for the perturbations u', linearized on the background balanced flow $\bar{\mathbf{u}}$:

$$\frac{\partial u'}{\partial t} + \bar{\mathbf{u}}\nabla u' + \mathbf{u}'\nabla\bar{u} - fv' + \frac{\partial \Phi'}{\partial x} = \mathcal{F}_u \ , \qquad (11)$$

where

$$\mathcal{F}_u = \frac{\partial \bar{u}}{\partial t} + \bar{\mathbf{u}}\nabla\bar{u} - f\bar{v} + \frac{\partial \bar{\Phi}}{\partial x} \qquad (12)$$

is the residual tendency, i.e. the residual when the balanced solution is injected into the primitive equations. If used in a systematic asymptotic approach with $Ro \ll 1$, the above approach yields no emission [*Reznik et al.*, 2001; *Vanneste*, 2008; *Plougonven et al.*, 2009]. More precisely, there may be an emission that is exponentially small in Ro, and hence not described by the above heuristic approach. Emission appears at finite Ro, when the advection on the lhs and the forcing on the rhs are both strong enough.

Several studies have investigated variations on this approach, using different sets of equations (for momentum and potential temperature in *Snyder et al.* [2009], for horizontal divergence and vorticity in *Wang et al.* [2010]; *Wang and Zhang* [2010]). They consistently show that the structure (location, orientation, intrinsic frequency) of the wave-packet is mainly determined by the background flow, (i.e. the *lhs* operator), not by the forcing:

the latter is large-scale and bears no resemblance with the produced waves [*Snyder et al.*, 2009]. In other words, and as confirmed using ray-tracing, *'the effects of propagation dominate over the source'* [*Wang et al.*, 2010]. The latter does matter to determine the amplitude of the emitted waves, i.e. they do not arise merely as an instability but require a forcing to be present in (11). Given the importance of propagation effects, diagnostics of the large-scale flow such as the Okubo-Weiss parameter (e.g. *Lapeyre et al.* [1999]), which appears in the description of wave capture, are likely as important as traditionnaly used diagnostics of imbalance.

In summary, different dipole experiments have shown the robustness of Jet Exit Region Emission (JEREmission). The crucial ingredients are strong velocities in the jet core, combined with along-jet variations: the first leads to strong advection ($\bar{\mathbf{u}}\nabla u'$ in equation (11)), the second produces a forcing, e.g. as in equation (12) (a zonally symmetric jet does not by itself produce waves). The advection allows this forcing to project onto fast Largangian timescales (shorter than $1/f$).

This linearization is in part inspired by Ford's work on Lighthill radiation [*Reeder and Griffiths*, 1996; *Plougonven and Zhang*, 2007]. Essential differences need to be emphasized to avoid confusion: in the case of Lighthill radiation, the scale separation between the vortical flow and the GW implies that the *lhs* operator is that for GW on a background of fluid at rest [*Plougonven and Zhang*, 2007; *Plougonven et al.*, 2009]. One important consequence is that the quadrupolar form of the forcing partly determines the weakness emission [*Ford et al.*, 2000, 2002]. For JEREmi waves, the scale separation is the opposite, and advection plays a crucial role to allow projection of the forcing onto fast intrinsic timescales. The higher-order derivatives of the large-scale forcing enhances the small-scale part of the forcing, and hence this projection. Fundamental conclusions concerning regarding Lighthill radiation [*Ford et al.*, 2002] no longer hold, and this motivates a sharp distinction between the generation mechanism at play in stratified dipoles or baroclinic life cycles and Lighthill radiation [*Zhang*, 2004; *McIntyre*, 2009].

7. IMPACTS AND PARAMETERIZATIONS

A major motivation driving recent research on atmospheric gravity waves is their role in transferring momentum towards the middle atmosphere (e.g. *Fritts and Alexander* [2003]). Constraints from observations and simulations, along with a better physical understanding, are needed to improve parameterizations in Atmospheric General Circulation Models (GCMs) (section 7.1). Yet gravity waves emitted from atmospheric jets and fronts also matter for other impacts, such as their local contributions to mixing and turbulence (section 7.2), and also to temperature-dependent phenomena (section 7.3).

While all the studies described above focus on the atmosphere, the same dynamical mechanisms that have been discussed in sections 4 and 6 are also active in the ocean, as discussed in section 7.4.

7.1. Momentum fluxes and parameterizations

Gravity waves are crucial to the general circulation of the stratosphere and mesosphere because they transfer momentum upward [*Andrews et al.*, 1987]. Atmospheric General Circulation Models (GCMs) typically include two parameterizations, one for orographic gravity waves and one for non-orographic gravity waves. The latter generally have an arbitrarily fixed source at a given level, tuned in order to produce a reasonnable stratospheric circulation [*Kim et al.*, 2003]. While parameterizations of convective sources of gravity waves have been elaborated and implemented in the last decade [*Beres et al.*, 2004, 2005; *Song and Chun*, 2005], parameterizations of waves produced by jets and fronts remain exceptionnal: *Rind et al.* [1988] included waves generated by wind shear at the level of the tropospheric jet stream. *Charron and Manzini* [2002] and *Richter et al.* [2010] have used the frontogenesis function [*Miller*, 1948; *Hoskins*, 1982] in the mid-troposphere (600 hPa) as a diagnostic to identify active source regions. *Richter et al.* [2010] prescibed the emitted waves with a Gaussian phase speed spectrum centred on the local wind, and kept the amplitudes as a tunable parameter. Improvements included a reduction of the cold pole bias and a better variability of the stratospheric circulation (frequency of Stratospheric Sudden Warmings), although they are not solely due to the changes in the GW parameterization (the addition of Turbulent Mountain Stress also contributed).

Implementing successfully a new parameterization with variable source, without degrading other features of the GCM's circulation, already is a significant achievement. Yet, the parameterizations described above remain heuristic, and progress is needed to include more physical understanding. Pathways to improve parameterizations of jets and fronts as sources include the systematic use of observational datasets (e.g. *Gong et al.* [2008] for radiosonde observations), numerical modeling (e.g. *Zülicke and Peters* [2006]) and theoretical developments (e.g. *Lott et al.* [2010]). *Zülicke and Peters* [2008] have elaborated a parameterization of inertia-gravity wave generation in poleward-breaking rossby waves, using the cross-stream Lagrangian Rossby number as a central quantity to diagnose emission, and describing the upward propagation with a WKB approximation. Mesoscale simulations and observations of ten cases were used to validate their approach.

Motivation to render the non-orographic sources more realistic (e.g. variable in time and space) includes evidence from studies of GW sources and needs from GCM modelling: different lines of evidence (idealized simulations of *Sato et al.* [2009], balloon observations *Hertzog et al.* [2008] and real-case simulations *Plougonven et al.* [2012]) point to oceanic regions in the mid-latitudes (i.e. to non-orographic GW sources) as significant sources. Regarding modelling, it is evidently unsatisfactory and unphysical not to link emitted waves to the flow that is exciting them. In practice, the poor represenation of gravity waves has been emphasized as a likely cause of important biases in GCMs *Pawson et al.* [2000]; *Austin et al.* [2003]; *Eyring and Co-Authors* [2007]. Yet more fundamentally, *Haynes* [2005] concludes his review of stratospheric dynamics by emphasizing that *'further (and potential greater) potential uncertainty enters through the extreme difficulty in simulating potential changes in gravity wave sources in the troposphere.'*

7.2. Transport, mixing and turbulence

Gravity waves contrbitue in several ways to transport and mixing. *Danielsen et al.* [1991] proposed, based on the analysis of airborne measurements, that the differential advection due to a low-frequency, large scale wave can induce laminar structures, favoring cross-jet transport and mixing. Irreversible mixing is then achieved by smaller-scale gravity waves when they break. *Pierce and Fairlie* [1993] thus suggested that inertia-gravity waves contribute to transport across the edge of the polar vortex, but called for further investigation for this effect to be quantified. Observational evidence for the production of laminae by inertia-gravity waves has been described by *Teitelbaum et al.* [1996] and *Pierce and Grant* [1998]. In another case study explicitly addressing this process, *Tomikawa et al.* [2002] found the contribution of inertia-gravity waves to be negligible.

In the numerical simulations of *O'Sullivan and Dunkerton* [1995], significant displacements due to inertia-gravity waves appeared in plots of the potential vorticity near the tropopause, which were interpreted as a signature of transport. *Moustaoui et al.* [1999] argued, based on observations and the numerical results of *O'Sullivan and Dunkerton* [1995], that gravity waves could promote cross-tropopause mixing.

In summary, there is evidence that inertia-gravity waves can produce laminae, and strong arguments that this will promote mixing. However, quantifying such contribution of gravity waves to mixing remains an issue.

The breaking of gravity waves will produce small-scale mixing and turbulence (e.g. *Fritts et al.* [2003]). The latter is of importance for aviation and forecasting of turbulence *Sharman et al.* [2006, 2012]. It is of particular importance to predict occurrences of clear-air turbulence (CAT), and the tropopause region near the jet stream is a major source of CAT events (e.g. [*Kim and Chun*, 2011]). Now, case studies have proven inertia-gravity waves in the vicinity of the jet-stream to be one mechanism leading to CAT [*Lane et al.*, 2004; *Koch et al.*, 2005] by locally enhancing shear. *Knox et al.* [2008] claimed to predict CAT from jet-generated IGWs as an application of Lighthill radiation, yet for several reasons Lighthill radiation here does not apply [*Plougonven et al.*, 2009; *Knox et al.*, 2009]. In fact, further investigation of this case *Trier et al.* [2012] has recently showed that gravity waves due to convection were at least partly responsible for the turbulence events analyzed by *Knox et al.* [2008].

7.3. Temperature dependent phenomena

Propagating gravity waves induce reversible temperature fluctuations. These can be of importance for phenomena that depend on temperature, and particularly those with a threshold. High frequency waves, as generated from convection and orography, will be most efficient in producing substantial temperature fluctuations, yet inertia-gravity waves have also been found to contribute.

At high latitudes, gravity waves contribute in this way to polar stratospheric clouds (PSCs). Orographic waves are a priori the main source of waves involved [*Carslaw et al.*, 1998] and for which clear and systematic effects have been documented and the impact on PSCs discussed (e.g. *Dörnbrack et al.* [2002]; *Hertzog et al.* [2002a]; *Mann et al.* [2005]; *Eckermann et al.* [2009]). The contribution from orographic waves is well established (e.g. *McDonald et al.* [2009]; *Alexander et al.* [2011]) and is more emphasized than that of non-orographic waves. Yet observational case studies have shown that gravity waves generated by jets and fronts can also produce PSCs, both in the Antarctic [*Shibata et al.*, 2003] and in the Artcic *Hitchman et al.* [2003]; *Buss et al.* [2004]; *Eckermann et al.* [2006].

Another example is the freeze-drying of air entering the stratosphere in the Tropical Tropopause Layer [*Fueglistaler et al.*, 2009]. Gravity waves contribute to temperature fluctuations that will affect the freeze-drying process [*Potter and Holton*, 1995; *Jensen et al.*, 1996], but it likely does not modify significantly the final water vapor mixing ratios [*Jensen and Pfister*, 2004]. In any case, convection is here the relevant source for the gravity waves involved.

7.4. In the ocean

One motivation for many of the studies on the limitations of balance (section 4.3) comes from the need to understand dissipation in the ocean [*Wunsch and Ferrari*, 2004]. The prevalent balances (hydorstasy and geostrophy, or some forms of gradient-wind balance) and the implied energy cascade to large scales implies a conundrum: what are the pathways for energy, injected by the wind forcing into geostrophic motions, toward the small-scales, where it can be dissipated [*McWilliams*, 2003]? Interaction of balanced motions with internal gravity waves and inertial oscillations constitutes one possible route [*Müller et al.*, 2005]. Several studies of unbalanced instabilities have been undertaken to quantify the efficiency of this route (e.g. *Molemaker et al.* [2005] and refs. therein). Recent high-resolution numerical simulations, both idealized [*Molemaker et al.*, 2010] and realistic [*Capet et al.*, 2008a, b], have rather emphasized the appearance, at short scales, of frontal instabilities. Such instabilities are however absent from other high-resolution simulations of upper-ocean geostrophic turbulence *Klein et al.* [2008], calling for further investigation. Now, while internal waves or inertial oscillations may play a role in the forward energy cascade leading to dissipation, it is those forced by ther mechanisms, particularly winds, that are likely involved [*Gertz and Straub*, 2009]. In both cases, the focus has moved away from spontaneously generated gravity waves.

Danioux et al. [2012] have recently investigated specifically the spontaneous generation of waves from upper-ocean turbulence in an idealized setting. Surface quasi-geostrophy (SQG) captures well the dynamics of the baroclinically unstable current and the turbulent mesoscale and submesoscale eddy field. In particular, SQG leads to large Rossby numbers at small scales [*Juckes*, 1994], and hence spontaneous generation. The generation is hence very localized (i.e. very intermittent spatially), which is consistent with an exponential dependence on Rossby number. Once generated however, the waves contribute to a more homogeneously distributed gravity wave field at depth, where the flow is much weaker. This generation is small (the energy in the gravity waves is 10^5 times weaker than the energy in the balanced flow) in comparison to inertia-gravity waves generated by winds (e.g. *D'Asaro et al.* [1995]). The generation occurs near the grid-scale, and further investigations will be necessary to assess more firmly the intensity and realism of such generation.

Polzin [2008, 2010]It has argued that wave-capture was playing a role in the ocean, and more generally that the consideration of horizontally varying background flows fundamentally modifies interactions between waves and the mean flows. However, detailled evidence for the occurence of wave capture in the ocean is still lacking. Observation and simulations of this faces one major difficulty in the ocean: near the surface, the major source of near-inertial motions are the surface winds, forcing large-scale motions (several hundreds to a thousand of kilometers) that are then distorted by the mesoscale, balanced vortices (scales of ten to a few hundred kilometers) to finer and finer scales [*Young and Jelloul*, 1997; *Klein and Smith*, 2001]. If waves undergoing capture are present, it will be at scales smaller than those of the mesoscale vortices, with amplitudes weaker than the wind-forced near-inertial oscillations, making them difficult to observe and simulate.

8. DISCUSSION AND PERSPECTIVES

Current knowledge from observations, theory and modelling studies on internal gravity waves emanating from jets and fronts has been reviewed. Below we discuss to what extent the different threads of investigation tie up together to provide a comprehensive understanding. Focusing on generation mechanisms, we summarize salient points, emphasize limitations so as to determine, critically, what should be preserved as robust conclusions, and identify what open questions constitute essential challenges.

8.1. On generation mechanisms

The generation mechanism that has most often been invoked is geostrophic adjustment (section 4.1), not only in observations (*Kaplan et al.* [1997]; *Pavelin et al.* [2001]; *Plougonven et al.* [2003]), but also in numerical simulations [*O'Sullivan and Dunkerton*, 1995] and sometimes in analytical studies [*Fritts and Luo*, 1992].

We wish to emphasize that the recurrent reference to geostrophic adjustment turns out to be unhelpful and argue that it should be avoided. It gives the misleading impression that there is, readily available, a theoretical paradigm for understanding the emission of gravity waves by jets and fronts, with foundations going back several decades to the work of *Rossby* [1938]. We argue that studies of geostrophic adjustment are in fact unhelpful for three reasons: **1-** they take the imbalance as part of a given initial condition, hence circumventing the essential difficulty, i.e. to understand how, why and where this imbalance is produced. **2-** The background flows for which the adjustment problem is well-posed theoretically, and for which results are available, are simple flows: axially or zonally symmetric, or with small Rossby number *Ro*. Relevant flows in practice are more complex (with spatial and temporal variations, locally large *Ro*). **3-** The classical scenario (imbalance propagating away as IGW, leaving a balanced flow behind) is valid only for the simple configurations afore-mentionned. This does not describe the phenomena observed and simulated near jets and fronts, where the emission is continuous and no simple, final adjusted state can be identified.

Now, it is true also that the notion of geostrophic adjustment can be extended, e.g. to include adjustment of perturbations on a background flow [*Tuyl and Young*, 1982; *Plougonven and Zeitlin*, 2005]. It can be stretched to describe the response to arbitrary, time-dependent injection of imbalance [*Weglarz and Lin*, 1997; *Chagnon and Bannon*, 2005a, b]. The traditional initial condition problem is then a particular case, with a forcing that is a Dirac δ function of time. With such a generalized definition however, geostrophic adjustment loses its precise meaning and encompasses all linear responses to a prescribed forcing, for instance, convectively generated waves (diabatic forcing). Hence we prefer to preserve a precise meaning for 'geostophic adjustment' and continue below to use it in its traditional acceptation (section 4.1).

In summary, geostrophic adjustment has been repeatedly invoked as the mechanism responsible for emission near jets and fronts, partly through lack of a better explanation and partly because of the presence of a strong, large-scale imbalance in the vicinity of the waves.

The following picture, generalizing the notion of adjutment, has guided intuition: the nonlinear evolution of a balanced flow leads to the appearance and growth of localized regions of imbalance. This imbalance partly projects onto gravity waves. The 'production' of imbalance may persist, so that the flow does not appear to adjust, i.e. the imbalance does not decrease and disappear (at least not on timescales of a few inertial periods) and gravity waves are continuously emitted. Now this phenomenology, as found in case studies (section 3) or in idealized experiments (section 6), differs from that described by classical geostrophic adjustment: first, the emission takes place continuously in time, not just in a short initial period. Second, the imbalance is not found to decay after the appearance of waves: for instance, it is stationary in the dipole. Concomitantly, the flow does not evolve simply to a balanced state that can be predicted in advance, e.g. in baroclinic life cycles the flow continues its complex, non-linear evolution which comprises imbalance. Third, the waves do not necessarily propagate away: for example, waves emitted in the dipole remain as an inherent part of the dipole. In baroclinic life cycles, only part of the waves generated near the upper-level jet leak away into the stratosphere. Hence we believe it is preferable to distinguish the emission by jets and fronts from geostrophic adjustment (*McIntyre* [2001], p1723 and 1731). Keeping the term 'adjustment' (because of the guiding image sketched above, which generalizes adjustment to a situation where the imbalance is conituously forced), we advise to use the terms spontaneous balanced adjustment [*Zhang*, 2004; *Wang and Zhang*, 2010] or spontaneous adjustment emission [*Ford et al.*, 2000; *Viúdez and Dritschel*, 2006], or simply spontaneous emission.

Over the past two decades, substantial progress has been achieved in understanding and quantifying how balanced motions may create imbalance and gravity waves spontaneously [*Vanneste*, 2013]. We first summarized mechanisms for spontaneous emission that have been identified analytically (section 4). Lighthill radiation (section 4.2.2), which has been very inspiring as the first clear mechanism of gravity wave emission from balanced motions, explains waves that have spatial scales larger than the balanced flow (with $Ro > 1$) generating them. It is useful to explain waves generated from intense vortices such as cyclones and mesoscylones *Schecter* [2008]. Unbalanced instabilities and transient generation (sections 4.3 and 4.4) describe how shear couples gravity waves and balanced motions, leading to emission in the form of unstable modes or transient bursts. These have scales comparable to or somewhat larger than the Potential Vorticity (PV) anomalies that are sheared. The range of applicability of these mechanisms remains to be evaluated, but two points are worth noting: first, unbalanced instabilities have been difficult to exhibit in dedicated laboratory studies because of their weakness (weak growth rates and/or low level of saturation, see Section 6.1). Second, the coupling of gravity waves and PV anomalies in shear may be more relevant for other flow configurations, where other processes such as wave-breaking [*Plougonven et al.*, 2010] produce small-scale PV anomalies that are subsequently sheared. In other words, these theoretical mechanisms for the spontaneous generation of gravity waves from balanced motions have not, so far, been found to apply and explain the emission of waves from jets and fronts in real cases.

In all three mechanisms, emission occurs when and where the appropriate scales (timescales and spatial scales) match: the scales of the balanced flow and the scales of potential inertia-gravity waves, i.e. consistent with the dispersion relation. In the configurations most relevant to jets and fronts (plane parallel sheared flows), studies have emphasized the importance of differential advection (i.e. shear) for coupling balanced motions and gravity waves: the slow, balanced motions connect to fast gravity wave motions thanks to Doppler shifting. Finally, note that there are many connections between these different mechanisms (sections 4.2, 4.3 and 4.4), some unbalanced instabilities being described as Lighthill radiation for instance. The fact that these mechanisms do not apply easily to cases found in real flows makes it necessary to consider more complex flows.

8.2. Jet Exit Region Emitted (JEREmi) waves

One remarkable outcome from observations and numerical modelling has been the robustness of the paradigm put forward by *Uccelini and Koch* [1987], and the dynamical understanding obtained since. Observational case studies (sections 3) and idealized simulations (6.4 and 6.5) have emphasized jet exit regions, upstream of a ridge and also, less frequently, of a trough, as a favored location for large-amplitude, sub-synoptic inertia-gravity waves (see section 3 and figure 5). The convergence of different approaches and the recurrence of this configuration in numerous studies are indications of the robustness of this result.

Theory has highlighted propagation effects, namely *'wave-capture'*, as a mechanism enhancing IGW in such a region of the flow (section 5.3), the large-scale strain and vertical shear determining certain of the wave characteristics. Simulations of idealized baroclinic life cycles (section 6.4) have also highlighted jet exit regions (see Figure 12). A further simplification of the flow has consisted in restricting to dipoles that have a nearly steady propagation. Several different modelling studies have robustly identified a low-frequency wave packet in the front of the dipole, with characteristics consistent with wave capture, as an inherent part of the dipoles, steadily propagating with them (see Figure 15). The emission mechanism has been explained as the linear response to the differences between the balanced and the full tendencies (see Section 6.5). The key point is that the dynamics are linearized on the background of a balanced approximation of the dipole[13]. The response is not very sensitive to the specific shape of the forcing but rather to the background flow used in the linearization.

The explanation of waves found in dipoles is an encouraging result, because of the similarity of these JEREmi (Jet Exit Region Emitted) waves with waves identified in more complex, idealized flows, and of the similarity of these latter waves with those described in observational studies. Nonetheless, revisiting observations with the understanding gained from theory and idealized simulations remains largely to be done in order to assess: **1)** what proportion of the wave field can be said to be affected by wave capture?, **2)** how systematic is the presence of such waves in jet exit regions?, **3)** why are amplitudes found in idealized simulations weaker than those observed?, and **4)** how much IGWs leak upward or propagate out of the region of strong strain? A further, fundamental issue is **5)** to understand the impact, for the interaction of waves with the mean flow, of this effect due to horizontal variations of the backgound flow, which is traditionnally ignored.

Other issues, beyond the case of IGW in jet exit regions, remain: how can this understanding guide the elaboration of parameterizations of jets and fronts as gravity waves sources? An essential issue that remains to be addressed concerns the role of moisture, idealized studies having until now focused on dry dynamics.

8.3. Waves from other processes

JEREmi waves are not the only waves present in the vicinity of jets and fronts, there are other potential sources of gravity waves near jets and fronts: first, extant idealized modelling studies have simulated a richer array of gravity waves, e.g. with waves emanating from surface fronts (sections 6.3 and 6.4). Second, these simulations have limitations such as the absence of moist processes or of a boundary layer. The parameterizations of these small-scale processes have their own uncertainties, yet these processes are of great importance: for instance, diabatic heating acts directly on the buoyancy and at small-scales, and is therefore a very efficient forcing for gravity waves. Case studies have recurrently mentionned the possible important role of moisture (see Section 3). Addition of moisture in idealized baroclinic life cycles will have a priori two implications: one is to accelerate and intensify the development of baroclinic instability (e.g. *Waite and Snyder* [2012]), which should enhance the excitation of gravity waves through spontaneous generation [*Reeder and Griffiths*, 1996; *Wang and Zhang*, 2006]. The other is to excite, through moist convection, additional waves. Those produced on small-scales from convective cells should have strikingly different characteristics (short horitzontal wavelengths (tens of km), long vertical wavelengths (5-10 km), and correspondingly high intrinsic frequencies). On the other hand, the large scale envelope of convection may contribute to the gravity wave field on larger scale, and this contribution will be more difficult to isolate.

Idealized moist simulations will contribute to guide our understanding, as for the impacts of moisture on the predictability of mesoscale weather [*Zhang et al.*, 2007], but they necessarily involve parameterizations convective and boundary layer processes, which are themselves quite uncertain. The implication is that further studies of moist generation of gravity waves from fronts will call strongly for observational constraints. Combined studies involving both simulations and observations should be an important step to provide a complete description of waves near moist fronts [*Zhang et al.*, 2011].

In a similar vein, additional complexity relative to idealized baroclinic life cycles may come from the generation of gravity waves from small scale turbulent motions, e.g. emission from shear instability. Previous studies on the subject have conclusively ruled out a straightforward, linear connection, but studies of the nonlinear development of the shear instability have shown that this mechanism should be considered as a source of gravity waves (section 4.5). Yet, the numerical configurations used remained quite idealized. Here again, observations will play a key role in constraining the realism of numerical simulations. A fundamental difficulty here again is the complexity of the background flow, involving a wide range of scales from the synoptic motions to the small-scale turbulence.

8.4. Perspectives

Now, both points above have emphasized the complexity that will be encountered in exploring gravity waves generated by jets and fronts as one explores finer scales. Moist convection and small-scale turbulence are themselves challenges for modelling and observation. It will likely be impossible to draw a simple, deterministic and convincing picture of the way gravity waves are generated from these processes in a complex flow environment such as a cold front within a baroclinic wave. Yet, the demand from applications (parameterizations for GCMs, forecasting of turbulence) may not call for such a deterministic picture. Observations should play a key role (see also challenges discussed in section 3.2). Global high-resolution datasets have been obtained, and the combined use of different observational platforms along with modeling promises to provide global descriptions of the gravity wave field in coming years. We believe one way forward will be to analyze such high-resolution datasets to produce flow-dependent characterizations of gravity waves (e.g. rather than quantify the mean GW activity at a given location, quantify it relative to flow configuration). This can bring practical answers to the needs of climate and forecast models. Presently, GCMs that include a parameterization of non-orographic waves are the exception, and there is much room for improving on the heuristic relation used to connect the emitted waves to the tropospheric flow. The trend towards stochastic parameterizations (*Palmer* [2001], and *Eckermann* [2011]; *Lott et al.* [2012a] for gravity waves specifically) is in phase with new descriptions of the gravity wave field [*Hertzog et al.*, 2012].

The perspective of quantifying jets and fronts as sources of gravity waves, and hence of measuring and parameterizing their variability, will make GCMs more physical, and should improve their internal variability. It will also set the stage for investigations of the variability of this forcing, of its evolution in a changing climate and of the implications, as questionned by *Haynes* [2005] (see Section 7.1).

GLOSSARY

Balanced models: approximate model that relies on balance relations which diagnostically relates several variables (e.g. velocity and pressure in geostrophic balance) to simplify the dynamics. Evolution of the flow typically reduces to one equation (conservation of Potential Vorticity), and the balance relations (e.g. hydostrasy and geostrophy for the quasi-geostrophic approximation) make it possible to *invert* the Potential Vorticity to recover all fields, and in particular the velocity (see *Hoskins et al.* [1985], and section 4.2).

Baroclinicity: measure of how the isolines of the density field and of the pressure field are misaligned. In the atmosphere, baroclinicity is strongest where there are strong horizontal thermal gradients, as in mid-latitudes, and is associated to vertical shear through thermal wind balance (e.g. *Holton* [1992]).

Inertia-gravity wave: gravity wave having a low frequency (close to the lower bound of the gravity wave spectrum, i.e. f the Coriolis parameter). See section 1.

Intrinsic frequency: : frequency in the frame moving with the fluid. The intrinsic frequency $\hat{\omega}$ is related to the ground based frequency ω by $om\hat{e}ga = omega - \mathbf{k}\,\mathbf{U}$, where $\mathbf{k}$ is the wavenumber and $\mathbf{U}$ is the background wind (see section 5).

Polar Night Jet: intense westerly jet that forms in the winter stratosphere, at high latitudes (typically 60°) and altitudes higher than 20 km. It encloses the polar vortex, and isolates it from mid-latitude air.

Rossby number: ratio U/fL, where U is a typical order of magnitude for wind velocity, L is a typical horizontal scale, and f is the Coriolis parameter. This compares the advective timescale L/U with the inertial timescale $1/f$, and is typically small at mid-latitudes at synoptic scales.

Superpressure balloons: balloons used for atmospheric measurements, with an envelope that is not extendable. At the level where the balloons drift, the gas inside has a pressure larger than the environment, so that the balloon remains fully inflated and the full device has a constant density. It therefore drifts along an isopycnic surface, and may be considered a quasi-Lagrangian tracer (see *Hertzog et al.* [2007] and section 2.3).

Unbalanced instabilities: instabilities in a rotating fluid that involves unbalanced motions. These are of interest in regimes where balance is expected or even dominant (e.g. weak Rossby number), and hence the term preferentially refers to instabilities that couple balanced and unbalanced motions (section 4.3).

ACKNOWLEDGMENTS. The authors are grateful to C. Snyder and J. Vanneste for careful reading of the manuscript and judicious remarks, to D. Durran for precious advice, to S. Wang for proofreading and to A. Kara for providing time to advance this project. They also wish to thank C. Snyder, J. Vanneste, O. Bühler, M.E. McIntyre, R. Rotunno, M. Reeder, T. Lane, C. Epifanio, T. Dunkerton, A. Medvedev, F. Lott and A. Hertzog for instructive and stimulating discussions on the subject. FZ acknowledges funding support from US National Science Foundation under grants: 0904635 and 1114849. RP acknowledges support from the European EMBRACE project.

NOTES

1. *Trexler and Koch* [2000] have compared observations from wind profilers and from a surface mesonetwork, and concluded that the latter may be limited to detecting waves that affect primarily the lower atmosphere.
2. The observational filter corresponding to superpressure ballons and radiosondes is also displayed
3. MLS, AMSU-A, AIRS, GPS, and CLAES; AIRS has much better horizontal resolution
4. The observations have their own biases, and in particular underestimate gravity waves with high intrinsic frequencies, which primarily affects orographic waves in this region *Plougonven et al.* [2008].
5. Some numerical simulations are also included in the present section because they are closely tied to the analytical results.
6. which has been refined as spontaneous balance adjustment in *Wang and Zhang* [2010], so as to avoid any confusion with a generalization of geostrophic adjustment that would simply include adjustment to higher-order balances than geostrophy (e.g. cyclo-geostrophic balance, see *Holton* [1992])
7. These low order models can been interpreted as describing the motions of a swinging spring [*Lynch*, 2002], or of a spring tied to a pendulum [*Vanneste*, 2006, 2008]. The small parameter equivalent to the Rossby number is the ratio of the (slow) pendulum to the (fast) spring oscillation frequencies.
8. This is in contrast with unbalanced instabilities, which require an initial deviation (however small) from the unstable balanced state *Vanneste* [2008]. The growing amplitudes of the waves will depend on this initial condition, linear theory providing only the growth rate, and the final amplitude of the waves will depend on the nonlinear saturation of the instability (e.g. *Gula et al.* [2009a]).
9. Shear instabilities are here treated separately from the other unbalanced instabilities because they occur on small scales such that the background rotation is generally not considered. In other terms, they occur at large Rossby numbers, such that balance (and imbalance) are not relevant for their development.
10. The dispersion relationships for waves in stratified fluid and in shallow water differ crucially here: in shallow water, short-scale waves necessarily have large frequencies and fast group velocities (recall $\omega^2 = f^2 + gH\,(k^2 + l^2)$). Wave capture can not occur in shallow water flows with Froude numbers smaller than unity.

11.The example of two-dimensional frontogenesis simulations had shown how spurious gravity waves could easily be produced and mistaken for spontaneously generated waves (see discussion of *Snyder et al.* [1993] on *Gall et al.* [1988]).

12.the study of *Bush et al.* [1995], which identified waves coming from the surface cold front, discarded them as a numerical artefact.

13.The forcing is also deduced from this balanced dipole.

REFERENCES

Afanasyev, Y. (2003), Spontaneous emission of gravity waves by interacting vortex dipoles in a stratified fluid: laboratory experiments, *Geophys. Astrophys. Fluid Dyn.*, *97*(2), 79–95.

Afanasyev, Y., P. Rhines, and E. Lindhal (2008), Emission of inertial waves by baroclinically unstable flows: Laboratory experiments with altimetric imaging velocimetry, *J. Atmos. Sci.*, *65*(doi:10.1175/2007JAS2336.1), 250–262.

Alexander, M., and co authors (2008), Global estimates of gravity wave momentum flux from High Resolution Dynamics Limb Sounder Observations, *J. Geophys. Res.*, *113*(D15S18), doi:10.1029/2007JD008,807.

Alexander, M., and et. al. (2010), Recent developments in gravity-wave effects in climate models and the global distribution of gravity-wave momentum flux from observations and models, *Q.J.R. Meteorol. Soc.*, *136*, 1103–1124.

Alexander, M., J. Holton, and D. Durran (1995), The gravity wave response above deep convection in a squall line simulation, *J. Atmos. Sci.*, *52*, 2212–2226.

Alexander, S., A. Klecociuk, M. Pitts, A. McDonald, and A. Arevalo-Torres (2011), The effect of orographic gravity waves on Antarctic polar stratospheric cloud occurrences and composition, *J. Geophys. Res.*, *116*(D06109), doi:10.1029/2010JD015,184.

Andrews, D., J. Holton, and C. Leovy (1987), *Middle atmosphere dynamics*, Academic Press.

Aspden, J., and J. Vanneste (2009), Elliptical instability of a rapidly rotating, strongly stratified fluid, *Phys. Fluids*, *21*, 074,104.

Aspden, J., and J. Vanneste (2010), *IUTAM Symposium on Turbulence in the Atmosphere and Oceans*, chap. Inertia-gravity-wave generation: a geometric-optic approach, Springer.

Austin, J., et al. (2003), Uncertainties and assessment of chemistry-climate models of the stratosphere, *Atm. Chem. Phys.*, *3*, 1–27.

Bacmeister, J., S. D. Eckermann, P. Newman, L. Lait, K. Chan, M. Loewenstein, M. Proffitt, and B. L. Gary (1996), Stratospheric horizontal wavenumber spectra of winds, potential temperature and atmospheric tracers observed by high-altitude aircraft, *J. Geophys. Res.*, *101*, 9441–9470.

Badulin, S., and V. Shrira (1993), On the irreversibiility of internal wave dynamics due to wave trapping by mean flow inhomogenities. Part 1: Local analysis, *J. Fluid Mech.*, *251*, 21–53.

Baer, F., and J. Tribbia (1977), On complete filtering of gravity modes through nonlinear initialization, *Mon. Weath. Rev.*, *105*, 1536–1539.

Bakas, N., and B. Farrell (2008), Momentum and energy transport by gravity waves in stochastically driven stratified flows. Part II: radiation of gravity waves from a Gaussian jet, *J. Atmos. Sci.*, *65*(7), 2308–2325.

Bakas, N., and B. Farrell (2009a), Gravity waves in a horizontal shear flow. Part I: Growth mechanisms in the absence of potential vorticity perturbations., *J. Phys. Oceanogr.*, *39*, 481–496.

Bakas, N., and B. Farrell (2009b), Gravity waves in a horizontal shear flow. Part II: Interaction between gravity waves and potential vorticity perturbations., *J. Phys. Oceanogr.*, *39*, 497–511.

Batchelor, G. (1967), *An introduction to fluid dynamics*, Cambridge University Press.

Beres, J., M. Alexander, and J. Holton (2004), A method of specifying the gravity wave spectrum above convection based on latent heating properties and background wind, *J. Atmos. Sci.*, *61*, 324–337.

Beres, J., R.R.Garcia, B. Boville, and F. Sassi (2005), Implementation of a gravity wave source spectrum parameterization dependent on the properties of convection in the Whole Atmosphere Community Climate Model (WACCM), *J. Geophys. Res.*, *110*(D10108), doi:10.1029/2004JD005,504.

Bluestein, H., and M. Jain (1985), Formation of mesoscale lines of precipitation - severe squall lines in Oklahoma during the spring, *J. Atmos. Sci.*, *42*(16), 1711–1732.

Blumen, W. (1972), Geostrophic adjustment, *Reviews of Geophysics and Space Physics*, *10*(2), 485–528.

Blumen, W., and R. Wu (1995), Geostrophic adjustment: frontogenesis and energy conversion, *J. Phys. Oceanogr.*, *25*, 428–438.

Boccara, G., A. Hertzog, R. Vincent, and F. Vial (2008), Estimation of gravity-wave momentum fluxes and phase speeds from long-duration stratospheric balloon flights. 1. Theory and simulations, *J. Atmos. Sci.*, *65*, 3042–3055.

Bokhove, O., and T. Shepherd (1996), On hamiltonian balanced dynamics and the slowest invariant manifold, *J. Atmos. Sci.*, *53*, 276–297.

Bosart, L., W. Bracken, and A. Seimon (1998), A study of cyclone mesoscale structure with emphasis on a large-amplitude inertia-gravity wave, *Mon. Weath. Rev.*, *126*, 1497–1527.

Brunet, G., and M. Montgomery (2002), Vortex Rossby waves on smooth circular vortices. Part I. Theory, *Dyn. Atmos. Ocean*, *35*, 153–177.

Bühler, O. (2009), *Waves and mean flows*, 341pp pp., Cambridge University Press.

Bühler, O., and M. McIntyre (1999), On shear-generated gravity waves that reach the mesosphere. Part II: wave propagation, *J. Atmos. Sci.*, *56*, 3764–3773.

Bühler, O., and M. McIntyre (2003), Remote recoil: a new wave-mean interaction effect, *J. Fluid Mech.*, *492*, 207–230.

Bühler, O., and M. McIntyre (2005), Wave capture and wave-vortex duality, *J. Fluid Mech.*, *534*, 67–95.

Bühler, O., M. McIntyre, and J. Scinocca (1999), On shear-generated gravity waves that reach the mesosphere. Part I: wave generation, *J. Atmos. Sci.*, *56*, 3749–3763.

Bush, A., J. McWilliams, and W. Peltier (1995), Origins and evolution of imbalance in synoptic-scale baroclinic wave life cycles, *J. Atmos. Sci.*, *52*, 1051–1069.

Buss, S., A. Hertzog, C. Hostettler, T. Bui, D. Lüthi, and H. Wernli (2004), Analysis of a jet stream induced gravity wave associated with an observed stratospheric ice cloud over Greenland, *Atmos. Chem. Phys.*, *4*, 1680–7324/acp/2004–4–1183.

Cahn, A. (1945), An investigation of the free oscillations of a simple current system, *J. Atmos. Sci.*, *2*(2), 113–119.

Camassa, R. (1995), On the geometry of an atmospheric slow manifold, *Physica D*, *84*, 357–397.

Capet, X., J. McWilliams, M. Molemaker, and A. Schepetkin (2008a), Mesoscale to submesoscale transition in the california current system: Part I: Flow structure, eddy flux and observational tests, *J. Phys. Oceanogr.*, *38*, 44–69.

Capet, X., J. McWilliams, M. Molemaker, and A. Schepetkin (2008b), Mesoscale to submesoscale transition in the california current system: Part III: energy balance and flux, *J. Phys. Oceanogr.*, *38*, 2256–2269.

Carslaw, K., et al. (1998), Increased stratospheric ozone depletion due to mountain-induced atmospheric waves, *Nature*, *391*, 675–678.

Chagnon, J., and P. Bannon (2005a), Wave response during hydrostatic and geostrophic adjustment. Part I: Transient dynamics, *J. Atmos. Sci.*, *62*, 1311–1329.

Chagnon, J., and P. Bannon (2005b), Wave response during hydrostatic and geostrophic adjustment. Part I: Potential vorticity conservation and energy partitioning, *J. Atmos. Sci.*, *62*, 1330–1345.

Charney, J. (1948), On the scale of atmospheric motions, *Geophys. Publ. Oslo*, *17*(2), 1–17.

Charron, M., and E. Manzini (2002), Gravity waves from fronts: parameterization and middle atmosphere response in a general circulation model, *J. Atmos. Sci.*, *59*, 923–941.

Chimonas, G., and J. Grant (1984), Shear excitation of gravity waves. Part II: upscale scattering from Kelvin-Helmholtz waves, *J. Atmos. Sci.*, *41*, 2278–2288.

Clark, T., T. Hauf, and J. Kuettner (1986), Convectively forced internal gravity waves: results from two-dimensional numerical experiments, *Q.J.R. Meteorol. Soc.*, *112*, 899–925.

Cram, J., R. Pielke, and W. Cotton (1992), Numerical simulation and analysis of a pre-frontal squall line. Part II: Propagation of the squall line as an internal gravity wave, *J. Atmos. Sci.*, *49*, 209–225.

Cunningham, P., and D. Keyser (2000), Analytical and numerical modelling of jet streaks: barotropic dynamics, *Q.J.R. Meteorol. Soc.*, *126*, 3187–3217.

Danielsen, E., R. S. Hipskind, W. Starr, J. Vedder, S. Gaines, D. Kley, and K. Kelly (1991), Irreversible transport in the stratosphere by internal waves of short vertical wavelength, *J. Geophys. Res.*, *96*(D9), 17,433–17,452.

Danioux, E., J. Vanneste, P. Klein, and H. Sasaki (2012), Spontaneous inertia-gravity wave generation by surface-intensified turbulence, *J. Fluid Mech.*, *in press*.

D'Asaro, E., C. Eriksen, M. Levine, P. Niiler, C. Paulson, and P. V. Meurs (1995), Upper-ocean inertial currents forced by a strong storm. Part I: data and comparison with linear theory, *J. Phys. Oceanogr.*, *25*, 2909–2936.

Davis, C., and K. Emanuel (1991), Potential vorticity diagnostics of cyclogenesis, *J. Atmos. Sci.*, *119*, 1929–1953.

Davis, P., and W. Peltier (1979), Some Characteristics of the Kelvin-Helmholtz and Resonant Overreflection Modes of Shear Flow Instability and of Their Interaction through Vortex Pairing, *J. Atmos. Sci.*, *36*(12), 2394–2412.

Dewar, W., and P. Killworth (1995), Do fast gravity waves interact with geostrophic motions?, *Deep-Sea Research*, *42*(7), 1063–1081.

Dörnbrack, A., T. Birner, A. Fix, H. Flentje, A. Meister, H. Schmid, E. V. Browell, and M. J. Mahoney (2002), Evidence for inertia-gravity waves forming polar stratospheric clouds over Scandinavia, *J. Geophys. Res.*, *107*(D20), 8287, 10.1029/2001JD000,452.

Dritschel, D., and J. Vanneste (2006), Instability of a shallow-water potential-vorticity front, *J. Fluid Mech.*, *561*, 237–254.

Dritschel, D., and A. Viúdez (2003), A balanced approach to modelling rotating stably stratified geophysical flows, *J. Fluid Mech.*, *488*, 213–150.

Dunkerton, T. (1984), Inertia-gravity waves in the stratosphere, *J. Atmos. Sci.*, *41*, 3396–3404.

Eady, E. (1949), Long waves adn cyclone waves, *Tellus*, *1*, 33–52.

Eckermann, S. (2011), Explicitly Stochastic Parameterization of Nonorographic Gravity Wave Drag, *J. Atmos. Sci.*, *68*(8), 1749–1765.

Eckermann, S., and C. Marks (1996), An idealized ray model of gravity wave tidal interactions, *J. Geophys. Res.*, *101*, 21,195–21,212.

Eckermann, S., and C. Marks (1997), GROGRAT: a new model of the global propagation and dissipation of atmospheric gravity waves, *Adv. Space. Res.*, *20*(6), 1253–1256.

Eckermann, S., and R. Vincent (1993), VHF radar observations of gravity-wave production by cold fronts over Southern Australia, *J. Atmos. Sci.*, *50*, 785–806.

Eckermann, S., A. Dörnbrack, S. Vosper, H. Flentje, M. Mahoney, T. P. Bui, and K. Carslaw (2006), Mountain wave-induced polar stratospheric cloud forecasts for aircraft science flights during SOLVE/THESEO 2000, *Weather and Forecasting*, *21*, 42–68.

Eckermann, S., L. Hoffmann, M. H. adn D.L. Wu, and M. Alexander (2009), Antarctic NAT PSC belt of June 2003: Observational validation of the mountain wave seeding hypothesis, *Geophys. Res. Lett.*, *36*(L02807), doi:10.1029/2008GL036,629.

Einaudi, F., A. Bedard, and J. Finnigan (1989), A Climatology of Gravity Waves and Other Coherent Disturbances at the Boulder Atmospheric Observatory during MarchApril 1984, *jas*, *46*, 303–329.

Eom, J. (1975), Analysis of the internal gravity wave occurrence of 19 April 1970 in the Midwest, *Mon. Weath. Rev.*, *103*, 217–226.

Ern, M., and P. Preusse (2011), Implications for atmospheric dynamics derived from global observations of gravity wave momentum flux in stratosphere and mesosphere, *J. Geophys. Res.*, *116*(D19107), doi:10.1029/2011JD015,821.

Ern, M., P. Preusse, M. Alexander, and C. Warner (2004), Absolute values of gravity wave momentum flux derived from satellite data, *J. Geophys. Res.*, *109*(D20103), doi:10.1029/2006JD007,327.

Esler, J., and L. Polvani (2004), Kelvin-Helmholtz instability of potential vorticity layers: a route to mixing, *J. Atmos. Sci.*, *61*, 1392–1405.

Eyring, V., and Co-Authors (2007), Multimodel projections of stratospheric ozone in the 21st century, *J. Geophys. Res.*, *112*(D16303), doi:10.1029/2006JD008,332.

Fetzer, E., and J. Gille (1994), Gravity wave variance in LIMS temperatures. Part I: Variability and comparison with background winds, *J. Atmos. Sci.*, *51*, 2461–2483.

Ford, R. (1994a), The response of a rotating ellipse of uniform potential vorticity to gravity wave radiation, *Phys. Fluids*, *6*(11), 3694–3704.

Ford, R. (1994b), The instability of an axisymmetric vortex with monotonic potential vorticity in rotating shallow water, *J. Fluid Mech.*, *280*, 303–334.

Ford, R. (1994c), Gravity wave radiation from vortex trains in rotating shallow water, *J. Fluid Mech.*, *281*, 81–118.

Ford, R., M. E. McIntyre, and W. A. Norton (2000), Balance and the slow quasimanifold: some explicit results, *J. Atmos. Sci.*, *57*, 1236–1254.

Ford, R., M. E. McIntyre, and W. A. Norton (2002), Reply, *J. Atmos. Sci.*, *59*, 2878–2882.

Fovell, R., D. Durran, and J. Holton (1992), Numerical simulations of convectively generated stratospheric gravity waves, *J. Atmos. Sci.*, *49*, 1427–1442.

Fritts, D. (1980), Simlpe stability limits for vertically propagating unstable modes in a tanh(z) velocity profile with a rigid lower boundary, *J. Atmos. Sci.*, *37*, 1642–1648.

Fritts, D. (1982), Shear excitation of atmospheric gravity waves, *J. Atmos. Sci.*, *39*, 1936–1952.

Fritts, D. (1984), Shear excitation of atmospheric gravity waves. 2: Nonlinear radiation from a free shear-layer, *J. Atmos. Sci.*, *41*, 524–537.

Fritts, D., and M. Alexander (2003), Gravity wave dynamics and effects in the middle atmosphere, *Reviews of Geophysics*, *41*(1), 1003.

Fritts, D., and G. Nastrom (1992), Sources of mesoscale variability of gravity waves. Part II: Frontal, convective, and jet stream excitation, *J. Atmos. Sci.*, *49*(2), 111–127.

Fritts, D., C. Bizon, J. Werne, and C. Meyer (2003), Layering accompanying turbulence generation due to shear instability and gravity-wave breaking, *J. Geophys. Res.*, *108*(D8), 8452.

Fritts, D., B. Williams, C. She, J. Vance, M. Rapp, F.-J. Lbken, A. Mllemann, F. Schmidlin, and R. Goldberg (2004), Observations of extreme temperature and wind gradients near the summer mesopause with the MaCWAVE/MIDAS rocket campaign, *Geophys. Res. Lett.*, *31*(L24S06), doi:10.1029/2003GL019,389.

Fritts, D. C., and Z. Luo (1992), Gravity wave excitation by geostrophic adjustment of the jet stream. Part I: Two-dimensional forcing, *J. Atmos. Sci.*, *49*(8), 681–697.

Fueglistaler, S., A. E. Dessler, T. J. Dunkerton, I. Folkins, Q. Fu, and P. W. Mote (2009), Tropical Tropopause Layer, *Rev. Geophys.*, *47*(RG1004), doi:10.1029/2008RG000,267.

Gall, R., R. Williams, and T. Clark (1987), On the minimum scale of surface fronts, *J. Atmos. Sci.*, *44*, 2562–2574.

Gall, R., R. Williams, and T. Clark (1988), Gravity waves generated during frontogenesis, *J. Atmos. Sci.*, *45*(15), 2204–2219.

Garner, S. (1989), Fully Lagrangian numerical solutions of unbalanced frontogenesis and frontal collapse, *J. Atmos. Sci.*, *46*(6), 717–739.

Geller, M., and J. Gong (2010), Gravity wave kinetic, potential, and vertical fluctuation energies as indicators of different frequency gravity waves, *J. Geophys. Res.*, *115*(D11111), doi:10.1029/2009JD012,266.

Gertz, A., and D. Straub (2009), Near-Inertial Oscillations and the Damping of Midlatitude Gyres: A Modeling Study, *J. Phys. Oceanogr.*, *39*, 23382350.

Gettelman, A., P. Hoor, L. Pan, W. Randel, M. Hegglin, and T. Birner (2011), The extratropical upper troposphere and lower stratosphere, *Rev. Geophys.*, *49*(RG3003), 2011RG000,355.

Gill, A. E. (1982), *Atmosphere-ocean dynamics*, 662p pp., Academic Press.

Glendening, J. (1993), Nonlinear displacement of the geostrophic velocity jet created by mass imbalance, *J. Atmos. Sci.*, *50*, 1617–1628.

Gong, J., and M. Geller (2010), Vertical fluctuation energy in United States high vertical resolution radiosonde data as an indicator of convective gravity wave sources, *J. Geophys. Res.*, *115*(D11110), doi:10.1029/2009JD012,265.

Gong, J., M. Geller, and L. Wang (2008), Source spectra information derived from U.S. high-resolution radiosonde data, *J. Geophys. Res.*, *113*(D10106), doi:10.1029/2007JD009,252.

Gossard, E., and W. Hooke (1975), *Waves in the atmosphere. Developments in atmospheric science II*, 456pp pp., Elsevier Scientific Publishing Company.

Griffiths, M., and M. J. Reeder (1996), Stratospheric inertia-gravity waves generated in a numerical model of frontogenesis. I: Model solutions, *Q.J.R. Meteorol. Soc.*, *122*, 1153–1174.

Grivet-Talocia, S., F. Einaudi, W. Clark, R. Dennett, G. Nastrom, and T. VanZandt (1999), A 4-yr Climatology of Pressure Disturbances Using a Barometer Network in Central Illinois, *J. Atmos. Sci.*, *127*(7), 1613–1629.

Guest, F., M. Reeder, C. Marks, and D. Karoly (2000), Inertia-gravity waves observed in the lower stratosphere over Macquarie Island, *J. Atmos. Sci.*, *57*, 737–752.

Gula, J., R. Plougonven, and V. Zeitlin (2009a), Ageostrophic instabilities of fronts in a channel in a stratified rotating fluid, *J. Fluid Mech.*, *627*, 485–507.

Gula, J., V. Zeitlin, and R. Plougonven (2009b), Instabilities of two-layer shallow-water flows with vertical shear in the rotating annulus, *J. Fluid Mech.*, *638*, 27–47.

Hart, J. (1972), A laboratory study of baroclinic instability, *Geophys. Astrophys. Fluid Dyn.*, *3*, 181–209.

Haynes, P. (2005), Stratospheric dynamics, *Ann. Rev. Fluid Mech.*, *37*, 263–293.

Haynes, P., and J. Anglade (1997), The vertical-scale cascade in atmospheric tracers due to large-scale differential advection, *J. Atmos. Sci.*, *54*, 1121–1136.

Hertzog, A., and F. Vial (2001), A study of the dynamics of the equatorial lower stratosphere by use of ultra-long-duration balloons 2. Gravity waves, *J. Geophys. Res.*, *106*, 22,745–22,761.

Hertzog, A., C. Souprayen, and A. Hauchecorne (2001), Observation and backward trajectory of an inertia-gravity wave in the lower stratosphere, *Annales Geophysicae*, *19*, 1141–1155.

Hertzog, A., F. Vial, A. Dörnbrack, S. Eckermann, B. Knudsen, and J.-P. Pommereau (2002a), In situ observations of gravity waves and comparisons with numerical simulations during the SOLVE/THESEO 2000 campaign, *J. Geophys. Res.*, *D20*(doi:10.1029/2001JD001025), 8292.

Hertzog, A., F. Vial, C. Mechoso, C. Basdevant, and P. Cocquerez (2002b), Quasi-Lagrangian measurements in the lower stratosphere reveal an energy peak associated with near-inertial waves, *Geophys. Res. Let.*, *29*(8), 70.

Hertzog, A., G. Boccara, R. Vincent, F. Vial, and P. Coquerez (2008), Estimation of gravity-wave momentum fluxes and phase speeds from long-duration stratospheric balloon flights. 2. Results from the Vorcore campaign in Antarctica, *J. Atmos. Sci.*, *65*, 3056–3070.

Hertzog, A., M. Alexander, and R. Plougonven (2012), On the probability density functions of gravity waves momentum flux in the stratosphere, *J. Atmosph. Sci.*

Hertzog, A., et al. (2007), Stratéole/Vorcore - Long duration, superpressure balloons to study the antarctic stratosphere during the 2005 winter, *J. Ocean. Atmos. Tech.*, *24*, 2048–2061.

Hines, C. (1968), A possibile source of waves in noctilucent clouds, *J. Atmos. Sci.*, *25*, 937–942.

Hirota, I., and T. Niki (1985), A statistical study of inertia-gravity waves in the middle atmosphere, *J. Meteor. Soc. Japan*, *63*, 1055–1065.

Hitchman, M., M. Buker, G. Tripoli, E. Browell, W. Grant, T. McGee, and J. Burris (2003), Nonorographic generation of Arctic polar stratospheric clouds during December 1999, *J. Geophys. Res.*, *108*(D5), 8325.

Holton, J. R. (1992), *An introduction to dynamic meteorology*, third ed., Academic Press, London.

Hoskins, B., M. McIntyre, and A. Robertson (1985), On the use and significance of isentropic potential vorticity maps, *Q.J.R. Meteorol. Soc.*, *111*(470), 877–946.

Hoskins, B. J. (1982), The mathematical theory of frontogenesis, *Ann. Rev. Fluid Mech.*, *14*, 131–151.

Hoskins, B. J., and F. P. Bretherton (1972), Atmospheric frontogenesis models: mathematical formulation and solution, *J. Atmos. Sci.*, *29*, 11–37.

Jacoby, T., P. Read, P. Williams, and R. Young (2011), Generation of inertia-gravity waves in the rotating thermal annulus by a localized boundary layer instability, *Geophys. Astrophys. Fluid Dyn.*, *iFirst: 11 March 2011*(10.1080/03091929.2011.560151), 1–21.

Jensen, E., and L. Pfister (2004), Transport and freeze-drying in the tropical tropopause layer, *J. Geophys. Res.*, *109*(D02207), doi:10.1029/2003JD004,022.

Jensen, E., O. Toon, L. Pfister, and H. Selkirk (1996), Dehydration of the upper troposphere and lower stratosphere by subvisible cirrus clouds near the tropical tropopause, *Geophys. Res. Lett.*, *23*(8), 825–828.

Jewett, B., M. Ramamurthy, and R. Rauber (2003), Origin, evolution, and finescale structure of the St. Valentine's Day mesoscale gravity wave observed during STORM-FEST. Part III: Gravity wave genesis and the role of evaporation, *Mon. Weath. Rev.*, *131*(4), 617–633.

Jin, Y. (1997), *A numerical model study of the role of mesoscale gravity waves in rainband dynamics in the central United States during STORM-FEST (Ph.D. Dissertation)*, 318 pp. pp., North Carolina State University.

Joly, A., et al. (1997), The Fronts and Atlantic Stormtracks Experiment (FASTEX): scientific objectives and experimental design, *Bull. Amer. Meteorol. Soc.*, *78*(9), 1917–1940.

Juckes, M. (1994), Quasi-geostrophic dynamics of the tropopause, *J. Atmos. Sci.*, *51*, 2756–2768.

Kalashnik, M. V. (1998), Forming of frontal zones during geostrophic adjustment in a continuously stratified fluid, *Izvetiya, Atmospheric and Oceanic Physics*, *34*(6), 785–792.

Kalashnik, M. V. (2000), Geostrophic adjustment and frontogenesis in a continuously stratified fluid, *Izvetiya, Atmospheric and Oceanic Physics*, *36*(3), 386–395.

Kalnay, E. (2003), *Atmospheric modeling, data assimilation and predictability*, 341pp pp., Cambridge University Press.

Kaplan, M., S. Koch, Y.-L. Lin, R. Weglarz, and R. Rozumalski (1997), Numerical Simulations of a Gravity Wave Event over CCOPE. Part I: The Role of Geostrophic Adjustment in Mesoscale Jetlet Formation, *Mon. Weath. Rev.*, *125*, 1185–1211.

Kim, S.-Y., and H.-Y. Chun (2011), Statistics and Possible Sources of Aviation Turbulence over South Korea, *J. App. Meteor. Clim.*, *50*, 311–324.

Kim, Y.-J., S. Eckermann, and H.-Y. Chun (2003), An overview of the past, present and future of gravity-wave drag parametrization for numerical climate and weather prediction models, *Atmosphere-Ocean*, *41*, 65–98.

Klein, P., and S. L. Smith (2001), Horizontal dispersion of near-inertial oscillations in a turbulent mesoscale eddy field, *J. Mar. Res.*, *59*, 697–723.

Klein, P., B. Hua, G. Lapeyre, X. Capet, S. LeGentil, and H. Sasaki (2008), Upper ocean turbulence from high 3Dresolution simulations, *J. Phys. Oceanogr.*, *38*, 1748.

Knox, J., D. McCann, and P. Williams (2008), Application of the lighthill-ford theory of spontaneous imbalance to Clear-Air Turbulence forecasting, *J. Atmos. Sci.*, *65*, 3292–3304.

Knox, J., D. McCann, and P. Williams (2009), Reply, *J. Atmos. Sci.*, *66*, 2511–2516.

Knupp, K. (2006), Observational Analysis of a Gust Front to Bore to Solitary Wave Transition within an Evolving Nocturnal Boundary Layer, *J. Atmos. Sci.*, *63*(8), 2016–2035.

Koch, S., and R. Golus (1988), A mesoscale gravity-wave event observed during CCOPE. 1. Multiscale statistical analysis of wave characteristics, *Mon. Weath. Rev.*, *116*(12), 2527–2544.

Koch, S., and C. O'Handley (1997), Operational Forecasting and Detection of Mesoscale Gravity Waves, *Wea. Forecasting*, *12*, 253–281.

Koch, S., and S. Saleeby (2001), An automated system for the analysis of gravity waves and other mesoscale phenomena, *Weather and Forecasting*, *16*, 661–679.

Koch, S., R. Golus, and P. Dorian (1988), A mesoscale gravity wave event observed during CCOPE. Part II: Interactions between mesoscale convective systems and the antecedent waves, *Mon. Weath. Rev.*, *116*, 2545–2569.

Koch, S., F. Einaudi, P. Dorian, S. Lang, and G. Heymsfield (1993), A Mesoscale Gravity-Wave Event Observed during CCOPE. Part IV: Stability Analysis and Doppler-derived Wave Vertical Structure, *Mon. Weath. Rev.*, *121*, 2483–2510.

Koch, S., F. Zhang, M. Kaplan, Y. Lin, R. Weglarz, and C. Trexler (2001), Numerical simulations of a gravity wave event over CCOPE. Part III: The role of a mountain-plains solenoid in the generation of the second wave episode, *Mon. Weath. Rev.*, *129*(5), 909–933.

Koch, S., et al. (2005), Turbulence and gravity waves within an upper-level front, *J. Atmos. Sci.*, *62*, 3885–3908.

Koch, S. E., and P. B. Dorian (1988), A mesoscale gravity wave event observed during CCOPE. Part III: wave environment and possible source mechanisms, *Mon. Wea. Rev*, *116*, 2570–2591.

Koppel, L., L. Bosart, and D. Keyser (2000), A 25-yr Climatology of Large-Amplitude Hourly Surface Pressure Changes over the Conterminous United States, *Mon. Weath. Rev.*, *128*(1), 51–68.

Kuo, A. C., and L. M. Polvani (1997), Time-dependent fully nonlinear geostrophic adjustment, *J. Phys. Oceanogr.*, *27*, 1614–1634.

Kuo, A. C., and L. M. Polvani (2000), Nonlinear geostrophic adjustment, cyclone/anticyclone asymmetry, and potential vorticity rearrangement, *Phys. Fluids*, *12*(5), 1087–1100.

Kuo, H. (1997), A new perspective of geostrophic adjustment, *Dyn. Atmos. Ocean*, *27*, 413–437.

Kushner, P., M. McIntyre, and T. Shepherd (1998), Coupled kelvin-wave and mirage wave instabilities in semi-geostrophic dynamics, *J. Phys. Oceanogr.*, *28*, 513–518.

Lalas, D., and F. Einaudi (1976), On the characteristics of waves generated by shear layers, *J. Atmos. Sci.*, *33*, 1248–1259.

Lalas, D., F. Einaudi, and D. Fua (1976), The destabilizing effect of the ground on Kelvin-Helmholtz waves in the atmosphere, *J. Atmos. Sci.*, *33*, 59–69.

Lane, T., J. Doyle, R. Plougonven, R. Sharman, and M. Shapiro (2004), Numerical modeling of gravity waves and shearing instabilities above an observed jet, *J. Atmos. Sci.*, *61*, 2692–2706.

Lapeyre, G., B. Hua, and P. Klein (1999), Does the tracer gradient vector align with the strain eigenvectors in 2d turbulence?, *Phys. Fluids*, *11*, 3729–3737.

Lawrence, G., F. Browand, and L. Redekopp (1991), The stability of a sheared density interface, *Phys. Fluids*, *3*, 2360–2370.

LeDizès, S., and P. Billant (2009), Radiative instability in stratified vortices, *Phys. Fluids*, *21*(096602), doi:10.1063/1.3241,995.

Leith, C. (1980), Nonlinear normal mode initialization and quasi-geostrophic theory, *J. Atmos. Sci.*, *37*, 958–968.

Ley, B., and W. Peltier (1978), Wave generation and frontal collapse, *J. Atmos. Sci.*, *35*(1), 3–17.

Li, Q., J. Xu, J. Yue, W. Yuan, and X. Liu (2011), Statistical characteristics of gravity wave activities observed by an OH airglow imager at Xinglong, in northern China, *ANN.*

Geophys., *29*(doi:10.5194/angeo-29-1401-2011), 1401–1410.

Lighthill, J. M. (1952), On sound generated aerodynamically, I. General theory, *Proc. Roy. Soc. London*, *211*(A), 564–587.

Lighthill, J. M. (1978), *Waves in Fluids*, Cambridge University Press.

Lin, Y., and F. Zhang (2008), Tracking gravity waves in baroclinic jet-front systems, *J. Atmos. Sci.*, *65*, 2402–2415.

Lin, Y.-L., and R. Goff (1988), A case study of solitary wave in the atmosphere originating near a region of deep convection, *J. Atmos. Sci.*, *45*, 194–205.

Lindzen, R., and M. Fox-Rabinowitz (1989), Consistent vertical and horizontal resolution, *Mon. Weath. Rev.*, *117*, 2575–2583.

Lindzen, R., and K.-K. Tung (1976), Banded convective activity and ducted gravity waves, *Mon. Weath. Rev.*, *104*, 1602–1617.

Liu, A., and G. Swenson (2003), A modeling study of 02 and OH airglow perturbations induced by atmospheric gravity waves, *J. Geophys. Res.*, *108*(D4), 4151.

Lorenz, E. (1980), Attractor sets and quasi-geostrophic equilibrium, *J. Atmos. Sci.*, *37*, 1685–1699.

Lorenz, E. (1986), On the existence of a slow manifold, *J. Atmos. Sci.*, *43*, 1547–1557.

Lorenz, E., and V. Krishnamurty (1987), On the nonexistence of a slow manifold, *J. Atmos. Sci.*, *44*, 2940–2950.

Lott, F. (1997), The transient emission of propagating gravity waves by a stably stratified shear layer, *Q.J.R. Meteorol. Soc.*, *123*, 1603–1619.

Lott, F., H. Kelder, and H. Teitelbaum (1992), A transition from Kelvin-Helmholtz instabilities to propagating wave instabilities, *Phys. Fluids*, *4*(9), 1990–1997.

Lott, F., R. Plougonven, and J. Vanneste (2010), Gravity waves generated by sheared potential vorticity anomalies, *J. Atmos. Sci.*, *67*(DOI:10.1175/2009JAS3134.1), 157–170.

Lott, F., L. Guez, and P. Maury (2012a), A stochastic parameterization of non-orographic gravity waves: Formalism and impact on the equatorial stratosphere, *Geophys. Res. Lett.*, *39*(L06807), 10.1029/2012GL051,001.

Lott, F., R. Plougonven, and J. Vanneste (2012b), Gravity waves generated by sheared three-dimensional potential vorticity anomalies, *J. Atmos. Sci.*

Lovegrove, A., P. Read, and C. Richards (2000), Generation of inertia-gravity waves in a baroclinically unstable fluid, *Q.J.R. Meteorol. Soc.*, *126*, 3233–3254.

Luo, Z., and D. Fritts (1993), Gravity wave excitation by geostrophic adjustment of the jet stream. Part II: Three dimensional forcing, *J. Atmos. Sci.*, *50*(1), 104–115.

Lynch, P. (2002), *Geometric Methods and Models, Vol. II, Large-Scale Atmosphere-Ocean Dynamics*, chap. The swinging spring: A simple model for atmospheric balance., pp. 64–108, Cambridge University Press.

Machenhauer, B. (1977), On the dynamics of gravity oscillations in a shallow water model, with applications to normal mode initialization, *Contrib. Atmos. Phys.*, *50*, 253–271.

MacKay, R. (2004), *Energy localisation and transfer*, chap. Slow manifolds, pp. 149–192, World Sci.

Mahalov, A., M. Moustaoui, B. Nicolaenko, and K. Tse (2007), Computational studies of inertia-gravity waves radiated from upper tropospheric jets, *Theoretical and Computational Fluid Dynamics*, *21*(6), 399–422.

Mamatsashvili, G., V. Avsarkisov, G. Chagelishvili, R. Chanishvili, and M. Kalashnik (2010), Transient Dynamics of Nonsymmetric Perturbations versus Symmetric Instability in Baroclinic Zonal Shear Flows, *J. Atmos. Sci.*, *67*(9), 2972–2989.

Mann, G., K. S. Carslaw, M. P. Chipperfield, and S. Davies (2005), Large nitric acid trihydate particles and denitrification caused by mountain waves in the Arctic stratosphere, *J. Geophys. Res.*, *110*(D08202), doi:10.1029/2004JD005,271.

Mastrantonio, G., F. Einaudi, D. Fua, and D. Lalas (1976), Generation of gravity waves by jet streams in the atmosphere, *J. Atmos. Sci.*, *33*, 1730–1738.

Matsumoto, S. (1961), A note on geosrophic adjustment and gravity waves in the atmosphere, *J. Meteor. Soc. Japan*, *39*, 18–28.

McDonald, A., S. George, and R. Woollands (2009), Can gravity waves significantly impact PSC occurence in the Antarctic?, *Atmos. Chem. Phys.*, *9*, 8825–8840.

McIntyre, M. (2001), Global effects of gravity waves in the middle atmosphere: a theoretical perspective, *Adv. Space Res.*, *27*(10), 1723–1736.

McIntyre, M. (2009), Spontaneous imbalance and hybrid vortex-gravity wave structures, *J. Atmos. Sci.*, *66*, 1315–1326.

McIntyre, M., and M. Weissman (1978), On radiating instabilities and resonant overreflection, *J. Atmos. Sci.*, *35*, 1190–1196.

McWilliams, J. (2003), *Nonlinear Processes in Geophysical Fluid Dynamics*, chap. Diagnostic force balance and its limits, pp. 287–304, Kluwer.

McWilliams, J., and I. Yavneh (1998), Fluctuation growth and instability associated with a singularity of the balance equations, *Phys. Fluids*, *10*(10), 2587–2596.

McWilliams, J., M. Molemaker, and I. Yavneh (2001), From stirring to mixing of momentum: cascades from balanced flows to dissipation in the oceanic interior, in *Aha Huliko'a Proceedings*, pp. 59–66.

McWilliams, J. C., and P. R. Gent (1980), Intermediate models of planetary circulations in the atmosphere and ocean, *J. Atmos. Sci.*, *37*(8), 1657–1678.

Miller, J. (1948), On the concept of frontogenesis, *J. Meteorology*, *5*, 169–171.

Molemaker, M., J. McWilliams, and I. Yavneh (2001), Instability and equilibration of centrifugally stable stratified Taylor-Couette flow, *Phys. Rev. Lett.*, *86*(23), 5270–5273.

Molemaker, M., J. McWilliams, and I. Yavneh (2005), Baroclinic instability and loss of balance, *J. Phys. Oceanogr.*, *35*, 1505–1517.

Molemaker, M., J. McWilliams, and X. Capet (2010), Balanced and unbalanced routes to dissipation in an equilibrated Eady flow, *J. Fluid Mech.*, *654*, 35–63.

Moustaoui, M., H. Teitelbaum, P. van Velthoven, and H. Kelder (1999), Analysis of gravity waves during the POLINAT experiment and some consequences for stratosphere-troposphere exchange, *J. Atmos. Sci.*, *56*, 1019–1030.

Müller, P., J. McWilliams, and M. Molemaker (2005), *Marine Turbulence: Theories, Observations and Models*, chap. Routes to dissipation in the ocean: the 2d/3d turbulence conundrum., pp. 397–405, Cambridge University Press, Cambridge.

Muraki, D., and C. Snyder (2007), Vortex dipoles for surface quasigeostrophic models, *J. Atmos. Sci.*, *64*, 2961–2967.

Murayama, Y., T. Tsuda, R. Wilson, H. Nakane, S. Hayashida, N. Sugimoto, I. Matsui, and Y. Sasano (1994), Gravity wave activity in the upper stratosphere and lower mesosphere observed with the Rayleigh lidar at Tsukuba, Japan, *Geophys. Res. Lett.*, *21*(14), 1539–1542.

Nakamura, N. (1988), Scale slection of baroclinic instability - effects of stratification and nongeostrophy, *J. Atmos. Sci.*, *45*(21), 3253–3267.

Nastrom, G., and D. Fritts (1992), Sources of mesoscale variability of gravity waves. part i: topographic excitation, *J. Atmos. Sci.*, *49*(2), 101–109.

Nicholls, M., R. Pielke, and W. Cotton (1991), Thermally forced gravity waves in an atmosphere at rest, *J. Atmos. Sci.*, *48*(16), 1869–1884.

Obukhov, A. (1949), On the question of geostrophic wind (in Russian), *Izv. Akad. Nauk. SSSR Ser. Geografs.-Geofiz.*, *13*(4), 281–306.

Olafsdottir, E., A. O. Daalhuis, and J. Vanneste (2008), Inertia-gravity-wave generation by a sheared vortex, *J. Fluid Mech.*, *569*, 169–189.

O'Sullivan, D., and T. Dunkerton (1995), Generation of inertia-gravity waves in a simulated life cycle of baroclinic instability, *J. Atmos. Sci.*, *52*(21), 3695–3716.

Ou, H. W. (1984), Geostrophic adjustment: a mechanism for frontogenesis, *J. Phys. Oceanogr.*, *14*, 994–1000.

Paegle, J. (1978), The transient mass-flow adjustment of heated atmospheric circulations, *J. Atmos. Sci.*, *35*, 1678–1688.

Palmer, T. (2001), A nonlinear dynamical perspective on model error: A proposal for non-local stochastic-dynamic parametrization in weather and climate prediction models, *Q.J.R. Meteorol. Soc.*, *127*(572), 279–304.

Pan, L., et al. (2010), The stratosphere-troposphere analyses of regional transport 2008 experiment, *Bull. Amer. Meteorol. Soc.*, *91*(DOI:10.1175/2009BAMS2865.1), 327–342.

Parsons, D., and P. Hobbs (1983), The mesoscale and microscale structure and organization of clouds and precipitation in mid-latitude cyclones. 11. Comparisons between observational and theorectical aspects of rainbands, *J. Atmos. Sci.*, *40*(10), 2377–2397.

Pavelin, E., and J. Whiteway (2002), Gravity wave interactions around the jet stream, *Geophys. Res. Lett.*, *29*(21), 2024–2027.

Pavelin, E., J. Whiteway, and G. Vaughan (2001), Observation of gravity wave generation and breaking in the lowermost stratosphere, *J. Geophys. Res.*, *106*(D6), 5173–5179.

Pawson, S., et al. (2000), The GCM-Reality Intercomparison Project for SPARC (GRIPS): scientific issues and initial results, *Bull. Amer. Meteor. Soc.*, *81*, 781–796.

Peters, D., P. Hoffmann, and M. Alpers (2003), On the appearance of inertia-gravity waves on the North-Easterly side of an anticyclone, *Meteo. Zeitschrift*, *12*(1), 25–35.

Pierce, R., and T. Fairlie (1993), Chaotic advection in the stratosphere: implications for the dispersal of chemically perturbed air from the polar vortex, *J. Geophys. Res.*, *98*(D10), 18,589–18,595.

Pierce, R., and W. Grant (1998), Seasonal evolution of Rossby and gravity wave induced laminae in ozonesonde data obtained from Wallops Island, Virginia, *Geophys. Res. Lett.*, *25*, 1859–1862.

Plougonven, R., and C. Snyder (2005), Gravity waves excited by jets: propagation versus generation, *Geoph. Res. Lett.*, *32*(L18892), doi:10.1029/2005GL023,730.

Plougonven, R., and C. Snyder (2007), Inertia-gravity waves spontaneously generated by jets and fronts. Part I: Different baroclinic life cycles, *J. Atmos. Sci.*, *64*, 2502–2520.

Plougonven, R., and H. Teitelbaum (2003), Comparison of a large-scale inertia-gravity wave as seen in the ECMWF and from radiosondes, *Geophys. Res. Let.*, *30*(18), 1954.

Plougonven, R., and V. Zeitlin (2002), Internal gravity wave emission from a pancake vortex: an example of wave-vortex interaction in strongly stratified flows, *Phys. of Fluids*, *14*(3), 1259–1268.

Plougonven, R., and V. Zeitlin (2005), Lagrangian approach to the geostrophic adjustment of frontal anomalies in a stratified fluid, *Geophys. Astr. Fluid Dyn.*, *99*(2), 101–135.

Plougonven, R., and F. Zhang (2007), On the forcing of inertia-gravity waves by synoptic-scale flows, *J. Atmos. Sci.*, *64*, 1737–1742.

Plougonven, R., H. Teitelbaum, and V. Zeitlin (2003), Inertia-gravity wave generation by the tropospheric mid-latitude jet as given by the fastex radiosoundings, *J. Geophys. Res.*, *108*(D21), 4686.

Plougonven, R., D. Muraki, and C. Snyder (2005), A baroclinic instability that couples balanced motions and gravity waves, *J. Atmos. Sci.*, *62*, 1545–1559.

Plougonven, R., A. Hertzog, and H. Teitelbaum (2008), Observations and simulations of a large-amplitude mountain wave breaking above the Antarctic Peninsula, *J. Geophys. Res.*, *113*(D16113), doi:10.1029/2007JD009,739.

Plougonven, R., C. Snyder, and F. Zhang (2009), Comments on 'application of the Lighthilll-Ford theory of spontaneous imbalance to clear-air turbulence forecasting', *J. Atmos. Sci.*, *66*, 2506–2510.

Plougonven, R., A. Arsac, A. Hertzog, L. Guez, and F. Vial (2010), Mesoscale simulations of the gravity wave field above antarctica during vorcore, *Quart. J. Roy. Meteorolog. Soc.*, *136*(650), 1371–1377.

Plougonven, R., A. Hertzog, and L. Guez (2012), Gravity waves over Antarctica and the Southern Ocean: consistent momentum fluxes in mesoscale simulations and stratospheric balloon observations, *in preparation for Quart. J. Roy. Meteorolog. Soc.*

Pokrandt, P., G. Tripoli, and D. Houghton (1996), Processes leading to the formation of mesoscale waves in the Midwest cyclone of 15 December 1987, *Mon. Weath. Rev.*, *124*, 2726–2752.

Polzin, K. (2008), Mesoscale EddyInternal Wave Coupling. Part I: Symmetry, Wave Capture, and Results from the Mid-Ocean Dynamics Experiment, *J. Phys. Oceanogr.*, *38*, 2556–2574.

Polzin, K. (2010), Mesoscale EddyInternal Wave Coupling. Part II: Energetics and Results from PolyMode, *J. Phys. Oceanogr.*, *340*, 789–801.

Potter, B., and J. Holton (1995), The role of monsoon convection in the dehydration of the lower tropical stratosphere, *J. Atmos. Sci.*, *52*(8), 1034–1050.

Powers, J. (1997), Numerical model simulation of a mesoscale gravity-wave event: sensitivity tests and spectral analyses, *Mon. Weath. Rev.*, *125*, 1838–1869.

Powers, J., and R. Reed (1993), Numerical simulation of the large-amplitude mesoscale gravity wave event of 15 December 1987 in the Central United States, *Mon. Weath. Rev.*, *121*, 2285–2308.

Preusse, P., S. Eckermann, and M. Ern (2008), Transparency of the atmosphere to short horizontal wavelength gravity waves, *J. Geophys. Res.*, *113*(10.1029/2007JD009682), D24,104.

Queney, P. (1948), The problem of air flow over mountains: A summary of theoretical studies, *Bull. Am. Meteorol. Soc.*, *29*, 16–26.

Ralph, F., M. Crochet, and S. Venkateswaran (1993), Observations of a mesoscale ducted gravity wave, *J. Atmos. Sci.*, *50*(19), 3277–3291.

Ralph, F., P. Neiman, and T. Keller (1999), Deep-tropospheric gravity waves created by leeside cold fronts, *J. Atmos. Sci.*, *56*, 2986–3009.

Ramamurthy, M., R. Rauber, B. Collins, and N. Malhotra (1993), A comparative study of large amplitude gravity wave events, *Mon. Weath. Rev.*, *121*(11), 2951–2974.

Rauber, R., M. Yang, M. Ramamurthy, and B. Jewett (2001), Origin, Evolution, and Finescale Structure of the St. Valentines Day Mesoscale Gravity Wave Observed during STORM-FEST. Part I: Origin and Evolution, *Mon. Weath. Rev.*, *129*(2), 198–217.

Read, P. (1992), Applications of singular systems analysis to baroclinic chaos, *Physica D*, *58*, 455–468.

Reeder, M. J., and M. Griffiths (1996), Stratospheric inertia-gravity waves generated in a numerical model of frontogenesis. Part II: Wave sources, generation mechanisms and momentum fluxes., *Q.J.R. Meteorol. Soc.*, *122*, 1175–1195.

Reznik, G., V. Zeitlin, and M. B. Jelloul (2001), Nonlinear theory of geostrophic adjustment. Part 1. Rotating shallow-water model, *J. Fluid Mech.*, *445*, 93–120.

Rhines, P., E. Lindahl, and A. Mendez (2006), Optical altimetry: A new method for observing rotating fluids with application to Rossby waves on a polar beta-plane., *J. Fluid Mech.*, *572*, 389–412.

Richiardone, R., and M. Manfrin (2003), A rain episode related to a mesoscale gravity wave, *Bull. Amer. Meteorol. Soc.*, *84*(10.1175/BAMS-84-11-1494), 1494–1498.

Richter, J., M. Geller, R. Garcia, H.-L. Liu, and F. Zhang (2007), Report on the gravity wave retreat, *SPARC Newsletter*, *28*, 26–27.

Richter, J., F. Sassi, and R. Garcia (2010), Toward a physically based gravity wave source parameterization in a general circulation model, *J. Atmos. Sci.*, *67*(doi:10.1175/2009JAS3112.1), 136–156.

Riedinger, X., S. LeDizès, and P. Meunier (2010a), Viscous stability properties of a Lamb-Oseen vortex in a stratified fluid, *J. Fluid Mech.*, *655*, 255–278.

Riedinger, X., P. Meunier, and S. LeDizès (2010b), Instability of a columnar vortex in a stratified fluid, *Exp. Fluids*, *49*, 673–681.

Riedinger, X., S. LeDizès, and P. Meunier (2011), Radiative instability of the flow around a rotating cylinder in a stratified fluid, *J. Fluid Mech.*, *672*, 130–146.

Rind, D., R. Suozzo, N. Balachandran, A. Lacis, and G. Russell (1988), The GISS global climate-middle atmosphere model. Part I: model structure and climatology, *J. Atmos. Sci.*, *45*(3), 329–370.

Rossby, C. (1938), On the mutual adjustment of pressure and velocity distributions in certain simple current systems II, *J. Mar. Res.*, *1*, 239–263.

Sakai, S. (1989), Rossby-kelvin instability: a new type of ageostrophic instability caused by a resonance between rossby waves and gravity waves, *J. Fluid Mech.*, *202*, 149–176.

Sato, K. (1994), A statistical study of the structure, saturation and sources of inertio-gravity waves in the lower stratosphere observed with the MU radar, *J. Atmos. Terr. Phys.*, *56*(6), 755–774.

Sato, K., and M. Yoshiki (2008), Gravity wave generation around the polar vortex in the stratosphere revealed by 3-hourly radiosonde observations at Syowa Station, *J. Atmos. Sci.*, *65*, 3719–3735.

Sato, K., S. Watanabe, Y. Kawatani, Y. Tomikawa, K. Miyazaki, and M. Takayashi (2009), On the origins of mesospheric gravity waves, *Geophys. Res. Lett.*, *36*(L19801), doi:10.1029/2009GL039,908.

Schecter, D. (2008), The spontaneous imbalance of an atmospheric vortex at high Rossby number, *J. Atmos. Sci.*, *65*, 2498–2521.

Schecter, D., and M. Montgomery (2006), Conditions that inhibit the spontaneous radiation of spiral inertia-gravity waves from an intense mesoscale cyclone, *J. Atmos. Sci.*, *63*, 435–456.

Schmidt, J., and W. Cotton (1990), Interactions between upper and lower tropospheric gravity waves on squall line structure and maintenance, *J. Atmos. Sci.*, *47*, 1205–1222.

Schneider, R. (1990), Large-Amplitude Mesoscale Wave Disturbances Within the Intense Midwest Extratropical Cyclone of 15 December 1987, *Weather and forecasting*, *5*, 533–558.

Schroeder, S., P. Preusse, M. Ern, and M. Riese (2009), Gravity waves resolved in ECMWF and measured by SABER, *Geophys. Res. Lett.*, *36*(L10805), doi: 10.1029/2008GL037,054.

Schubert, W., J. Hack, P. S. Dias, and S. Fulton (1980), Geostrophic adjustment in an axisymmetric vortex, *J. Atmos. Sci.*, *37*, 1464–1484.

Scinocca, J., and R. Ford (2000), The nonlinear forcing of large-scale internal gravity waves by stratified shear instability, *J. Atmos. Sci.*, *57*, 653–672.

Scolan, H., J.-B. Flor, and J. Gula (2011), Frontal instabilities and waves in a differentially rotating fluid, *J. Fluid Mech.*, *685*, 532–542.

Sharman, R., C. Tebaldi, G. Wiener, and J. Wolff (2006), An integrated approach to mid- and upper-level turbulence forcasting, *Weather and Forecasting*, pp. 268–287.

Sharman, R., S. Trier, T. Lane, and J. Doyle (2012), Source and dynamics of turbulence in the upper troposphere and lower stratosphere: a review, *Geophys. Res. Lett.*, *39* (L12803), doi:10.1029/2012GL051,996.

Shibata, T., K. Sato, H. Kobayashi, M. Yabuki, and M. Shiobara (2003), Antarctic polar stratospheric clouds under tempreature perturbations by nonorographic inertia-gravity waves observed by micropulse lidar at Syowa Station, *J. Geophys. Res.*, *108* (D3), 4105.

Shutts, G., and S. Vosper (2011), Stratospheric gravity waves revealed in NWP forecast models, *Q.J.R. Meteorol. Soc.*, *137* (655), 303–317.

Simmons, A., and B. Hoskins (1978), The life cycles of some nonlinear baroclinic waves, *J. Atmos. Sci.*, *35*, 414–432.

Snyder, C. (1995), Stability of steady fronts with uniform potential vorticity, *J. Atmos. Sci.*, *52* (6), 724–736.

Snyder, C., W. Skamarock, and R. Rotunno (1993), Frontal dynamics near and following frontal collapse, *J. Atmos. Sci.*, *50* (18), 3194–3211.

Snyder, C., D. Muraki, R. Plougonven, and F. Zhang (2007), Inertia-gravity waves generated within a dipole vortex, *J. Atmos. Sci.*, *64*, 4417–4431.

Snyder, C., R. Plougonven, and D. Muraki (2009), Forced linear inertia-gravity waves on a basic-state dipole vortex, *J. Atmos. Sci.*, *66* (11), 3464–3478.

Song, I.-S., and H.-Y. Chun (2005), Momentum flux spectrum of convectively forced internal gravity waves and its application to gravity wave drag parameterization. Part I: Theory, *J. Atmos. Sci.*, *62*, 107–124.

Spiga, A., H. Teitelbaum, and V. Zeitlin (2008), Identification and separation of the sources of inertia-gravity waves in the Andes Cordillera region, *Ann. Geophys.*, *26*, 2551–2568.

Stone, P. (1970), On non-geostrophic baroclinic instability: Part II, *J. Atmos. Sci.*, *27*, 721–726.

Sugimoto, N., and K. Ishii (2012), Spontaneous gravity wave radiation in a shallow water system on a rotating sphere, *J. Meteor. Soc. Jap.*, *90*, 101–125.

Sugimoto, N., K. Ishioka, and K. Ishii (2008), Parameter sweep experiments on spontaneous gravity wave radiation from unsteady rotational flow in an f-plane shallow water system, *J. Atmos. Sci.*, *65*, 235–249.

Sutherland, B. (2006), Rayleigh wave - internal wave coupling and internal wave generation above a model jet stream, *J. Atmos. Sci.*, *63*, 1042–1055.

Sutherland, B., and W. Peltier (1995), Internal gravity wave emission into the middle atmosphere from a model tropospheric jet, *J. Atmos. Sci.*, *52*, 3214–3235.

Sutherland, B., C. Caulfield, and W. Peltier (1994), Internal gravity wave generation and hydrodynamic instability, *J. Atmos. Sci.*, *51*, 3261–3280.

Sutyrin, G. (2007), Ageostrophic instabilities in a horizontally uniform baroclinic flow along a slope, *J. Fluid Mech.*, *588*(DOI: 10.1017/S0022112007006829), 463–473.

Sutyrin, G. (2008), Lack of balance in continuously stratified rotating flows, *J. Fluid Mech.*, *615*(DOI: 10.1017/S0022112008004059), 93–100.

Taylor, M., and M. Bishop (1995), All-sky measurements of short-period waves imaged in the OI (557.7 nm), Na(589.2 nm) and near-infrared OH and O2(0,1) nightglow emissions during the Aloha-93 campaign, *Geophys. Res. Lett.*, *22*(20), 2833–2836.

Teitelbaum, H., M. Moustaoui, J. Ovarlez, and H. Kelder (1996), The role of atmospheric waves in the laminated structure of ozone profiles, *Tellus*, *48A*, 442–455.

Tepper, M. (1951), On the dessication of a cloud bank by a propgating pressure wave, *Mon. Weath. Rev.*, *79*, 61–70.

Thomas, L., R. Worthington, and A. McDonald (1999), Inertia-gravity waves in the troposphere and lower stratosphere associated with a jet stream exit region, *Ann. Geophysicae*, *17*, 115–121.

Thorncroft, C., B. Hoskins, and M. McIntyre (1993), Two paradigms of baroclinic-wave life-cycle behaviour, *Q.J.R. Meteorol. Soc.*, *119*, 17–55.

Tokioka, T. (1970), Non-geostrophic and non-hydrostatic stability of a baroclinic fluid, *J. Meteorol. Soc. Japan*, *48*, 503–520.

Tomikawa, Y., K. Sato, K. Kita, M. Fujiwara, M. Yamamori, and T. Sano (2002), Formation of an ozone lamina due to differential advection revealed by intensive observations, *J. Geophys. Res.*, *107*(D10(4092)), 10.1029/2001JD000,386.

Trexler, M., and S. Koch (2000), The Life Cycle of a Mesoscale Gravity Wave as Observed by a Network of Doppler Wind Profilers, *Mon. Weath. Rev.*, *128*, 2423–2446.

Trier, S., R. Sharman, and T. Lane (2012), Influences of moist convection on a cold season outbreak of Clear-Air Turbulence (CAT), *in press for Mon. Wea. Rev.*

Tse, K., A. Mahalov, B. Nicolaenko, and H. Fernando (2003), Quasi-equilibrium dynamics of shear-stratified turbulence in a model tropospheric jet, *J. Fluid Mech.*, *496*, 73–103.

Tuyl, A. V., and J. Young (1982), Numerical simulation of nonlinear jet streak adjustment, *Mon. Wea. Rev.*, *110*, 2038–2054.

Uccelini, L., and S. Koch (1987), The synoptic setting and possible energy sources for mesoscale wave disturbances, *Mon. Wea. Rev.*, *115*, 721–729.

Vallis, G. (1992), Mechanisms and parameterization of geostrophic adjustment and a variational approach to balanced flow, *J. Atmos. Sci.*, *49*, 1144–1160.

Vallis, G. (2006), *Atmospheric and oceanic fluid dynamics*, 745 pp., Cambridge University Press.

Vanneste, J. (2004), Inertia-gravity wave generation by balanced motion: revisiting the Lorenz-Krishnamurty model, *J. Atmos. Sci.*, *61*, 224–234.

Vanneste, J. (2006), Wave radiation by balanced motion in a simple model, *SIAM J. Appl. Dynam. Syst.*, *5*, 783–807.

Vanneste, J. (2008), Exponential smallness of inertia-gravity-wave generation at small rossby number, *J. Atmos. Sci.*, *65*, 1622–1637.

Vanneste, J. (2013), Balance and spontaneous wave generation in geophysical flows, *Ann. Rev. Fluid Mech.*, *45*, 147–172.

Vanneste, J., and I. Yavneh (2004), Exponentially small inertia-gravity waves and the breakdown of quasi-geostrophic balance, *J. Atmos. Sci.*, *61*, 211–223.

Vanneste, J., and I. Yavneh (2007), Unbalanced instabilities of rapidly rotating stratified shear flows, *J. Fluid Mech.*, *584*, 373–396.

Vaughan, G., and R. Worthington (2007), Inertia-gravity waves observed by the UK MST radar, *qjrms*, *133*(S2), 179–188.

Vautard, R., and B. Legras (1986), Invariant manifolds, quasi-geostrophy and initialization, *J. Atmos. Sci.*, *43*(4), 565–584.

Vincent, R., A. Hertzog, G. Boccara, and F. Vial (2007), Quasi-Lagrangian superpressure balloon measurements of gravity-wave momentum fluxes in the polar stratosphere of both hemispheres, *Geophys. Res. Lett.*, *34*(L19804), doi:10.1029/2007GL031,072.

Viudez, A. (2007), The origin of the stationary frontal wave packet spontaneously generated in rotating stratified vortex dipoles, *J. Fluid Mech.*, *593*, 359–383.

Viudez, A. (2008), The stationary frontal wave packet spontaneously generated in mesoscale dipoles, *jpo*, *38*, 243–256.

Viúdez, A., and D. Dritschel (2003), An explicit potential vorticity conserving approach to modelling nonlinear internal gravity waves, *J. Fluid Mech.*

Viúdez, A., and D. Dritschel (2006), Spontaneous generation of inertia-gravity wave packets by geophysical balanced flows, *J. Fluid Mech.*, *553*, 107–117.

Waite, M. L., and C. Snyder (2009), The mesoscale kinetic energy spectrum of a baroclinic life cycle, *J. Atmos. Sci.*, *66*(4), 883–901.

Waite, M. L., and C. Snyder (2012), Mesoscale energy spectra of moist baroclinic waves, *submitted to J. Atm. Sci.*

Walterscheid, R., J. Hecht, R. Vincent, I. Reid, J. Woithe, and M. Hickey (1999), Analysis and interpretation of airglow and radar observations of quasi-monochromatic gravity waves in the upper mesosphere and lower thermosphere over Adelaide, Australia (35S, 138E), *J. Atmos. Solar-Terr. Phys.*, *61*(6), 461–478.

Wang, L., and M. Geller (2003), Morphology of gravity-wave energy as observed from 4 years (1998-2001) of high vertical resolution U.S. radiosonde data, *J. Geophys. Res.*, *108*(doi:10.1029/2002JD002786), 4489.

Wang, S. (2008), *Gravity Waves from Vortex Dipoles and Jets (Ph.D. Dissertation)*, Texas A&M University.

Wang, S., and F. Zhang (2006), Sensitivity of mesoscale gravity waves to the baroclinicity of jet-front systems, *in press for Mon. Wea. Rev.*

Wang, S., and F. Zhang (2007), Sensitivity of mesoscale gravity waves to the baroclinicity of jet-front systems, *Mon. Weath. Rev.*, *135*, 670–688.

Wang, S., and F. Zhang (2010), Source of gravity waves within a vortex-dipole jet revealed by a linear model, *J. Atm. Sci.*, *67*, 1438–1455.

Wang, S., F. Zhang, and C. Snyder (2009), Generation and propagation of inertia-gravity waves from vortex dipoles and jets, *J. Atm. Sci.*, *66*, 1294–1314.

Wang, S., F. Zhang, and C. Epifanio (2010), Forced gravity wave response near the jet exit region in a linear model, *Q.J.R. Meteorol. Soc.*, *136*, 1773–1787.

Warn, T., and R. Ménard (1986), Nonlinear balance and gravity-inertial wave saturation in a simple atmospheric model, *Tellus*, *38A*, 285–294.

Warn, T., O. Bokhove, T. Shepherd, and G. Vallis (1995), Rossby number expansions, slaving principles, and balance dynamics, *Q.J.R. Meteorol. Soc.*, *121*, 723–739.

Weglarz, R., and Y.-L. Lin (1997), Nonlinear adjustment of a rotating homogeneous atmosphere to zonal momentum forcing, *Tellus*, *50A*, 616–636.

Williams, P., T. Haine, and P. Read (2005), On the generation mechanisms of short-scale unbalanced modes in rotating two-layer flows with vertical shear, *J. Fluid Mech.*, *528*, 1–22.

Williams, P., D. Fritts, C. She, and R. Goldberg (2006), Gravity wave propagation through a large semidiurnal tide and instabilities in the mesosphere and lower thermosphere during the winter 2003 MaCWAVE rocket campaign, *Annales Geophysicae*, *24*(doi:10.5194/angeo-24-1199-2006), 1199–1208.

Williams, P., T. Haine, and P. Read (2008), Inertiagravity waves emitted from balanced flow: Observations, properties, and consequences, *J. Atmos. Sci.*, *65*(11), 3543–3556.

Wilson, R., M.-L. Chanin, and A. Hauchecorne (1991), Gravity waves in the middle atmosphere observed Rayleigh by Lidar: 2. Climatology, *J. Geophys. Res.*, *96*, 5169–5183.

Wu, D., and S. Eckermann (2008), Global gravity wave variances from Aura MLS: characteristics and interpretation, *J. Atmos. Sci.*, *65*(12), 3695–3718.

Wu, D., and J. Waters (1996), Satellite observations of atmospheric variances: A possible indication of gravity waves, *Geophys. Res. Lett.*, *23*, 36313634.

Wu, D., P. Preusse, S. Eckermann, J. Jiang, M. de la Torre Juarez, L. Coy, and D. Wang (2006), Remote sounding of atmospheric gravity waves with satellite limb and nadir techniques, *Adv. Space Res.*, *37*, 22692277.

Wu, D. L., and F. Zhang (2004), A study of mesoscale gravity waves over the North Atlantic with satellite observations and a mesoscale model , *J. Geophys. Res.*, *109*(D22104), doi:10.1029/2004JD005,090.

Wu, R., and W. Blumen (1995), Geostrophic adjustment of a zero potential vorticity flow initiated by a mass imbalance, *J. Phys. Oceanogr.*, *25*, 439–445.

Wunsch, C., and R. Ferrari (2004), Vertical mixing energy and the general circulation of the oceans, *Annu. Review Fluid Mech.*, *36*, 281–314.

Yamazaki, Y., and W. Peltier (2001a), The existence of subsynoptic-scale baroclinic instability and the nonlinear evolution of shallow disturbances, *J. Atmos. Sci.*, *58*, 657–683.

Yamazaki, Y., and W. Peltier (2001b), Baroclinic instability in an Euler equations-based column model: the coexistence of a deep synoptic scale mode and shallow subsynoptic scale modes, *J. Atmos. Sci.*, *58*, 780–792.

Yan, X., N. Arnold, and J. Remedios (2010), Global observations of gravity waves from High Resolution Dynamics Limb Sounder temperature measurements: A year-long record of temperature amplitude and vertical wavelength, *J. Geophys. Res.*, *115*(D10113), doi:10.1029/2008JD011,511.

Yavneh, I., J. McWilliams, and M. Molemaker (2001), Non-axisymmetric instability of centrifugally stable stratified taylor-couette flow, *J. Fluid Mech.*, *448*, 1–21.

Yeh, T. (1949), On energy dissipation in the atmosphere, *J. Meteor.*, *6*, 1–16.

Young, W., and M. B. Jelloul (1997), Propagation of near-inertial oscillations through a geostrophic flow, *J. Mar. Res.*, *55*, 735–766.

Zeitlin, V. (2008), Decoupling of balanced and unbalanced motions and inertia-gravity wave emission: Small versus large rossby numbers, *J. Atmos. Sci.*, *65*(11), 3528–3542.

Zeitlin, V., S. Medvedev, and R. Plougonven (2003), Frontal geostrophic adjustment, slow manifold and nonlinear wave phenomena in one-dimensional rotating shallow-water. Part 1: Theory, *J. of Fluid Mech.*, *481*, 269–290.

Zhang, D.-L., and J. Fritsch (1988), Numerical simulation of the meso-b scale structure and evolution of the 1977 Johnstown flood. Part III: Internal gravity waves and the squall line, *J. Atmos. Sci.*, *45*, 12521268.

Zhang, F. (2004), Generation of mesoscale gravity waves in upper-tropospheric jet-front systems, *J. Atmos. Sci.*, *61*(4), 440–457.

Zhang, F., and S. Koch (2000), Numerical simulations of a gravity wave event over CCOPE. Part II: Waves generated by an orographic density current, *Mon. Weath. Rev.*, *128*(8), 2777–2796.

Zhang, F., S. Koch, C. Davis, and M. Kaplan (2000), A survey of unbalanced flow diagnostics and their application, *Adv. Atmos. Sci.*, *17*(2), 165–183.

Zhang, F., S. Koch, C. Davis, and M. Kaplan (2001), Wavelet analysis and the governing dynamics of a large amplitude mesoscale gravity wave event along the east coast of the united states, *Q.J.R. Meteorol. Soc.*, *127*, 2209–2245.

Zhang, F., S. Koch, and M. Kaplan (2003), Numerical simulations of a large-amplitude gravity wave event, *Meteo. Atmos. Phys.*, *84*, 199–216.

Zhang, F., S. Wang, and R. Plougonven (2004), Potential uncertainties in using the hodograph method to retrieve gravity wave characteristics from individual soundings, *Geophys. Res. Lett.*, *31*(L11110), doi:10.1029/2004GL019,841.

Zhang, F., N. Bei, R. Rotunno, and C. Snyder (2007), Mesoscale predictability of moist baroclinic waves: Convection permitting experiments and multistage error growth dynamics, *J. Atmos. Sci.*, *64*, 3579–3594.

Zhang, F., M. Zhang, K. Bowman, L. Pan, and E. Atlas (2009), Aircraft measurements and numerical simulations of gravity waves in the extratropical utls region during the start08 field campaign, in *The 13th Conference on Mesoscale Processes*.

Zhang, F., J. Wei, and S. Wang (2011), Dynamics and impacts of gravity waves in the baroclinic jet-front systems with moist convection, in *The 14th AMS conference on mesoscale processes*.

Zhang, S., and F. Yi (2005), A statistical study of gravity waves from radiosonde observations at Wuhan (30 degrees N, 114 degrees E) China, *Ann. Geophys.*, *23*, 665–673.

Zhang, S., and F. Yi (2007), Latitudinal and seasonal variations of inertieal gravity wave activity in the lower atmosphere over central China, *J. Geophys. Res.*, *112*(D05109), doi:10.1029/2006JD007,487.

Zhang, S., and F. Yi (2008), Intensive radiosonde observations of gravity waves in the lower atmosphere over Yichang (111 degrees 18 ' E, 30 degrees 42 ' N), China, *Ann. Geophys.*, *26*(7), 2005–2018.

Zhu, X., and J. Holton (1987), Mean fields induced by local gravity-wave forcing in the middle atmosphere, *J. Atmos. Sci.*, *44*(3), 620–630.

Zülicke, C., and D. Peters (2006), Simulation of inertia-gravity waves in a poleward breaking Rossby wave, *J. Atmos. Sci.*, *63*, 3253–3276.

Zülicke, C., and D. Peters (2008), Parameterization of strong stratospheric inertiagravity waves forced by poleward-breaking rossby waves, *Mon. Wea. Rev.*, *136*, 98–119.

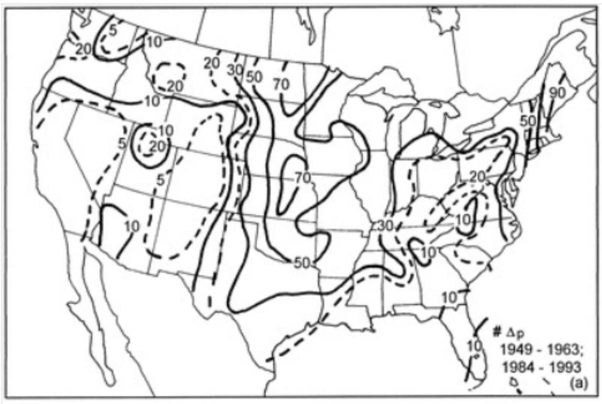

Figure 1. Distribution of large hourly surface pressure changes (defined to be greater than 4.25 hPa.), as diagnosed from the surface barograph network by *Koppel et al.* [2000]. The data covers 25 years (1949 – 1963 and 1984 – 1993).

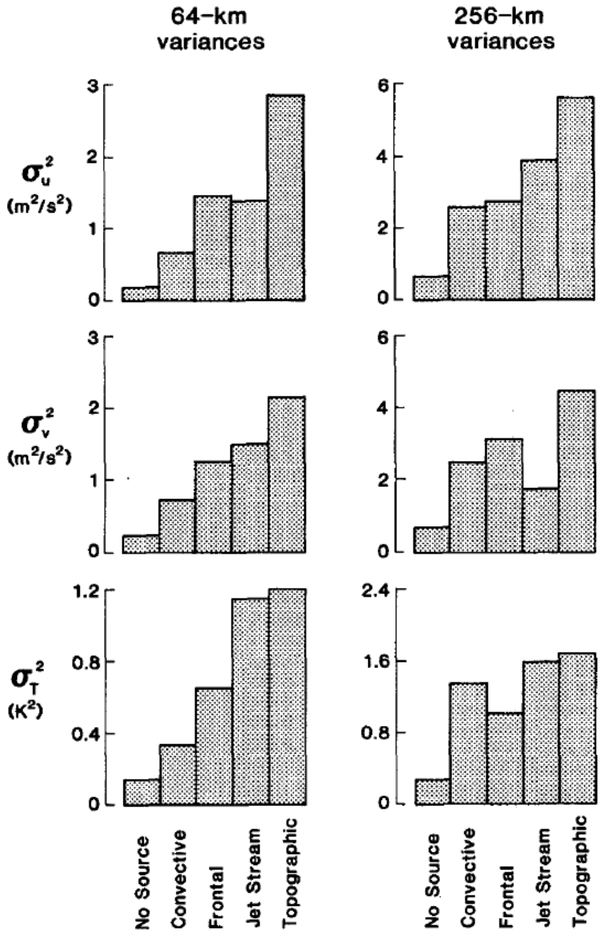

Figure 2. Average variances of the zonal (top) and meridional (middle) wind components, and of temperature (bottom), for flight segments of 64 (left) and 256 km (right). Inspection of the flow has allowed to categorize segments by the expected source of gravity waves. (Adapted from *Fritts and Nastrom* [1992]).

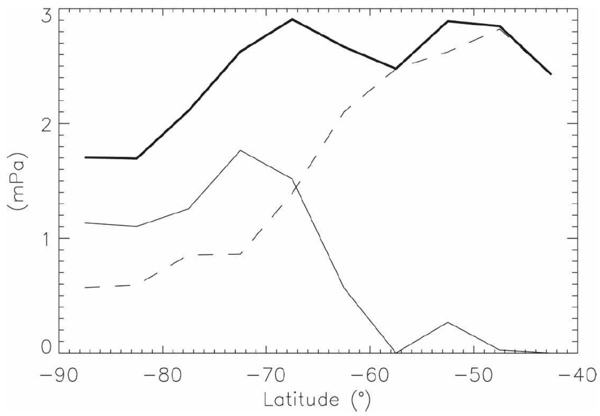

Figure 3. Latitudinal distribution of zonal mean, density weighted absolute momentum flux carried by waves over orographic regions (thin solid), by waves over non-orographic regions (thin dashed), and by both types of waves (thick solid), as estimated by [*Hertzog et al.*, 2008] from balloon observations.

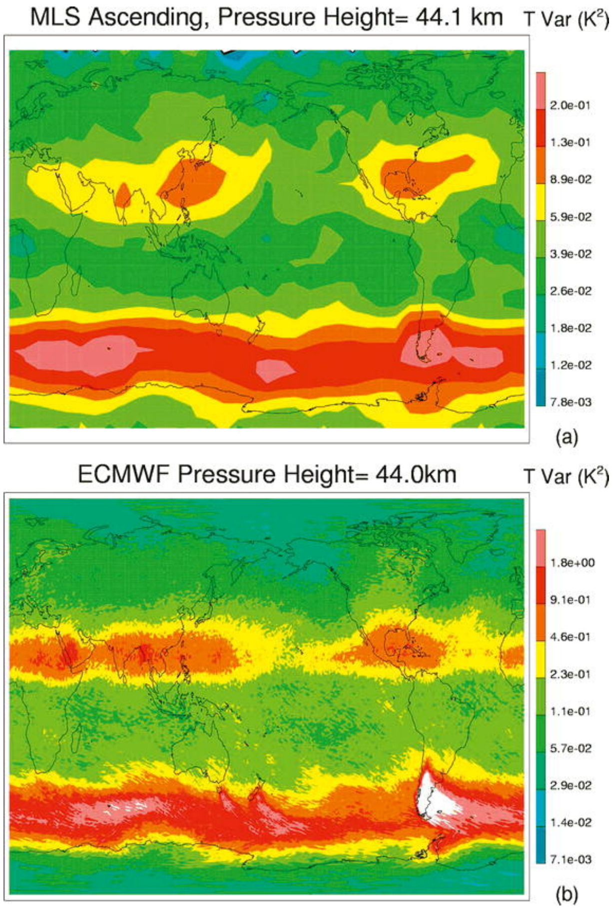

Figure 4. Monthly-mean temperature variances at 44-km pressure altitude from from (a) satellite observations from the Aura Microwave Limb Sounder, and (b) the ECMWF analyses at resolution TL799L91 for August 2006. For the latter, only horizontal wavelengths longer than 300 km were retained.

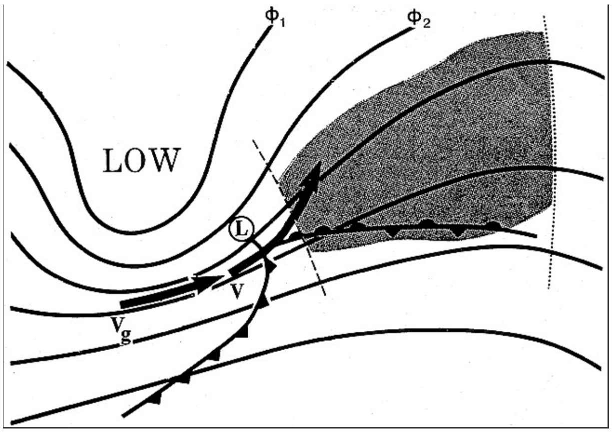

Figure 5. Flow configuration identified by *Uccelini and Koch* [1987] (UK87) as conducive to intense gravity waves: lines of geopotential in the mid-troposphere and surface fronts are indicated. Just downstream of the inflection axis (dashed line) the wind has a significant cross-stream ageostrophic component (wind vector crossing isolines of geopotential) and intense gravity waves are recurrently found (shaded region).

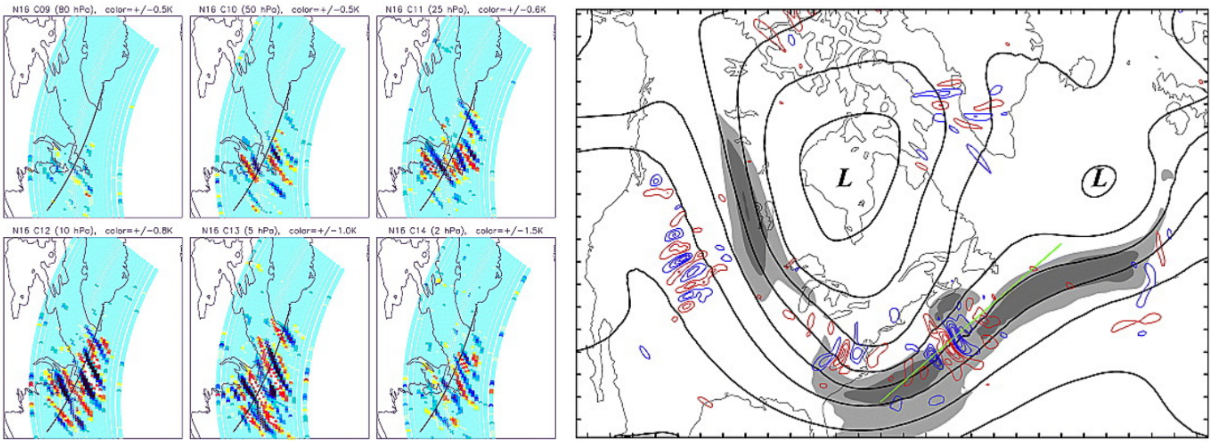

Figure 6. Comparison of gravity waves in satellite observations and in mesoscale simulations, from *Wu and Zhang* [2004]. Left panel: radiance perturbations from different channels of the NOAA 16 AMSU-A at 0630 UT on 20 January, showing gravity wave perturbations at different heights. Right panel: geopotential height (thick contours every 20 dam) and maxima of wind speed (shaded regions) at 300-hPa, and 80-hPa horizontal divergence (every 3 105 s1; blue, positive; red, negative) from the MM5 simulations at 1800 UT on 19 January (starting on 19 January at 0000 UT). Simulated amplitudes of wind and temperature perturbations are 10 $m\,s^{-1}$ and 5 K respectively.

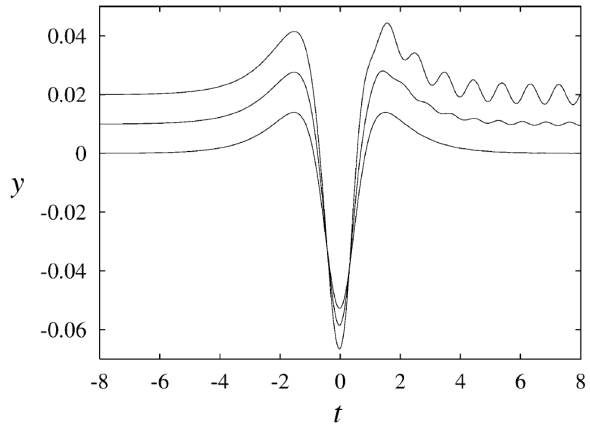

Figure 7. Evolution of $y(t)$, one of the 2 fast variables of the Lorenz-Krishnamurty model, as calculated by *Vanneste* [2004], for Rossby numbers $\epsilon = 0.15$ (upper curve, offset by 0.02), $\epsilon = 0.125$ (middle curve, offset by 0.01) and $\epsilon = 0.1$ (lower curve). The balanced evolution of the flow leads to temporary variations of y near $t = 0$. For $\epsilon = 0.15$, conspicuous fast oscillations are excited and remain thereafter. This emission is very sensitive to ϵ (exponential dependence).

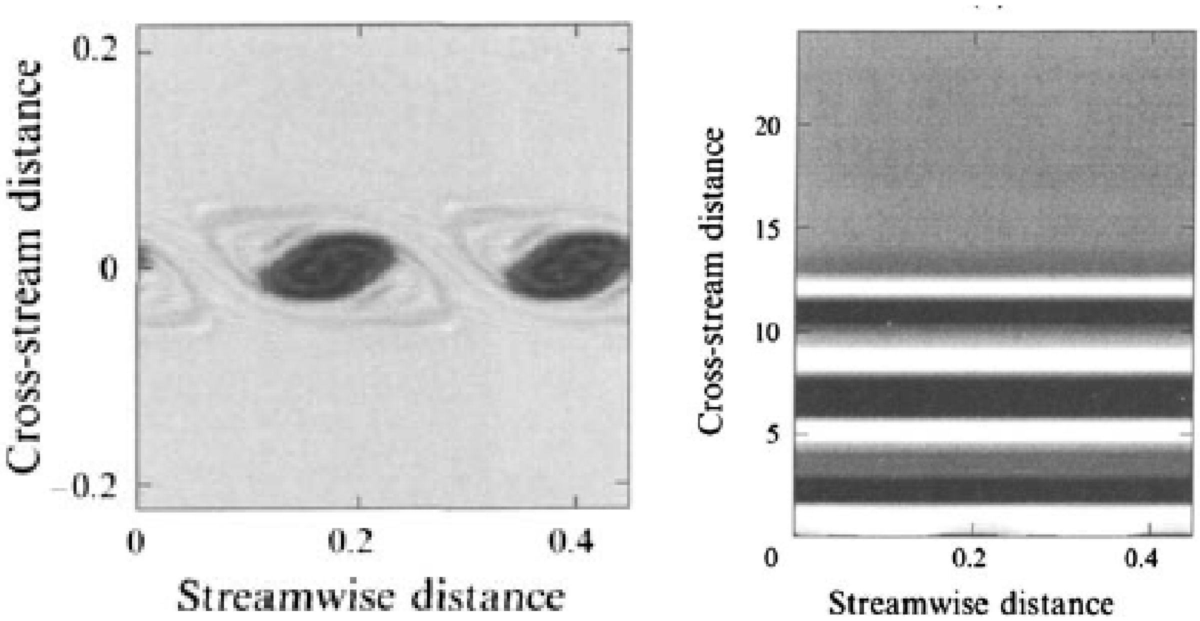

Figure 8. From *Ford* [1994c]: roll-up of the unstable potential vorticity strip (left) as seen from the potential vorticity distribution, and radiation of gravity waves in the far-field (right), as seen from the time derivative of the surface height. Note the large scale separation between the two phenomena.

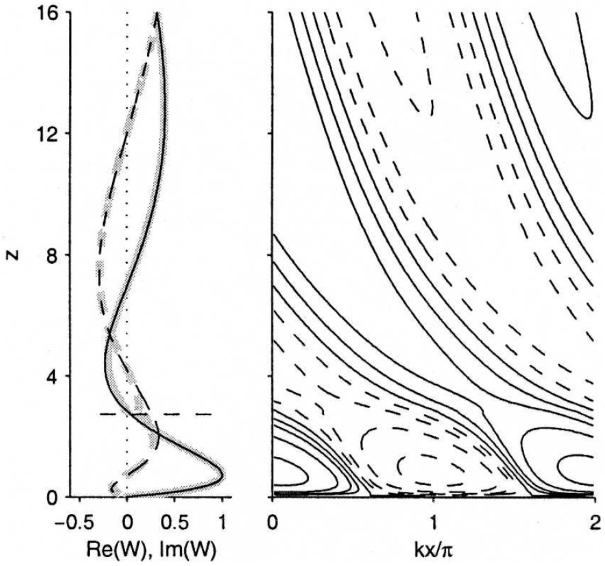

Figure 9. Vertical structure $W(z)$ for a normal mode of an unbalanced baroclinic instability in a vertical shear [*Plougonven et al.*, 2005]: the left panel shows the real (plain line) and imaginary parts of $W(z)$, with the horizontal dashed line indicating the inertial critical level. The right panel shows a vertical cross-section in the (x, z) plane, through one wavelength of the mode. Also shown in the left panel are asymptotic approximations of the balanced edge wave near the surface (below the ICL, obtained asymptotically in Rossby number), and a far field approximation of sheared gravity waves aloft (above the ICL).

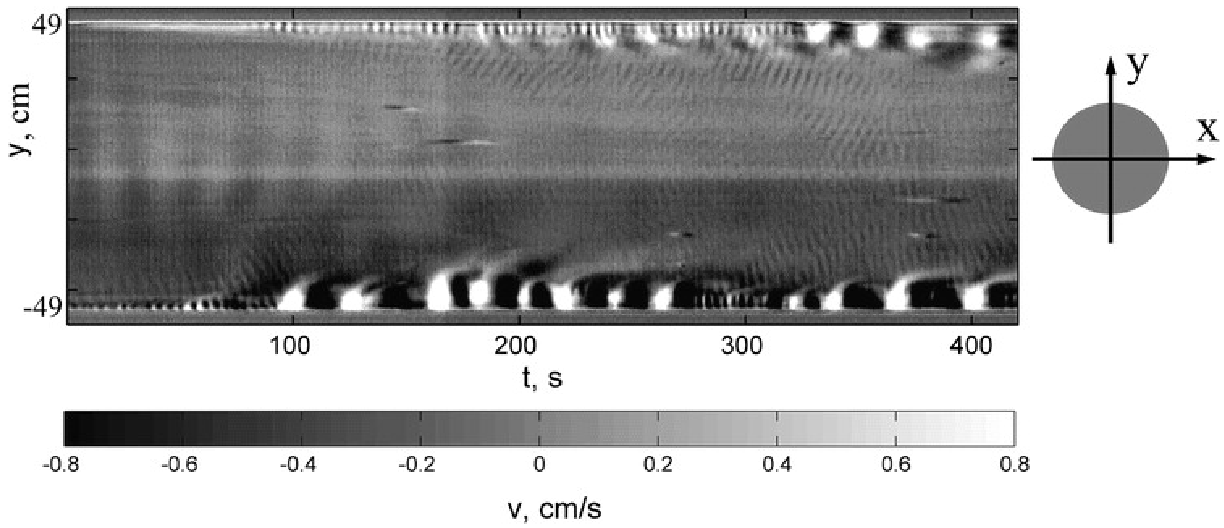

Figure 10. Hovmöller plot showing the x component of the gradient wind velocity along the y axis across the tank in the experiment of *Afanasyev et al.* [2008]. Features near the walls ($y = \pm 49$cm) describe the baroclinic instabilty of the coastal jet. The intentionally narrow grayscale range makes the short-scale inertial waves visible. They are emitted from the shorter-scale meanders of the coastal jet and propagate into the quiescent interior of the tank.

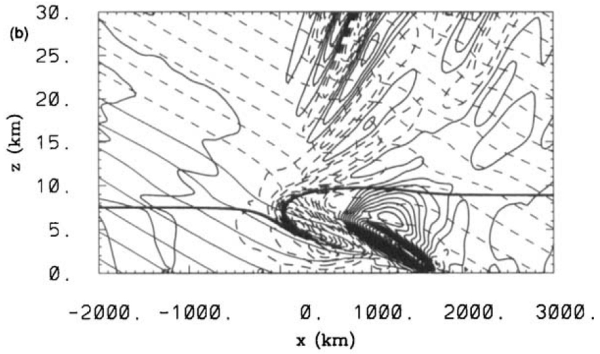

Figure 11. Isotachs of vertical velocity (thick lines, contour interval $5m\,s^{-1}$) in the two-dimensional simulation of frontogenesis of *Griffiths and Reeder* [1996] which produced the most stratospheric waves. Also shown is the tropopause (thick line) and the cross-front velocity (contour interval $5m\,s^{-1}$).

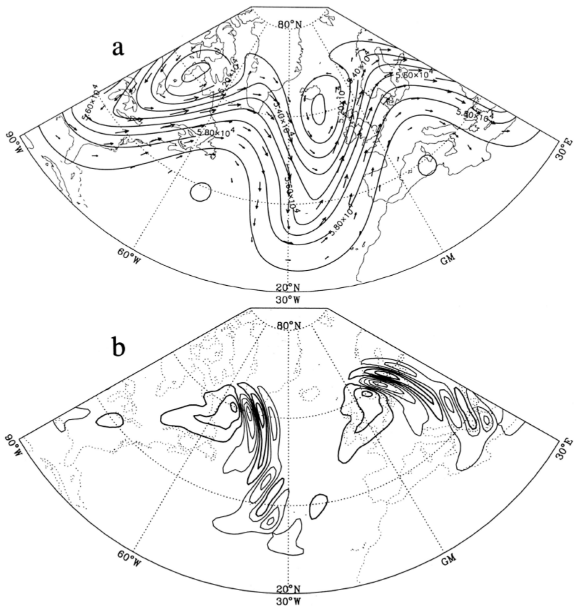

Figure 12. *a)* Geopotential height and wind at 503 hPa, at day 10 of the idealized baroclinic life cycle of *O'Sullivan and Dunkerton* [1995], and *b)* divergence of the horizontal wind at 130 hPa at the same time. Adapted from *O'Sullivan and Dunkerton* [1995].

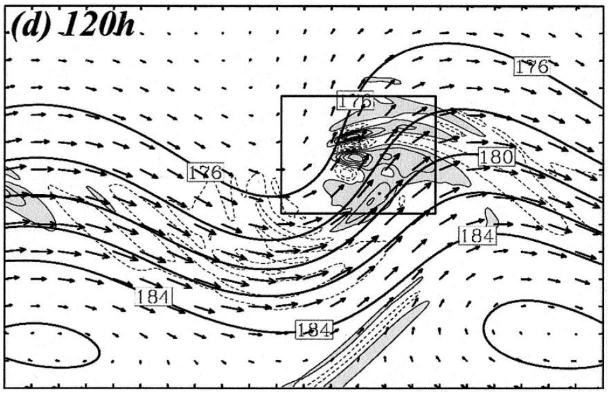

Figure 13. Pressure and divergence of horizontal wind, at $z = 13$km, in the baroclinic life cycle simulated by *Zhang* [2004]. Distance between the tick marks is 300 km.

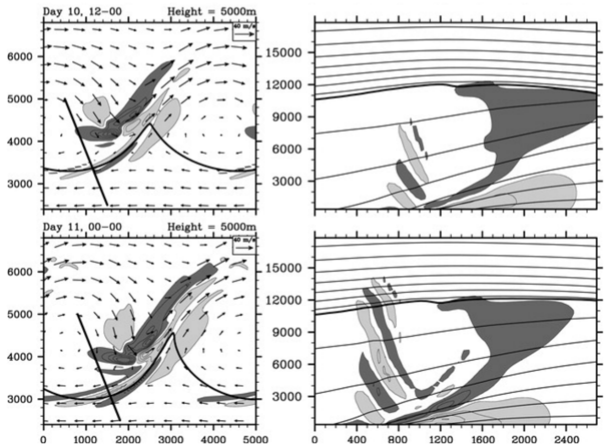

Figure 14. Inertia-gravity waves appearing ahead of cold surface fronts in a life cycle with enhanced surface anticylonic shear. Left: horizontal maps of $\nabla\, \mathbf{u}_H$ at $z = 5$km, with one surface isentrope (thick line) to depict the surface fronts; right: vertical cross sections through the line segments indicated in the left panels (height in m, distance along section in km, southern end of the section to the left). The top and botton panels are separated by 12 hours. Adapted from *Plougonven and Snyder* [2007].

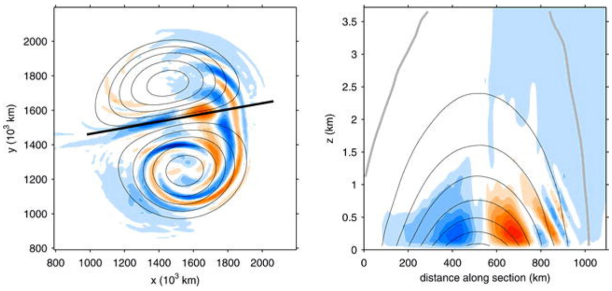

Figure 15. Horizontal (left) and vertical (right) cross-sections of the vertical velocity (colors) in a surface dipole, from *Snyder et al.* [2007]. Also shown are contours of potential temperature (left, at $z = 125m$) and of section-parallel horizontal flow. The horizontal cross-section of w corresponds to $z = 62.5m$.